# NOBLE METALS IN THE MERENSKY HORIZON, BUSHVELD IGNEOUS COMPLEX

# A STUDY OF THE DISTRIBUTION OF SOME NOBLE METALS IN THE MERENSKY HORIZON, BUSHVELD IGNEOUS COMPLEX

By

Yuko Teruta, B.Sc.

A Thesis

Submitted to the School of Graduate Studies

in Partial Fulfilment of the Requirements

for the Degree

Master of Science

McMaster University

October 1974

MASTER OF SCIENCE (1974) McMASTER UNIVERSITY
(Geology) Hamilton, Ontario.

Title: A Study of the Distribution of Some Noble Metals in the Merensky Horizon, Bushveld Igneous Complex

Author: Yuko Teruta, B.Sc. (McMaster University)

Supervisor: Dr. James H. Crocket

Number of Pages: xii, 137

Scope and Contents Neutron activation analysis has been applied to the simultaneous determination of Pt, Pd, Ir and Au in a diamond drill core from the Lonrho property (Western Platinum Limited) on the Merensky horizon, Bushveld Igneous Complex, South Africa.

Analytical results for Pt, Pd, Ir and Au in a total of 65 samples, including 25 whole rock, 19 separated sulphide and 21 oxide samples are presented. Chemical analyses by fusion-gravimetric and atomic absorption methods are used to determine S, Cr, Ni and Cu in whole rock samples. Profiles along the core length were obtained for the four noble metals and these were correlated with the mineralogical and petrographic character of the core. The sulphide and oxide data were used to evaluate the proportion of total platinum group metals contributed by these mineral phases.

## ACKNOWLEDGEMENTS

The author wishes to express her sincere thanks and gratitude to her supervisor, Dr. J.H. Crocket, for his kind assistance and discussion of problems throughout the course of the work. She is also indebted to Dr. D.M. Shaw and Mr. J.R. Muysson, chemical analyst. Dr. Shaw kindly gave the author permission to use his atomic absorption equipment.

The samples were provided by Western Platinum Limited. The interest of Mr. H.H. Bird (Falconbridge Exploration Limited), Mr. A.M. Clarke and Dr. A.R. Graham (Falconbridge Nickel Mines Limited) is deeply appreciated. Financial support of Western Platinum Limited and the National Research Council of Canada made the study possible.

The competence and reliability of Mrs. J. Allen, who typed this thesis, has been very much appreciated.

TABLE OF CONTENTS

Table of Contents (continued)

# LIST OF TABLES

List of Tables (continued)

# LIST OF FIGURES

List of Figures (continued)

## LIST OF PLATES

# ABSTRACT

Neutron activation analysis was used to determine the Pt, Pd, Ir and Au contents in a single 27 inch diamond drill core from the Lonrho property (Western Platinum Limited) on the Merensky horizon, some 25 miles east of Rustenburg, Western Transvaal, South Africa. Fusion-gravimetric and atomic absorption methods were applied to the determination of S, Cr, Ni and Cu contents in whole rock samples. A total of 65 samples including 25 one-inch whole rock core samples, 19 separated sulphide and 21 oxide samples were analysed.

The rock is a feldspathic pyroxenite consisting mainly of cumulus orthopyroxene, intercumulus plagioclase and accessory biotite, clinopyroxene, chromite, magnetite and sulphides. Localized concentration of oxides (chromite and magnetite) in bands occurs in the top half of the core. Extensive hydrous alteration is observed in the middle of the core and occasionally elsewhere. Part of the sulphide has crystallized from the intercumulus liquid apparently in equilibrium with silicates, while other sulphides show close spatial relationship with hydrous secondary silicates occurring mainly along cleavages in altered silicates. This

secondary sulphide may result from reaction of primary sulphides with hydrous solutions of deuteric origin during the alteration of primary silicates.

Pt, Pd and Au are all highly enriched in the central portion of the core in association with hydrous secondary silicate alteration and high content of secondary sulphides. Pd and Ir are enriched in sulphides throughout the core and Pd is closely related to pentlandite. Sulphides (and oxides) account for approximately 20 and 40% of total whole rock Pd and Ir respectively. From the dispersion of Pd and Ir contents in different sulphides from the same one inch core specimen it is inferred that much of the Pd probably occurs in discrete minerals, whereas Ir may be in true lattice solid solution.

Pt and Au do not show clear enrichment in separated sulphides and oxides which account for only 5% of the whole rock total for these elements. The heterogeneous distribution of Pt suggests the presence of discrete Pt minerals as a major source of this metal, particularly in the Pt-rich central portion of the core. Metallic gold is probably a significant contributor to total whole rock gold.

# CHAPTER I

## INTRODUCTION

The major sources of platinum group metals are, at present, South Africa, the U.S.S.R. and Canada. Although primary platinum in economic concentrations is invariably associated with basic and ultra-basic rocks, types of occurrences differ considerably. In South Africa, platinum and palladium are recovered mainly from the Merensky Reef of the Bushveld Igneous Complex where they are mined as principal economic metals. In the U.S.S.R. and Canada, the platinoids are recovered mainly from magmatic Cu-Ni sulphide deposits as by-products from such deposits as Noril'sk and Sudbury.

Nearly all the production of platinum in South Africa is derived from the Merensky Reef, a pegmatitic pyroxenite discovered to be platiniferous in 1924 by a prospector, A. F. Lombaard. It was later named in honor of Dr. Hans Merensky who was in charge of the prospecting. Although almost 50 years have passed since this eventful discovery, the true origin and relationships of this pegmatoid to its

host Bushveld Igneous Complex have been a most controversial subject amongst geologists and still remain open to considerable discussion.

The Merensky Reef, normally bounded on top and bottom by thin chromitite seams, is characterized by high platinum metal values within or adjacent to the top and bottom chromite bands. Schneiderhöhn and Moritz (1931) analysed sulphide and silicate minerals from the Merensky Reef for platinum metals by microdrilling of polished sections, followed by direct analysis by emission spectrography. In the samples examined by them no discrete platinum minerals were observed and they concluded that the platinum metals were in solid solution in sulphides. They also found that the highest platinum metal contents were in the earliest sulphides, pyrite and pyrrhotite.

The well-established occurrence of discrete platinum metal minerals in the Merensky Reef (Wagner, 1929, p. 226; Ramdohr, 1969, p. 354; Stumpfl, 1962; Cousins, 1969, etc.) indicates, however, that only part of the total platinum metal content can be in solid solution in sulphides. Although distinctive platinum metal-sulphide mineral associations are apparent, it is by no means clear whether the platinum metals are in solid solution or are mechanically admixed as discrete minerals with the sulphides.

The occurrence of platinum metals in dunitic rocks such as the Mooihock and Onverwacht pipes in the Bushveld Complex is characterized by two important features including: 1) enrichment associated with spinel group minerals, particularly massive or segregation-type chromite and 2) concentration in the younger portions of the pipes.

A suggested explanation is that low solubility of platinum metals in silicate lattices has led to concentration in residual magmatic fluids or melts, where they have finally crystallized as native metals, sulphides, arsenides or antimonides depending on the availability of these elements.

Having studied platinum metals in the Inaglinsk Massif, U.S.S.R., Razin et al. (1965) appeal to substantial solid solution or adsorption of platinum metals in silicates, whereas Cousins (1969) maintains that the Merensky Reef and other Bushveld chromites are free of platinum metals although supporting analytical data are not presented.

Thus, the relative importance of oxides, sulphides, silicates and discrete platinoid minerals as carriers of the noble metals in economic deposits remains obscure. With this situation in mind, it was decided to conduct a study of the distribution of the noble metals

in whole rock samples, sulphide grains and oxides (mainly spinel group minerals) from the Merensky Reef.

The study was carried out on a single 27-inch diamond drill core from the Lonrho property (Western Platinum Limited, South Africa), a mine currently operating in the Merensky Reef some 25 miles east of Rustenburg. Pt, Pd, Ir and Au were determined by neutron activation on whole rock and separated sulphide and oxide samples. The mineralogy of the whole rock samples and purity of the separated grains were evaluated by microscopic observations of thin and polished sections and X-ray powder diffraction. Chemical analyses by fusion-gravimetric and atomic absorption methods were used to determine S, Cr, Ni and Cu in whole rock samples.

Throughout the thesis the platinum group metals will be referred to as PGM. For the purpose of discussion, gold is included in the PGM for convenience.

It was hoped by consideration of these data that a better understanding of the geochemical behaviour of noble metals during crystallisation of a basic magma would be obtained.

# CHAPTER II

## OUTLINE OF PREVIOUS WORK

The geology, mineralogy and geochemistry of the Bushveld Igneous Complex has been investigated and described, amongst others, by Wagner (1929), Hall (1932), Lombaard (1934), Wager and Brown (1967), Willemse (1969), L. Liebenberg (1970) and Cousins (1956-1973). The outline below is taken from these studies.

### 2.1. General Geology of the Bushveld Igneous Complex

The Bushveld Igneous Complex occupies a lobate area in the Central Transvaal with one axis striking in a general east-westerly direction and measuring 288 miles in length, and the other extending from north of Pretoria for 153 miles to the north. The area taken up by the Complex is about 26,000 square miles, including that covered by younger formations. The accompanying map depicts the areal relationships (Fig. 1).

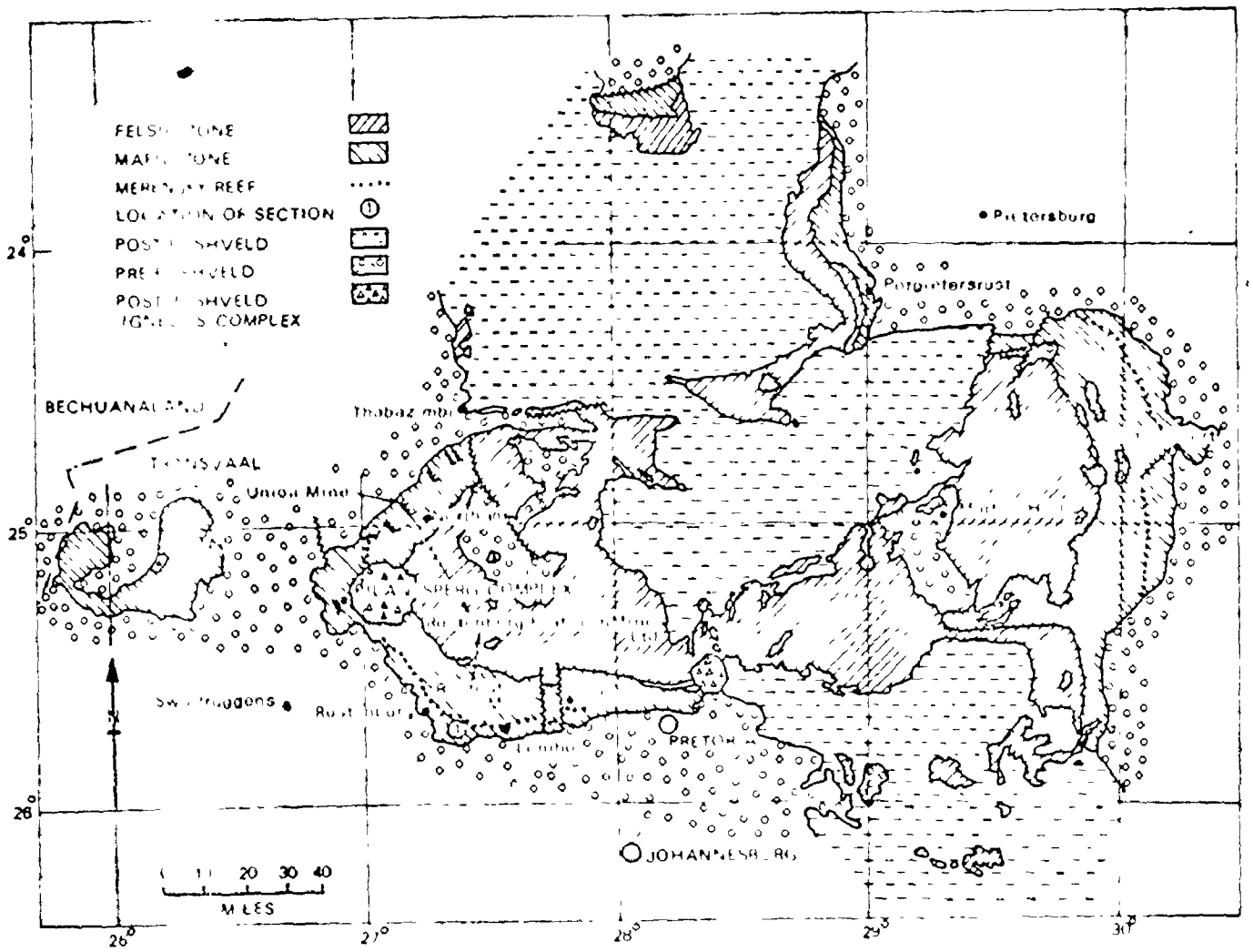


Fig. 1 GEOLOGICAL PLAN OF THE BUSHVELD COMPLEX SHOWING THE MERENSKY REEF
(After C.A. Cousin, 1969)

The Complex comprises essentially five adjoining, basin-shaped masses of igneous rocks. A typical section, where such a basin is followed from the margin inwards, consists of a gabbroic marginal zone, a layered succession of mafic and ultramafic rocks, and towards the centre or roof of the structure "red rocks", viz. felsite, leptite, granophyre and granite, called Bushveld Granite.

The absolute age of the Bushveld granite was determined as 1954±30 million years (Nicolaysen, 1958; Davies et al. 1970). Most of the determinations, however, were made on material from the Bushveld granites, whose relations to the mafic and ultramafic rocks of the intrusion are in doubt (Hess, 1960, p. 164). One Rb-Sr determination of 2050±50 m.y. was obtained on biotite from a pyroxenite (Jackson, 1967). Previously, the Bushveld was considered to be of Late Precambrian age.

Although there is doubt about the order in which some of the rocks of the Bushveld Complex were emplaced, they are usually grouped in the following chronological order:

1. deposition of the Transvaal System, including contemporaneous volcanic rocks;

2. diabase intruded as sills in the Transvaal System;

3. Epicrustal rocks including felsite, leptite, granophyre and microgranite;

4. the Layered Sequence of mafic and ultramafic rocks comprising the Bushveld Complex proper, and

5. a later plutonic phase represented by the Bushveld granite.

The Transvaal System, having an average total thickness of 20,000 feet, is 300 miles long and 100 miles wide. It makes up 85 percent of the circumference of the Complex and consists mainly of shale, dolomite, andesite and quartzite. The System is characterized by uniform deposition over extensive areas so that marker-horizons can be followed for hundreds of miles along the strike, far beyond the main basin of the Complex.

Although comparatively little research has been done on the diabase sheets in the Transvaal System, they are known at a number of horizons. Each retains roughly the same stratigraphic position over long distances of strike, but locally they migrate from one horizon to another for no clear reason. These "diabase" sheets comprise a considerable variety of mafic rocks, although the most common type is a plagioclase and clinopyroxene rock. Cousins (1962) believes they represent contemporaneous (extrusive) lava and not intrusive sills.

The roof of the Layered Sequence of mafic and ultramafic rocks is formed by felsite, granophyre, fine-grained silica-rich rocks called leptite and microgranite. The thickness of these rocks varies with locality and is over 15,000 feet thick in places. The mode of formation of these rocks is not clear. They may be feldspathized sediments, or they may represent somewhat coarsely crystalline, slowly cooled felsite.

The Layered Sequence of mafic and ultramafic rocks comprises a thickness of the order of 25,000 feet. It is subdivided into the Basal, Critical, Main and Upper Zones (Fig. 2). The major subdivisions are based on the following marker horizons: the main Chromitite Seam, the Merensky Reef and the Main Magnetite Seam.

The Basal Zone comprises essentially ultramafic rocks, mostly monomineralic bronzitite with occasional interbedded layers and large masses of peridotite. The lower boundary of this zone is not definite because the outer or basal contact of the Complex is very irregular. In places, for example, the Main Zone is in contact with marginal pre-Bushveld sedimentary rocks for long distances. The Basal Zone displays marked layering although the individual units are rather thick. In the Eastern Transvaal its exposed thickness is of the

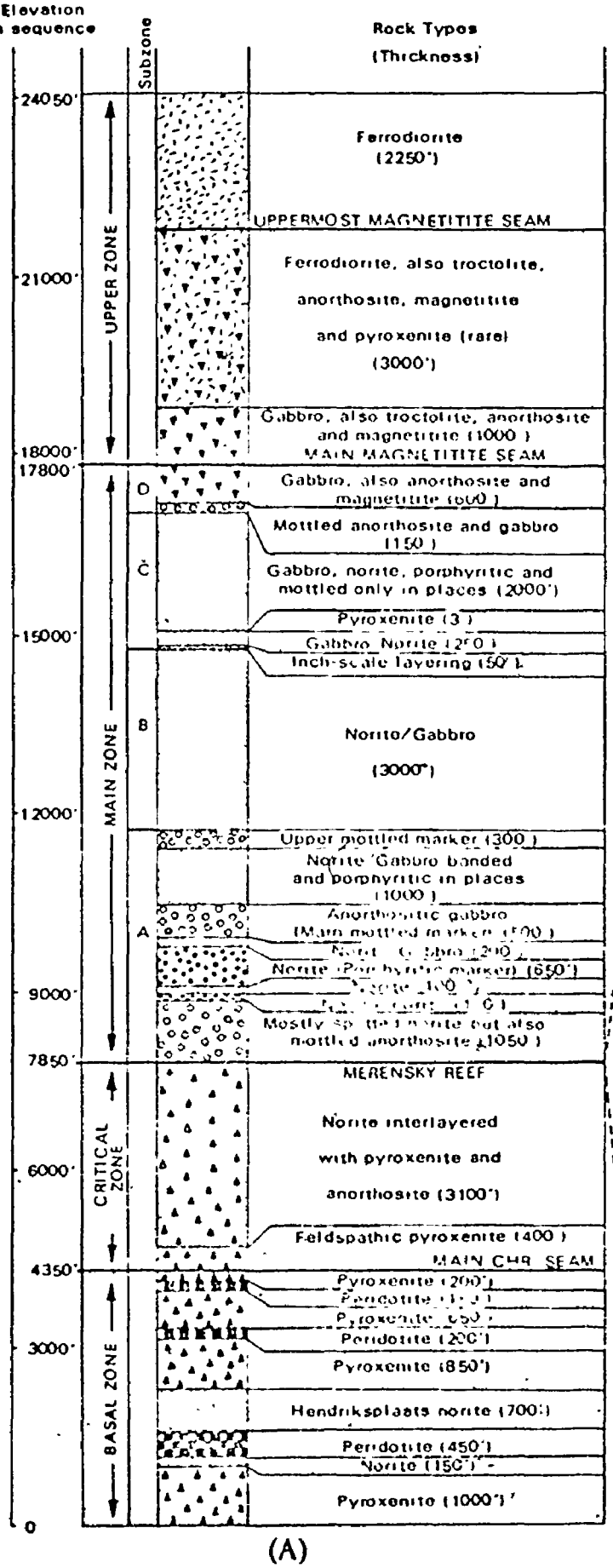


Fig. 2 (A) THE LAYERED SEQUENCE IN THE EASTERN TRANSVAAL (after Willemse, 1969) and (B) GENERALIZED DIAGRAMMATIC PROFILE THROUGH THE MERENSKY SUITE OF ROCKS

order of 4,500 feet. Southeast and northwest of Rustenburg a thickness of 1,500-1,800 feet was calculated according to Willemse (1964). In the far western Transvaal the Basal Zone forms a basin-like structure and the rocks are pyroxenite and harzburgite.

The Critical Zone displays layering of a grand scale involving rocks ranging from banded norite to a variable succession of pyroxenite, norite, anorthosite and chromitite. The maximum thickness of this zone in the Eastern Transvaal is about 3,500 feet, but in the faulted and folded area south of the Steelpoort River, the zone is locally sometimes only 500 feet thick. Southeast of Rustenburg the thickness ranges from 1,140 to 2,190 feet. Most of the chromitite seams occur in this zone. The upper and lower markers of the zone are the Merensky Reef and the Main Chromitite Seam respectively.

The Main Zone consists of a great thickness of gabbroic rocks forming a prominent ridge and mountainous country. This zone is generally considered to be noritic towards the base and gabbroic higher up in the sequence. Many of the rocks contain both clino- and ortho-pyroxene in variable amounts. The thickness of the Main Zone is about 17,000 feet in the Eastern Transvaal and 10,000 feet in the Rustenburg Sector (Willemse, 1964).

The Upper Zone includes continuous and persistent seams of titano-magnetite, interlayered with anorthosite, in a mass of gabbroidal to dioritic rocks. It is up to 6,300 feet thick in the Eastern Transvaal, but only 5,000 feet in the Rustenburg and Pretoria areas (Willemse, 1964).

Extensive areas in the central portion of the Complex are occupied by the Bushveld Granite. This granite is essentially intrusive into the Epicrustal rocks, i.e. the felsite, granophyre, leptite and microgranite. The granite body is essentially basin-shaped in form and has as its roof mostly felsite, granophyre and fragments of the Transvaal System.

## 2.2. Mineralogy of the Bushveld Igneous Complex

The compositional variation of the major minerals in the Layered Sequence has been presented by Willemse (1969), as shown in Fig. 3. The change in plagioclase composition over the Layered Sequence is remarkably small, ranging from An 85 in norite of the Basal Zone to An 60 at the top of the Main Zone. It is only at the top of the Upper Zone that the change is somewhat rapid where the anorthite content drops to An 30. Variation in the composition of orthopyroxene is more marked. It ranges from 10 to 60 mole percent $FeSiO_3$ from the Basal Zone to the top of the Main Zone.

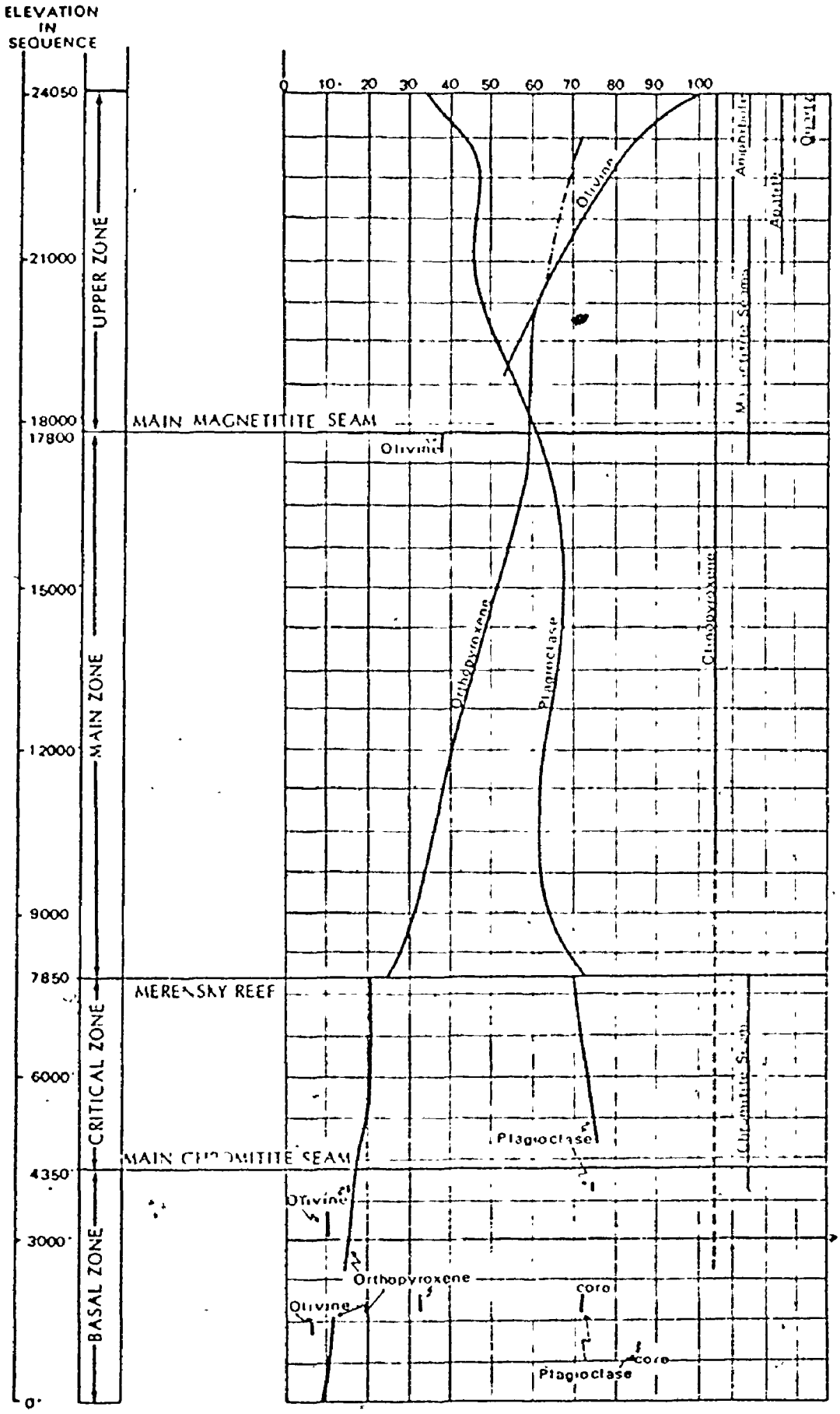


Fig. 3 THE MINERAL VARIATION IN THE LAYERED SEQUENCE: $FeSiO_3$(MOL.%) IN ORTHOPYROXENE, $Fe_2SiO_4$ (MOL%)

A very significant feature is the appearance and disappearance and the relative concentration of certain mineral phases. A few outstanding examples are as follows: Forsteritic olivine is a prominent constituent of the Basal Zone. It is unknown from the Critical Zone but has been reported from the Merensky Reef pegmatoid in the Western Transvaal. Then for thousands of feet of the Main Zone there is no olivine until the Main Magnetitite Seam is reached. In the Upper Zone olivine is again widespread, but here is hortonolite to fayalite becoming more iron-rich upward in the succession.

The oxide minerals, chromite and magnetite, are generally mutually exclusive. From the vicinity of the Merensky Reef downwards, chromiferous rocks are abundant, and magnetite is absent for all practical purposes. Chromite occurs in thin layers or chromitite seams between the Merensky Reef and the Main Chromitite Seam. Cousins (1969) recognizes Upper, Middle and Lower (= Main Chromite Seam) Chrome groups in the Critical Zone in both the Eastern and Western Bushveld. Neither chromite nor magnetite is prominent in the rocks above the Bastard Reef, a horizon immediately overlying the Merensky Reef, until the Upper Zone is reached. Here magnetite becomes so abundant that over a thickness of 5,000 feet 26 seams of magnetite have been reported in a typical profile (Willemse, 1969).

Regarding the pyroxenes, orthopyroxene is prevalent in the Basal, Critical and Main Zones. Clinopyroxene is rare in the Basal Zone, subordinate to orthopyroxene in the Critical Zone and becomes a major mineral constituent in the Main Zone persisting throughout the entire Upper Zone. Orthopyroxene disappears in the upper horizons of the Upper Zone.

Biotite is a subordinate constituent of the mafic and ultramafic rocks generally, but is fairly abundant in the dioritic rocks toward the top of the Upper Zone. Hornblende is a major constituent of the diorite of the Upper Zone. Quartz is a regular constituent of the uppermost rocks of the Layered Sequence, but is also quite conspicuous in most of the anorthosites in the Main Zone even lower down in the sequence. Apatite is reported from different profiles from about 3,000 feet above the Main Magnetitite Seam and continues to be present higher in the sequence as a prominent constituent.

## 2.3. Textures of Bushveld Complex Rocks

Bushveld rocks are characterized by textures originating through bottom accumulation of settled (cumulus) crystals. The chief cumulus minerals found at various horizons are: Basal Zone, bronzite and olivine; Critical Zone, bronzite, plagioclase, augite and chromite;

Main Zone, pigeonite, plagioclase, ferroaugite, olivine, magnetite and apatite. Rhythmic layering results from the concentration of some cumulus phases relative to others. Most of the Basal and Critical Zones contain either one or two cumulus phases. The Main Zone is characterized by three cumulus phases, two pyroxenes and plagioclase. The Upper Zone rocks, in which six cumulus phases may occur, generally contain at least three and usually more cumulus phases. Hence, the Bushveld layered succession displays an important feature of the crystal fractionation of basaltic magmas, i.e. a gradual increase in the number of crystalline phases in equilibrium with successive liquids.

A few of the characteristic textures reported by Willemse (1969) include the following. In the Basal Zone forsteritic olivine almost invariably represents primary precipitate material and when orthopyroxene is also present, as in peridotite layers, it poikilitically encloses olivine indicating an interprecipitate origin. In pyroxenites of the Basal and Critical Zones orthopyroxene, in contrast, is cumulus in nature. In the upper Main Zone orthopyroxene encloses grains of clinopyroxene and even an orthopyroxene which contains exsolved clinopyroxene indicating original pigeonite.

Textures involving pyroxene and plagioclase dominate rocks above the Basal Zone. Two important textural types useful as horizon

markers are mottled anorthosite and porphyritic (Willemse, 1969) norite (= spotted norite, Liebenberg, 1970; Fig. 2B in this work). Mottled anorthosite, an important rock type in the Merensky Suite, is a plagioclase cumulate with dark coloured intercumulus clinopyroxene blotches 1 cm or more in diameter, giving a mottled appearance in a light coloured plagioclase background. Porphyritic or spotted norite forms the hanging wall and footwall rock of the Merensky pyroxenite. It is made up of distinctive clots of pyroxene less than 1 cm in diameter in a light coloured plagioclase matrix. Thus, the textural character of the ferromagnesian minerals depends very much on their relative volume with respect to the other mineral phases of the rocks.

Many of the textural relationships indicate that after accumulation of primary precipitate crystals, considerable interaction took place between these minerals and the interprecipitate liquid during the process of consolidation and compaction.

## 2.4. Chemical Studies of the Bushveld Complex Rocks

The most comprehensive study of the chemical composition of the rocks of the Bushveld Igneous Complex has been done by C.J. Liebenberg (1960, 1961) and L. Liebenberg (1970). As expected, general consistency prevails between chemical and mineralogical trends.

The averages of analyses from each zone were plotted on a Mg-(Fe+Mn)-(Na+K) diagram by Wager and Brown (1967, Fig. 217) and a Mg-($Fe^{2+}$+$Fe^{3+}$)-(K+Na) diagram by C. J. Liebenberg (Willemse, 1969). These plots suggest iron enrichment relative to magnesium, and feldspar enrichment relative to mafic minerals, upward in the Layered Sequence. On the appearance of plagioclase in the Critical Zone there is a sudden increase in the alkali content, although increasing alkali content does not continue to th[redacted] of the Layered Sequence. Through the Main Zone and a great part of the Upper Zone, the main trend of the overall differentiation is towards enrichment in iron. In the late Bushveld granites and related rocks, the alkalies are noticeably in excess of the femic constituents. A relatively high iron content is a general characteristic of the pegmatoidal rocks which are found in the Layered Sequence.

The variation of S, Ni and Cu at different stratigraphic horizons was studied by L. Liebenberg (1970). This work clearly illustrates the effect of differentiation on these elements.

The average S content of ultramafic and mafic rocks of the Basal Zone is about 200 ppm and 100 ppm respectively. The late hypabyssal norites at or near the contact with the main plutonic rocks of the Complex, and the ultramafic rocks in the Western Transvaal, which contain disseminated sulphides, have values very much higher than their unmineralized equivalents in the Eastern Transvaal.

The pertinent part of Liebenberg's diagram has been redrawn here as Fig. 4. The S content gradually decreases from the lowest exposed member of the Complex (900 ppm) to the upper part of the Critical Zone (30 ppm). A sudden increase occurs in the rocks of the Merensky Reef (mineralized pyroxenite + pegmatoid, 4850 ppm; unmineralized, 1460 ppm). The greater part of the Main Zone has values below 50 ppm. In the uppermost pyroxenite layer of the Main Zone the S content increases rapidly to 300 ppm. The maximum value in the normal layered rocks of the Complex occurs in the mineralized anorthosite below the Main Magnetitite Seam. A gradual decrease is again noted in the Upper Zone and below the uppermost magnetitite where a repetition of the conditions below the Main Magnetitite Seam appears.

In comparison with the Critical and the Main Zones, the Upper Zone is quite S-rich (average of 350 ppm). The most striking phenomenon in the variation curve for S is the repeated decreases in the Critical, Main and Upper Zones, which are followed by abrupt increases at the top of each of the zones respectively.

The Ni content of the mafic and the ultramafic rocks of the Complex is 100 and 700 ppm respectively and is lower than the terrestrial average for these rock types as compiled by Liebenberg and the

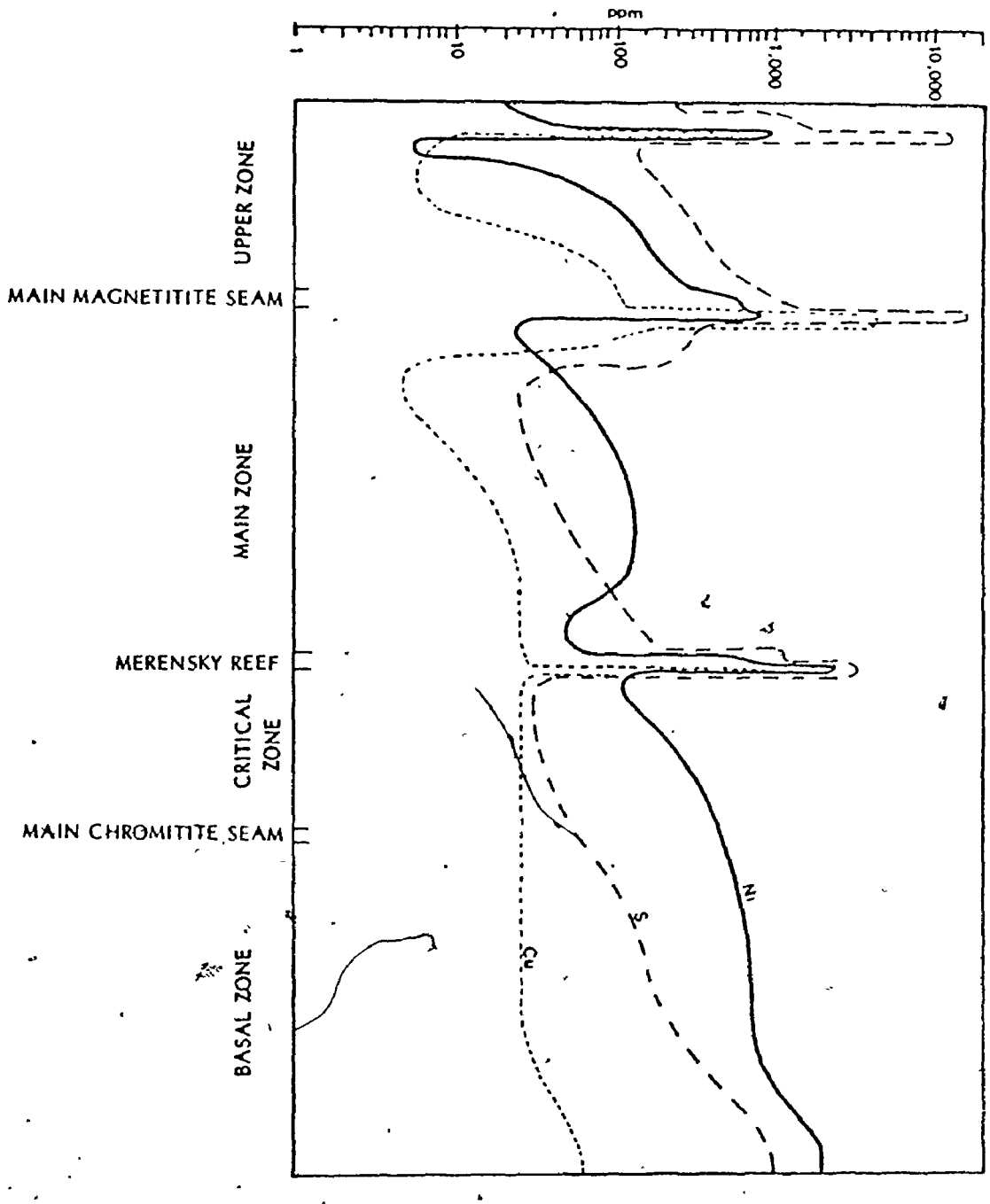


Fig. 4 VARIATION OF Ni, Cu AND S ON DIFFERENT STRATIGRAPHICAL HORIZONS IN THE BUSHVELD COMPLEX (after Liebenberg, 1970)

present writer (see Table 1 below). Nickel shows a gradual decrease from ultramafic rocks to the rocks of the Upper Zone. Nickel is much more enriched in the forsterite dunite (1,423 ppm) than in the hortonolite dunite (400 ppm) of the pipes in the Critical Zone. The capturing of Ni by Fe is clearly illustrated by the high Ni content (600 ppm) of the magnetitites and magnetite gabbros of the Upper Zone. Otherwise, owing to the chalcophile properties of Ni, this element varies sympathetically with S.

The average content of Cu in the ultramafic and mafic rocks is 35 and 25 ppm respectively. These values are lower than the average value for the corresponding rock types (Table 1). Norite interlayered with pyroxenite has generally a lower Cu content than the pyroxenite. The harzburgites at the base of the Complex have higher Cu contents than the pyroxenites higher up. Hortonolite dunite is enriched in Cu compared with forsterite dunite. A sudden increase occurs in the mineralized pyroxenite and pegmatoid in the Merensky Reef (876 ppm) and the mineralized anorthosite in the Main Zone (3,805 ppm). In the Fe-rich rocks of the Upper Zone, the magnetitites including those at the bottom and top of the Main Seam show lower Cu contents than mineralized anorthosite in the same zone.

Table 1. The S, Cr, Ni and Cu Contents of Bushveld Complex Rocks in Comparison with the World's Average for Mafic and Ultramafic Rocks

| | Average Ultramafic | | | ppm Mafic | | | | | |
|---|---|---|---|---|---|---|---|---|---|
| | 1 | 2 | 3 | 4 | 5 | 6 | 7 | 8 | 9 |
| S | 300 | 100 | - | 300 | 300 | 150 | 200 | - | - |
| Cr | 1600 | 2000 | 2400 | 170 | 200 | - | - | 140 | 980 |
| Ni | 2000 | 2000 | ~1500 | 130 | 160 | 150 | 700 | 75 | 435 |
| Cu | 10 | 20 | ~ 30 | 87 | 100 | 30 | 35 | 100 | 6 |

1+4 Turekian and Wedepohl (1961)

2+5 Vinogradov (1962)

3 Wyllie (1967, p. 354)

6 Average Bushveld magma after L. Liebenberg (1970)

7 Ultramafic rocks of Bushveld Complex after L. Liebenberg (ibid.)

8 Basaltic rocks after Hess and Poldervaart (1968)

9 Cumulus bronzite from the Merensky Reef after Atkins (1969)

With regard to the trace elements in pyroxenes of the Bushveld Complex, the work done by Atkins (1969) indicates that Cr decreases rapidly in both series of pyroxenes, and is approximately twice as abundant in augites compared with bronzites. Nickel decreases progressively with fractionation in both pyroxene series, the amount being greater in the Ca-poor pyroxene of a coexisting pair. Copper is usually present in low concentrations. Some Ca-rich pyroxenes, however, contain appreciable Cu, suggesting that the distribution of Cu is very irregular, if this element is present in the pyroxene structure. Alternatively, Cu may have been present as an immiscible sulphide intimately associated with pyroxene on a submicroscopic scale.

## 2.5. General Geology of the Merensky Reef

Generalized profiles across the Merensky Suite representative of the Western and Eastern Transvaal (after L. Liebenberg, 1970) are shown in Fig. 2B. In the past the feldspathic pyroxenite has generally been called the Merensky Reef. Currently, the Merensky Reef is defined as a norite, a pyroxenite or an olivine-bearing pegmatoid layer, occurring at the base of a feldspathic pyroxenite in the Rustenburg and Schilpadnest areas in the Western Transvaal and at the top of a

feldspathic pyroxenite in the Eastern Transvaal (Fig. 2B). The Merensky Reef dips inwards at angles of $5^{o}$ and $30^{o}$. The dip and strike remain uniform over long distances. The dip in the Rustenburg district averages $9.5^{o}$-$10^{o}$ N. At the Union Mine in the Northam area it is $23^{o}$ SE and in the northern Lydenburg district, about $25^{o}$ W (Newman, 1973).

The Merensky Suite constitutes the following rocks, in ascending order:

1. the footwall spotted and/or mottled anorthosite and/or norite.

The rocks are plagioclase cumulates in which pyroxene has an intercumulus relationship, except in the norites in which the pyroxene is also a cumulate. When the pyroxene crystals or clusters of pyroxene crystals are less than 1 cm in diameter, the adjective "spotted" is applied and when they are more than 1 cm, the adjective "mottled" is used (L. Liebenberg, 1970).

2. a thin layer of pure anorthosite which is almost barren of pyroxene.

In places this anorthosite contains isolated specks of sulphides which are interstitial to the feldspars. The thickness does not exceed one inch and the layer is absent in places.

3. the chromitite seams (usually not more than 2 inches thick)

These are developed at different horizons in the pyroxenite and are mostly restricted to horizons above/or below the pegmatoid. A chromite seam characteristically occurs at the contact of the feldspathic pyroxenite and anorthosite units.

4. the feldspathic pyroxenite

This unit contains the platinum metal values and averages 3 to 10 feet in thickness. It is characterized by a pegmatitic facies of the same composition averaging 1 to 3 feet. In the Eastern Transvaal this pegmatoid occurs near or at the top of the pyroxenite. More than one layer of pegmatoid is developed in some localities, e.g. three are observed in the Lydenburg District. In the Western Transvaal, the pegmatoid generally occurs at the base of the feldspathic pyroxenite. While the correlation of platinoid values with the pegmatitic layer is definite in the Western belt, a lack of such correlation in the Eastern belt is equally definite. However, in both belts, the platinoid values occur in the rock between the thin chromitite seams.

5. hanging-wall spotted norite or anorthosite which varies from 5 to 10 feet in thickness.

6. spotted norite or mottled anorthosite, 30-50 feet thick.

Immediately succeeding the mottled anorthosite is a second feldspathic pyroxenite approximately 12 feet in thickness known as the Bastard Reef. Disseminated sulphide with accompanying low platinum values usually occurs near the top or the base of the Bastard Reef. A chromitite seam at the base of this unit is also developed in some localities such as the Schilpadnest area. The Bastard Reef is, therefore, a repetition of the Merensky Reef with less intense mineralization. Although the hanging-wall succession of the Merensky Reef is uniform in both Eastern and Western belts, the footwall section shows marked thickness variations from one area to others.

Two major breaks in the continuity of the Merensky Reef are found. One is in the Western belt, north of the Pilanesberg, and is due to faulting while the second occurs in the Eastern belt by abutment against previously up-fold Pretoria sediments of the Transvaal System.

Local structures disturb the regularity of the plane of the Reef over limited areas. Two main types of structure known as "potholes" and "koppies" are present. A "pothole" is a local, basin-shaped depression generally circular to elliptical in shape. A "koppie" is a local, domed structure. These structures occur outside the

Merensky Suite as well. Reef containing these structures is still a pegmatitic pyroxenite and carries platinoid values with disseminated sulphides, similar to undisturbed Reef. Schmidt (1952), supported later by Ferguson and Botha (1964), suggested that potholes were the result of rotating eddies in the magma chamber.

## 2.6. Mineralogy of the Merensky Reef

The silicate minerals in the Merensky Suite have been studied by Wagner (1929), Lombaard (1934), Schmidt (1952), van Zyl (1970), and Ferguson and Wright (1970), among others. The results of these studies are summarized below.

1. The Footwall Spotted Anorthosite

This rock consists largely of idiomorphic bytownite (An 72-80). The spotted appearance is due to anhedral orthopyroxene (Fs 18-33) sparsely scattered between the plagioclase. Also present are isolated ragged grains of diallage (diopside with prominent parting along {100}) which are moulded on the orthopyroxene. The average volumetric mineral composition in the Rustenburg district is: plagioclase 84%, orthopyroxene 14%, clinopyroxene 2% and accessory biotite and magnetite less than 1% (van Zyl, 1970).

2. The Chromitite Seams

The chromitite seam consists of chromite grains poikilitically included in plagioclase, orthopyroxene and diallage in approximately equal proportions. Sulphide grains are always present. The chromite grains vary from octahedral crystals to embayed masses, the former being smaller than the embayed chromite. The base of the chromitite band is sharply defined against the anorthosite whereas the top is rather irregular with chromite grains being scattered in the overlying coarse feldspathic pyroxenite. van Zyl (1970) observed that the chromite occurs in four different ways: 1) as small euhedral crystals in the orthopyroxene, 2) as bigger euhedral to subhedral crystals in the margins of the orthopyroxene, indicating simultaneous crystallization with the orthopyroxene, 3) as enclosed crystals in the interstitial plagioclase, and 4) as large chromite crystals which are interstitial to the orthopyroxene and associated with hematite, ilmenite and magnetite.

3. The Feldspathic Pyroxenite

This rock is composed mainly of orthopyroxene (Fs 14-18) and plagioclase (An 70-76) with subordinate clinopyroxene. The average mode at Rustenburg is: plagioclase 14%, orthopyroxene 83%, clinopyroxene 2% and accessory biotite, phlogopite, chromite,

magnetite and sulphide 1%. Biotite, chromite, sulphides and quartz make up the minor constituents. Hornblende is very rare. Schmidt (1952) stated that no evidence could be found to support Wagner's statement (1929, p. 105) that magmatic hornblende is always present and locally abundant, particularly as a shell surrounding diallage. Orthopyroxenes are euhedral to subhedral and poikilitically enclosed in feldspar and diallage. The diallage is also interstitial to the orthopyroxene and forms occasional large anhedral to subhedral crystals up to several centimeters in diameter sparsely distributed throughout the rock. The texture resembles that of a porphyritic rock and the name pseudoporphyritic pyroxenitic diallage-norite was proposed by Wagner. The plagioclase tends to become subhedral to euhedral upwards from the base of the unit, until the orthopyroxenes are interstitial to the plagioclase in the overlying spotted anorthosite.

The order of crystallization is: orthopyroxene, diallage and plagioclase. In some cases diallage has been found to surround crystals of plagioclase completely. The periods of crystallization of diallage and plagioclase seem, therefore, to have overlapped. Where chromite grains are found in the feldspathic pyroxenite, they appear to have crystallized after the orthopyroxene but before the feldspar. The sulphides, biotite and quartz are the last minerals to crystallize and

belong to the same period of crystallization according to Schmidt (1952). van Zyl (1970) stated that the sulphides are interstitial to the silicates and were the last minerals to crystallize. Sulphide-silicate relationships in the samples examined in this study were found to be more variable (see Chapter IV).

4. The Pegmatitic Reef Facies*

The minerals forming the pegmatoidal pyroxenite of the Merensky Reef are: orthopyroxene, clinopyroxene, plagioclase, other silicates, sulphides, chromite and platinoid minerals.

Orthopyroxene is mostly subhedral to anhedral and varies considerably in size. The iron content of orthopyroxenes increases from 12% FeO (bronzite) at the base of the Reef to 21% at the top (hypersthene) (Schmidt, 1952). No zoning of crystals is reported.

Clinopyroxene is a subordinate mineral which occurs as large anhedral to subhedral crystals enclosing orthopyroxene and occasionally plagioclase. Clinopyroxene has replaced orthopyroxene as a result of reaction of orthopyroxene with the magma. The mineral has the optical properties of augite, although it is usually referred to as diallage.

* This is coarse grain facies of feldspathic pyroxenite.

Plagioclase is interstitial to pyroxene and olivine. It is sericitized and kaolinised, in part, and sometimes metasomatically replaced by sulphides. The anorthite content varies from An 82-86 at the base of the Reef to An 58-62, 42 inches above the base in the Rustenburg Platinum Mine (Schmidt, 1952). Most of the grains show strain shadows, but no zoning is reported.

Accessory silicates include biotite, quartz and olivine (Cousins, 1969; van Zyl, 1970). According to Wagner (1929, p. 105) both biotite and hornblende are reaction minerals but according to Schmidt (1952), both are primary minerals representing end-stage crystallization products of a magmatic residuum. Olivine occurs as an accessory mineral in the pegmatitic pyroxenite.

The sulphides consist mainly of intergrowths of pyrrhotite, pentlandite, chalcopyrite and pyrite, in order of abundance, and occur as small interstitial grains moulded on plagioclase. They are also found included in plagioclase and diallage, and have been seen to penetrate pyroxene, hornblende and biotite along fractures and cleavage planes. The sulphides are uniformly distributed throughout the rock making up about 1-2 percent (Schmidt, 1952), although in the Lonrho sampl a more complex distribution of sulphide is found. According

to L. Liebenberg (1970) the composition of sulphides is fairly constant from locality to locality although pyrite is absent and cubanite is present at certain localities, e.g. Dwars River area and north-west of Potgietersrus.

According to Zermatten (personal communication to Cousins, 1969) the primary mineral was probably nickeliferous pyrrhotite, which subsequently exsolved pentlandite and nickeliferous pyrite. Chalcopyrite shows considerable secondary redistribution. The sulphides are principally concentrated in the platinoid bearing portion of the pyroxenite in the pegmatitic layer of the Western Belt and in proximity to the chromite bands in the Eastern belt. Detailed sampling across the Reef at the Rustenburg Platinum Mine indicates that peak platinoid values normally occur in the Basal chromite band and that the peak sulphide values occur immediately above it. Redistribution of the sulphides causes some modification of this pattern.

Chromite is present, both as an accessory mineral in the pyroxenite, and concentrated into one or more thin seams at specific positions in the Reef. According to Cousins (1969) the chromite of the Reef has the following composition: $Cr_2O_3$-40.5%, FeO-32.6%, $Al_2O_3$-15.2%, MgO-9.7%, $TiO_2$-2.0%, Cr/Fe=1.1. Reef chromite

includes a small percentage of a magnetic variety having the composition: $Cr_2O_3$-37.2%, FeO-42.0%, $Al_2O_3$-9.8%, MgO-8.2%, $TiO_2$-2.8%, Cr/Fe=0.8. L. Liebenberg (1970) mentioned that two generations of chromite are present: firstly, roundish or euhedral grains which were the first to crystallize and, secondly, euhedral grains which crystallized more or less simultaneously with the sulphides. Rutile is also reported in the ores from Rustenburg and from Potgietersrus. According to van Zyl (1970) the textural relationship of the minerals indicate that the chromite crystallized later than the olivine, pyroxene, and plagioclase. This means that the chromite must be either a late crystallization product, or it has been introduced from a foreign source. This conclusion is at variance with Wager and Brown's (1967) who regard the chromite exclusively as a cumulus phase.

Platinoid minerals listed by Cousins (1969) as present in the Reef and confirmed by X-ray diffraction include: braggite, (Pt, Pd, Ni)S; ferro-platinum; sperrylite, $PtAs_2$; laurite, (Ru, Os, Ir)$S_2$; and various rare platinoid minerals such as the bismuth-tellurides of platinum and palladium; platinum telluride, $PtTe_2$; and cooperite, $BiPd_3$. Gold, alloyed with silver, copper, and up to 12% Zn, is also present. The different minerals containing the platinum group metals (PGM) are not homogeneously distributed along the strike of the Merensky Reef. In the Rustenburg area braggite is the main mineral which contains the PGM

(excluding perhaps the platinum alloys) with subordinate sperrylite and cooperite. L. Liebenberg (1970) noted that where platinum metal minerals are present in relatively large amounts, the Merensky Reef is in contact with or near sedimentary rocks, e.g. the Lydenburg district.

The greatest concentration of platinum metal minerals occurs in a mineralized skarn at Potgietersrus. Usually the minerals containing the PGM are in association with chalcopyrite. The coarse feldspathic pyroxenite in the Potgietersrus Platinum Field is the richest in PGM in the Bushveld and often assays above 7 cwts/ton (= 12 ppm). Some aspects of the geochemistry of the platinum group metals are discussed in Chapter V.

5. The Hanging Wall Spotted Norite

In passing from the Merensky Reef to the spotted anorthosite, plagioclase becomes more idiomorphic and orthopyroxene gradually develops an interstitial character. In addition, the diallage becomes more evenly distributed through the rock. The plagioclase is more basic than in the top part of the Reef (An 74-82). Orthopyroxene composition does not show a sympathetic variation.

## 2.7. Genesis of Bushveld Rocks with Particular Emphasis on the Merensky Reef

The origin of the Merensky Reef and the relationship of the mineralized pegmatoid to the associated rock types has repeatedly been debated amongst geologists working on the Bushveld Complex, but a complete explanation incorporating all the facts is not yet available. Willemse (1964) and Wager and Brown (1968, pp. 344-5) summarized the existing hypotheses on the genesis of the Complex and the Merensky Reef.

One school of thought, to which especially Wagner (1929, pp. 43-47), Hall (1932, pp. 278-283) and Lombaard (1934) belong, considers that two processes operated to produce the diversity of rocks. Firstly, differentiation at great depth produced magmas differing in composition. These were emplaced intermittently and then gravitative crystal-settling in situ took place, producing pyroxenite, anorthosite and chromitite, etc. The most popular alternative hypothesis for explaining local irregularities is that of multiple injections of contrasting magmas with similar bulk compositions to the individual layers (Truter, 1955; Coertz, 1958, etc.). According to this hypothesis the effect of differentiation in situ by crystal-settling was entirely subordinate.

The theory of differentiation at great depth to produce magmas differing in composition has been criticized from various viewpoints. After considering the difficulties involved in this postulate of differentiation in depth, Hess (1960) concluded that it is more reasonable to explain the changes in composition of the main crystalline phases and the changes of the phases with stratigraphic height by fractional crystallization in situ of undifferentiated basaltic magma. Wager and Brown (1967, p. 345) also mentioned: "There seems little doubt, from all the evidence now at our disposal, that the Bushveld basic rocks are the products of crystal accumulation from a basaltic magma".

Recent views favour the idea that the basic mass consists of four separate intrusions which developed simultaneously through crystallization in a group of interconnected magma chambers, e.g. Truter (1955) and Willemse (1964). According to Willemse (1964) transgressions of large magnitude suggest that the emplacement of magma took place in successive heaves. The effect of transgressions of large magnitude refers to the overlap of zonal component of one zone by the layers of the stratigraphically higher zone, as for example, transgression of the main plutonic phase by the Upper Zone near Northam. Compelling evidence to prove that influx of magma of highly variable composition during formation of the Layered Sequence is still problematic.

According to L. Liebenberg (1970) field relationships indicate that the main plutonic phase of the Bushveld clearly involved intrusion of at least two separate surges of magma. Convection-currents and gravity-settling of minerals took place and gave rise to the phase-layering in the Complex. Variation in the S content of the magma was responsible for the concentration of sulphides in the Layered Sequence. Most of the disseminated sulphide in the Bushveld Complex crystallized from an immiscible sulphide liquid trapped in the inter-cumulus pores. During crystallization of the Critical Zone the S content in the magma was relatively low and consequently mainly chalcopyrite was formed. Not enough Cu was present to remove all the S and its concentration therefore gradually increased. Immediately after the second magma surge, a copper-nickeliferous immiscible liquid formed during deposition of the Merensky Reef. During the crystallization of the Main Zone conditions were the same as in the Critical Zone, except that the oxidation potential of the magma during the crystallization of the upper part of the Main Zone was relatively high.

From petrographic data on the Merensky Suite in the Rustenburg district, van Zyl (1970) concluded that the rhythmic layering could best be explained by different heaves of homogeneous magma emplaced periodically from which fractional crystallization and gravi-

tative differentiation took place. According to van Zyl the norite-anorthosite unit may be subdivided into four sub-units: Basal, Pseudo-reef, Merensky Reef and Bastard Reef. His conclusions are supported by the following observations: 1) an almost perfect repetition of rock sequences in the various sub-units, 2) a regular decrease of ortho-pyroxene from the bottom to the top in each sub-unit, 3) a regular increase in the Fs content of the orthopyroxene from the bottom upwards in each sub-unit due to fractional crystallization and gravitational differentiation in situ, 4) almost identical Fs content of the orthopyroxene in the upper and lower portions of the different sub-units, 5) a regular decrease in the An content of the plagioclase from the bottom upwards in each sub-unit, and 6) the identical composition of the plagioclase in the basal portions of the different sub-units. The sharp contacts between the sub-units of the norite-anorthosite unit indicate that the lapse of time between the emplacement of the successive heaves of magma was probably long enough for each heave to crystallize almost completely before the next heave was emplaced. Atkins (1969) also noted the reversal of iron content in pyroxenes from the Merensky Reef horizon and those occurring some 370 m lower in the Critical Zone and concluded that this reversal was probably due to the fresh influx of undifferentiated magma which produced the platinoid and sulphide minerals of the Merensky Reef.

According to Wager (1968, p. 620) in the Critical Zone olivine is present in some layers and absent in others, especially in the Western Busvheld. This behaviour may well prove to be due to a succession of influxes of new magma other than that at the Merensky Reef horizon.

However, the coarseness of the pegmatitic reef and the presence of chromitite bands along its upper and lower contacts are problems still to be solved.

# CHAPTER III

# EXPERIMENTAL METHOD

## 3.1. Description and Location of the Samples

The diamond drill core was kindly provided by the Western Platinum Company from its Lonrho property operations on the Merensky Reef about 25 miles east of Rustenburg. Here the Merensky Suite shows a variation in width from 11.5 to 21.5 feet and dips at $1.0^{\circ}$ to the north (Newman, 1973). The thickness of the Merensky Reef proper (i.e. the pegmatitic facies of the pyroxenite) is understood to average 36-40 inches (Chilton, 1971).

The core sample, 1.75" in diameter X 27" in length, included the thin chromitite seam near the top of the Reef known to be associated with the highest PGM values. The approximate location of the core in a stratigraphic sense within the Reef is shown in Fig. 5. The core was first sawn in half lengthwise. One of the half-core pieces was sawn into 25 sections of approximately one inch length perpendicular to the core axis. A 1/8" slice was then taken from the flat face of each one-inch sample for preparation of a thin section.

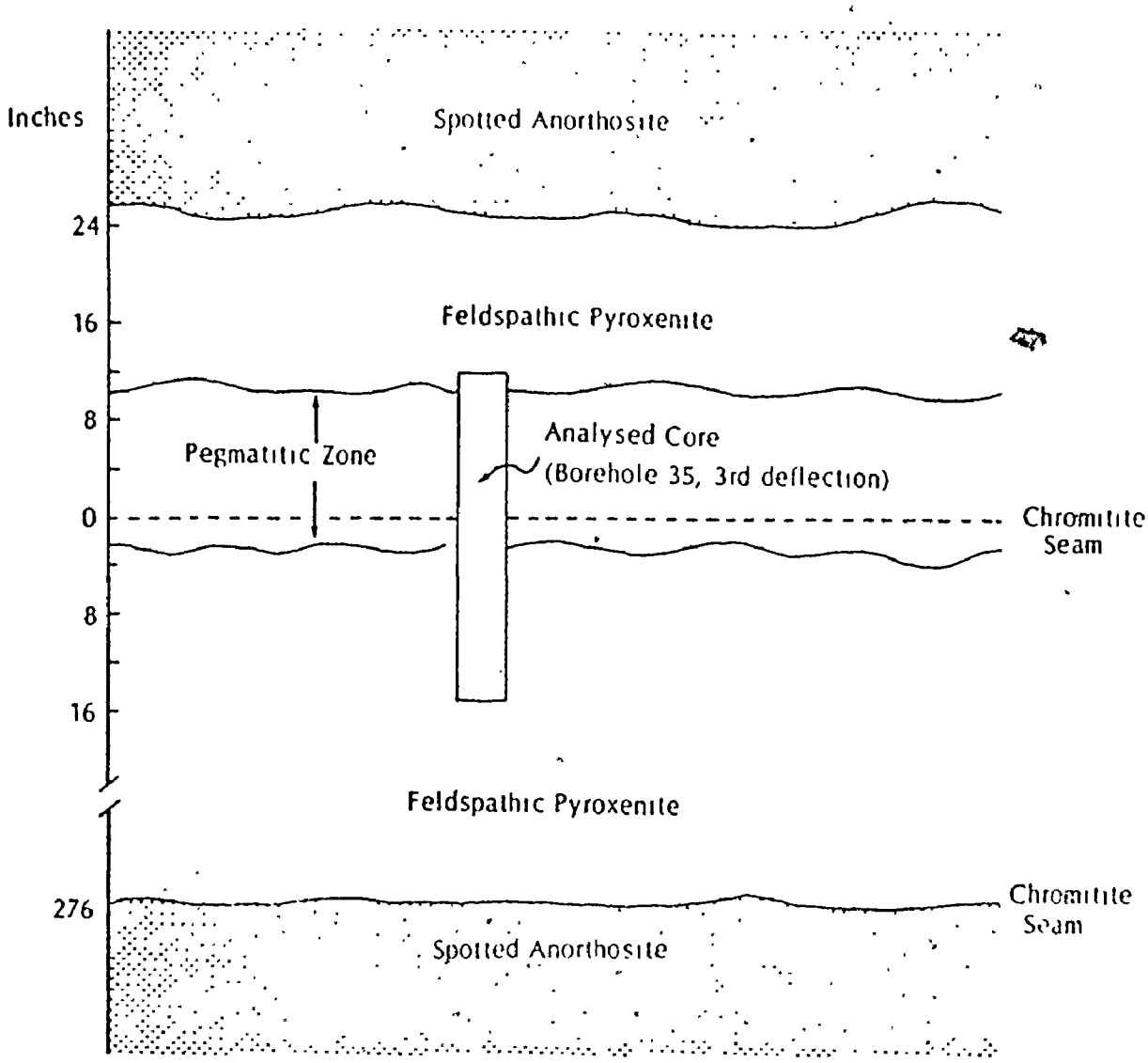


Fig. 5 LOCATION OF ANALYSED DRILL CORE SAMPLE, LONRHO MINE

The remainder was crushed and powdered for chemical analysis. Samples for chemical analysis were ground to pass 100 mesh. Polished sections were prepared from the uncut, half-core piece.

3.2. Sample Preparation of Separated Grains

Sulphide grains were sampled from the polished sections by microdrilling. Most analyses were carried out on single grain aggregates. However, if a sulphide grain was too small to yield a sample of c.a. 10 mg, several grains were combined if they had approximately the same mineral proportions (Separate Grain No. 7-2, 15-1, 17-2, 20-1, 20-2 and 20-3 in Table 11).

Oxide grains were separated by the following methods. From thin section observation, the samples rich in oxides, No. 1, 4, 7, 10 and 13 were chosen for mineral separation. The strongly magnetic portion of the 100-200 mesh size fraction was removed with a hand magnet. The powder was then run through a Franz magnetic separator at $10^{\circ}$ forward inclination and $20^{\circ}$-$30^{\circ}$ tilt at 0.1-0.2 amperes. About 70% chrome spinel concentrate was collected on the magnetic side after repeating this procedure several times. This concentrate was then run through at the same forward inclination, but a tilt $2.5^{\circ}$ or less and a current of 0.05 amperes or less. This procedure separated chrome spinel from other contaminants, mainly

pyroxene and plagioclase, which collected at the non-magnetic side. The procedure was repeated several times until maximum purity, as judged visually, was obtained.

The final mineral separates were always contaminated with talc and composite grains. These were removed as far as possible by hand picking under a binocular microscope. In some samples composite pyroxene-chromite grains consisting of inclusions of chrome spinel in pyroxene could not be effectively separated from pure pyroxene. A representative portion of such composite grains was counted under a binocular microscope to estimate the purity of such samples. Samples No. 7 and 10 which were of this type could only be purified to 50% even with many passes through the Frantz. These samples (No. 1-4, 4-4, 7-1, 7-2a, 2b, 10-1, 10-2 and 13-4 in Table 12) are called composite grains.

3.3. X-ray Powder Diffraction of Whole Rock Samples

The X-ray powder diffraction spectra of each whole rock core sample and twenty one samples of oxide concentrates and composite grains from samples, No. 1, 4, 7, 10 and 13 were taken with a Toshiba X-ray Diffractometer.

In the case of oxides and composite grains, the small amount of the sample available (20-80 mg) required use of the following method. Grains were first mixed with analytical grade acetone in an agate mortar, ground slightly with a pestle and coated on a thin glass slide with a small pipette. Using this technique, mineral orientations of samples were not completely random. Therefore, the intensities of the resulting spectra may not be exactly the same as those recorded in the literature. In order to minimize this weakness in the procedure, at least two spectra of the same sample were taken. The instrumental settings used for the experiments were as follows: Time constant 2 second, Counts per second 200, X-ray tube current 22 mA, X-ray tube voltage 35 KV, Cu-K$\alpha_1$, $\alpha_1$ = 1.54050 Å, Ni Filter, Scan range, $2\theta = 5\text{--}120^\circ$.

For calibration the spectrum of fused powdered silicon (Fisher Scientific Co. S-164, 78122, lot 724745) was taken and used for the construction of a curve of $2\theta_{\alpha_2} - 2\theta_{\alpha_1}$ versus $2\theta_{\alpha_1}$ (where $\alpha_1$ = very strong, $L_{III} \rightarrow K$ and where $\alpha_2$ = strong, $L_{II} \rightarrow K$ of Cu-$K_\alpha$) to check for diffraction by $K_{\alpha_2}$ which may cause incorrect interpretation of spectra.

The interpretation of spectra was based on literature values found in the following references: 1) Calculated X-ray Powder Patterns for Silicate Minerals (1969), 2) X-ray Powder Data for Ore Minerals (1962), 3) The X-ray Identification and Crystal Structures of Clay Minerals (1961), 4) Inorganic Index to the Powder Diffraction File (1967), 5) Powder Diffraction File, Search Manual, Minerals (1974) and 6) Selected Powder Diffraction Data for Minerals (1974).

## 3.4. Chemical Analyses

### 3.4.1. Determination of Total S Content in Whole Rock Sample

A flow chart of the analytical procedures is presented in Appendix I. Although the gravimetric determination of sulphur as barium sulphate is considered the most accurate method for determining sulphate concentrations greater than 10 mg/l (Heinrich et al., 1961), the barium sulphate precipitate is almost always contaminated through co-precipitation phenomena. Numerous papers have been written on the problem of obtaining a pure precipitate of barium sulphate (Vogel, 1961, p. 462; Willard et al., 1956, pp. 328-332 and 358-360), but its determination remains one of the least accurate in quantitative analysis (Heinrich et al., 1961, p. 59). The excellent agreement often observed between theoretical and experimental results is due in considerable measure to a cancellation of errors (Skoog et al., 1966, p. 203). In

order to minimize experimental errors in the present determinations, the optimum conditions known for each step were followed with caution. As the final precipitates of barium sulphate were white, they were not contaminated by barium chromate. The experimental errors are considered to be less than 0.1 percent of the total sulphur found from the experiences of the present author.

3.4.2. Determination of Cr, Ni and Cu Contents in Whole Rock Samples by Atomic Absorption Analyses

The experimental procedures for the atomic absorption methods are given in Appendix I.. Satisfactory, completely oxidised, fusions were confirmed for all samples by the presence of a diagnostic green colour of the melts when cooled. Despite extensive leaching of the melts, the observation of residue under a binocular microscope indicated that there were traces of unattacked brownish black material in samples, 9, 11, 16, 20 and 21. According to Jeffery (1974, p. 193) this loss of chromium, generally found to be of the order of 1 percent, was demonstrated for a sample of fuchsite from Nakilor, Uganda, containing 1.57 percent total chromium. The errors due to this step for chromium, therefore, are estimated as 1 percent of the concentration of Cr.

All reagents used were certified reagent chemicals. The standard solutions were prepared from the Johnson Matthey "Specpure" (Regd) $Cr_2O_3$ (J.M. 705), NiO (J.M. 895) and CuO (J.M. 40). The concentrations of the standard solutions were as follows:

| Cr | Ni | Cu | in ppm |
|---|---|---|---|
| 12.0 | 4.91 | 2.06 | |
| 60.0 | 11.6 | 5.15 | |
| 74.9 | 18.6 | 8.20 | |
| 150.0 | 39.6 | 22.0 | |

The blank solutions were prepared in the same way as the standards and samples. Furthermore, to test the validity of the experimental method, duplicate analyses of the U.S. Geological Survey Standards, W-1 and DTS-1 were conducted.

The results obtained for the above rocks were checked against published values in the literature (Flanagan, 1969; Fleischer, 1969) and they were within the range of the accepted values.

An atomic absorption spectrophotometer (Perkin-Elmer Model 303) was used with a recorder and model PR4 printer. All instrumental settings were as recommended in the Perkin-Elmer Analytical Methods Book (1973).

Sensitivity is defined as the concentration of metal in solution that gives a 1% absorption signal for the instrumental conditions designated in the above book. Sensitivity for Cr, Ni and Cu are as follows:

| Cr | Ni | Cu |
|---|---|---|
| 0.1 | 0.15 | 0.09 in μg/ml |

The concentrations of metals in samples were obtained from calibration curves constructed from sets of standard solutions. Readings of absorbance were recorded at least three times for each sample and standard, and their average value used for the determination of concentration of the element. The estimated errors in the metal concentrations due to the present experimental procedure (including instrumental fluctuation) are 5% for Cr, and 2% for Ni and Cu. The values of Cr concentration may be lower than actual ones in the samples, comparing only one value of the standard rock DTS-1 with that in literature, although no acceptable Cr value of DTS-1 by atomic absorption is reported. With respect to contribution of oxides to total noble metal values in whole rock, this error is not significant.

### 3.4.3. Determination of Pt, Pd, Ir and Au Contents by Neutron Activation Analyses

a) Sample Preparation: Powdered samples of 200 to 250 mg for whole rock analyses, 3 to 20 mg for sulphide grains and 20 to 80 mg for the oxides and composite grains were accurately weighed into labelled quartz ampoules of 2 mm inside diameter and sealed with a gas-oxygen flame. Oxide and composite grains were powdered in an agate mortar to 200 mesh. This procedure is said to be necessary for fusion of chromium compounds (Hartford, 1963). However, excess grinding was avoided, as this causes contamination from the grinding procedure, oxidation, and the absorption of difficultly removed water. For the weighing of small quantities of sulphide grains, a Micro Gram-atic Mettler Model M-5, six place balance (precision ±0.001 mg), was used.

b) Standard Preparation: Standard solutions of Pt, Pd, Ir and Au were prepared from Johnson Matthey "Specpure" platinum sponge (J.M. 1010), palladium sponge (J.M. 940), gold sponge (J.M. 73) and ammonium chloroiridate (J.M.C. 995) respectively. Following the procedures of Crocket et al. (1968), gold, palladium and iridium were combined into a single solution in 2 M HCl while platinum was prepared separately. The final concentrations of the standard solution were

5.341 μgm/gm Au, 19.42 μgm/gm Pd, 0.4079 μgm/gm Ir, and 604.1 μgm/gm Pt. As some of the oxides and sulphide samples were low in gold content, a secondary standard solution was prepared from the original stock solutions of each metal. The final concentrations of the second standard solution were 0.6652 μgm/gm Au, 19.40 μgm/gm Pd, and 0.4095 μgm/gm Ir in 2 M HCl. All standard solutions were prepared entirely by weighing using a top loading Mettler Model P 1200 N balance.

c) Irradiation: To prepare standards for irradiation, the standard solutions were accurately weighed into quartz ampoules with a capillary glass pipette. After reweighing to obtain the weight of solution, about 50 mg of 100-200 mesh fused quartz powder was added to adsorb the solution. The ampoules were then put in a drying oven at $70^{\circ}$-$75^{\circ}$C overnight, and sealed with a gas-oxygen flame. Irradiation units consisted of 4 to 6 samples and 4 standards (2 containing Au, Pd, and Ir, and 2 containing Pt) packaged together in an aluminum radiation can. Arrangement of samples and standards was such that each sample was positioned adjacent to the same number of standards in order to minimize error due to flux variation during irradiation.

Samples and standards were irradiated in the McMaster Research Reactor at an average total flux of $2 \times 10^{13}$ n/cm$^2$/sec. The neutron flux varies with position in the reactor, thus the same reactor loading position (7D) was used for all irradiations. Whole rock samples were irradiated at 2 MW/hr (megawatt per hour) for 12 hrs. and cooled for 24 hrs., sulphide grains at 5 MW/hr. for 24 hrs. with cooling for 48 hrs. Oxides and composite grain samples were irradiated at 1.5 MW/hr for 4 days, cooled for 5 days, and then re-irradiated for 12 hrs. and finally cooled for 12-20 hrs. The second irradiation is required to induce sufficient 13.5 hr. $^{109}$Pd activity as that generated during the first irraidation is lost during the first 48 hr. cooling period. Depending on the Reactor's power condition the above irradiation schedule was adjusted to obtain the same total MW/hr for every set of samples.

As sensitivity is dependent upon induced activity, the nuclide with highest yield is the best for the element concerned. For this reason, $^{109}$Pd, $^{192}$Ir and $^{199}$Pt were used for the respective elements. Despite the somewhat higher yield of $^{194}$Ir, $^{192}$Ir is preferred because of the convenience of the 74 day half-life and its distinctive gamma spectrum. The pertinent nuclear reactions are:

26.7% $^{108}Pd(n,\gamma)$ 13.46 hr. $^{109}Pd$ ($\beta^-$ only)

37.3% $^{191}Ir(n,\gamma)$ 74.3 day $^{192}Ir$ ($\gamma$: 136, 320, 470 KeV)

7.21% $^{198}Pt(n,\gamma)$ 0.5 hr. $^{199}Pt \xrightarrow{\beta^-}$ 3.12 day $^{199}Au$ ($\gamma$: 158 KeV)

100% $^{197}Au(n,\gamma)$ 2.695 day $^{198}Au$ ($\gamma$: 412 KeV)

d) Chemical Procedures: Comprehensive analytical procedures for Pt, Pd, Ir and Au by neutron activation have been described by Crocket et al. (1968) and Keays (1968). The procedure used in this study employs selected parts of the above procedures with necessary modifications as required and it will only be presented in flow chart form (Fig. 6). The purification steps for Au and Pt are largely omitted because the application of high resolution gamma spectroscopy does not require the higher radiochemical purity. However, the following modifications were necessary partly because of sample composition and long irradiation time:

i) $Fe(OH)_3$ scavenging was required for purification of all Pd samples because of the long irradiation time.

ii) Complete precipitation of Pd-DMG was ensured by adding an excess of 1.5% of dimethylglyoxime solution at room temperature and allowing the solution to stand at least 1 hour (Vogel, 1961, p. 512).

iii) Due to the very refractory nature of spinels, the oxide and composite grain samples were subjected to higher fusion temperatures. The melting temperature of the NaOH-$Na_2O_2$ flux was increased by decreasing the proportion of NaOH used.

iv) High levels of $^{51}Cr$ activity were occasionally found in Ir from oxide and composite grain samples. To minimize this contamination the 6 M HCl solution of Ir obtained after the ion exchange step was made basic and scavenged by precipitation of $Fe(OH)_3$ - $Cr(OH)_2$. The repetition of this step was impractical because of the large volume of solution to be handled.

v) A difficulty often encountered in the practical chemistry complexes of Ir(IV) and Ir(III) is that oxidation of tri- to tetravalent or reduction of tetra- to trivalent iridium may very easily occur (Griffith, 1967, p. 229). Therefore, in the final reduction of Ir-chloride complex to Ir metal with zinc, 5-10 mls of $H_2O_2$ were added to the Ir(III) solution two or three times in order to obtain Ir(IV). Another difficulty is that iridium is never quantitatively precipitated by zinc (Walsh and Hausman, 1963, p. 422). Accordingly, the precipitation of Ir by Zn was repeated at least three times from boiling solution.

In order to avoid cross contamination of samples, zirconium fusion crucibles were gamma counted before and after each experiment. The crucibles were cleaned immediately after use by fusing $Na_2O_2$ in them. In general, the activities found were: a) 27.8 day $^{51}Cr$ activity in crucibles used for oxide analyses (300-400 cpm after 3 weeks), b) 85 day $^{46}Sc$ activity in crucibles used for whole rock analyses (very low levels). No activity remained in crucibles used for sulphide analyses.

## Fig.6 FLOW CHART FOR ANALYTICAL PROCEDURES

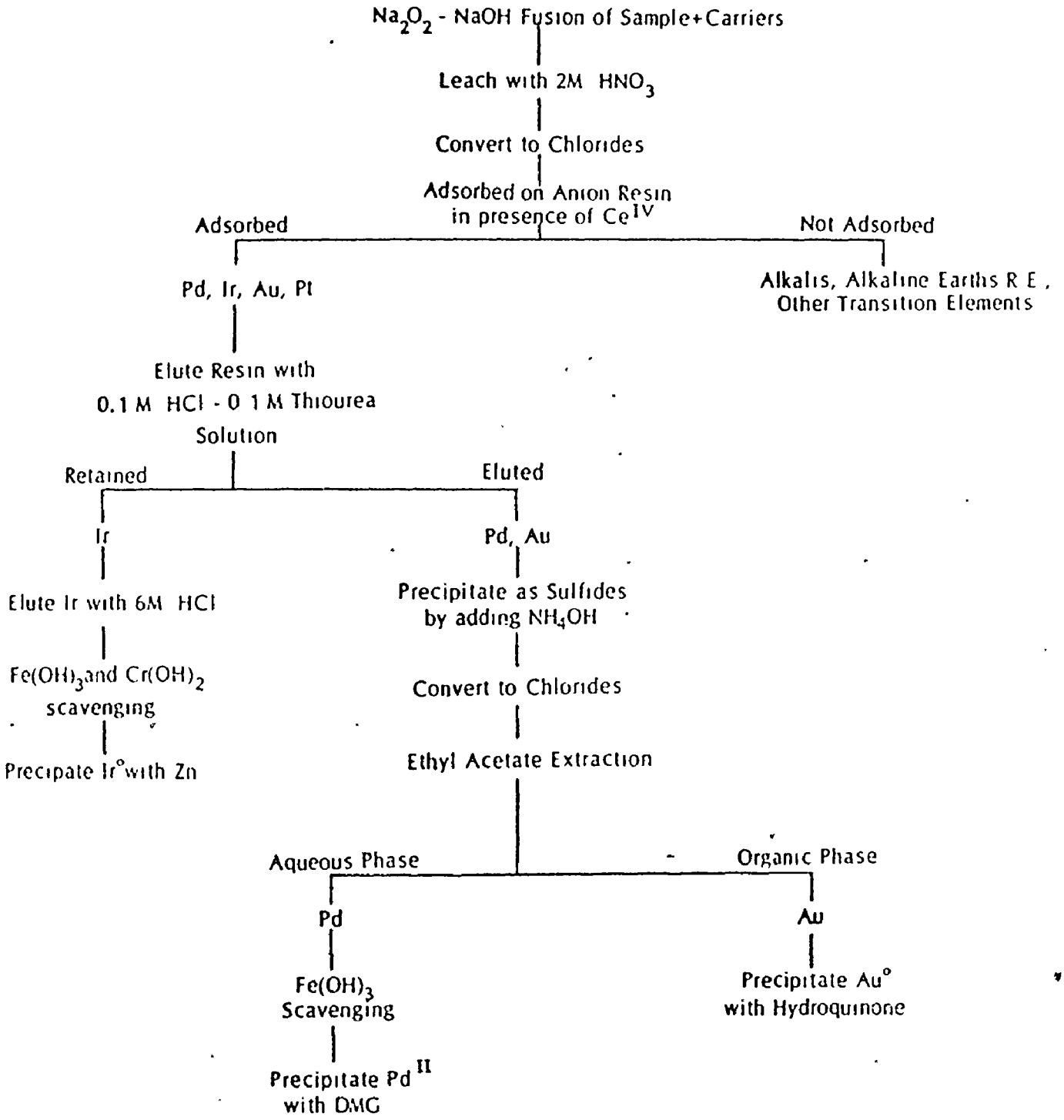


Anion Resin: Fisher Certified, Rexyn 201
$Cl^-$ form, 100 - 200 mesh

DMG : Dimethylglyoxime

e) Counting Procedures: For beta counting a Nuclear Chicago beta counter, consisting of a scaler-timer, an automatic sample changer and a gas flow Geiger-Mueller counting tube with coincidence shielding was used. The detector had an average background of 3.0 counts/min. Electronic drift in the counter was monitored by a uranium standard source. Dead time corrections were unnecessary for count rates up to 10,000 counts/min.

For gamma counting a Model 4410 Nuclear Data System employing a 50 MHz Analog-to-Digital Converter and an 8K Computer for data processing was employed. The effecting capacity of the system was 3000 channels after the various control programs were loaded into the memory. Output was to a TC33ASR teletype. The 8K computer was programmed to subtract backgrounds and integrate photopeak areas so that net photopeak counts could be obtained directly in the readout. The detector was a Canberra coaxial Ge(Li) crystal of 30 $cm^3$ nominal volume which gave a peak to compton ratio of 11 and a resolution of 3.4 KeV (FWHM) for the 1.17 MeV photopeak of $^{60}Co$.

Both platinum and gold were measured in the gold gamma spectrum. The 412 KeV photopeak of $^{198}Au$ is a measure of $^{199}Au$ while the 158 KeV photopeak of $^{199}Au$ is mostly due to a nuclear reaction

on Pt (see p. 52), and thereby is a measure of this element. However, the 158 KeV radiation can be produced not only from $^{198}Pt(n,\gamma)^{199}Pt \xrightarrow{\beta^-} {}^{199}Au$ but also by the reaction $^{197}Au(2n,\gamma)^{199}Au$. The procedure for determination of platinum radiation in the 158 KeV region is as follows:

Let A be a sample spectrum with a 412 KeV photopeak from $^{198}Au$ radiation produced from the $^{197}Au(n,\gamma)^{198}Au$ reaction, and 158 KeV and 208 KeV photopeaks from $^{199}Au$ radiation which is produced from both $^{198}Pt(n,\gamma)^{199}Pt \xrightarrow{\beta^-} {}^{199}Au$ and $^{197}Au(2n,\gamma)^{199}Au$ processes. Let B be a pure Au standard spectrum with a major 412 KeV photopeak from $^{198}Au$ radiation and minor 158 KeV and 208 KeV photopeaks from the $^{197}Au(2n,\gamma)^{199}Au$ process only. Let C be a pure Pt standard spectrum with a major 158 KeV photopeak from Au and minor 412 KeV photopeak from $^{198}Au$. The latter photopeak results from minor gold contamination which is invariably present in the platinum standard solution. Use x and y to refer to 158 KeV and 412 KeV radiation respectively and the symbolism $y_A$ to mean the peak area of the 412 KeV radiation in the sample spectrum. The corrected 158 KeV peak area in the Pt standard, $x'_C$, is obtained from 1) below:

$$x'_C = x_C - y_C(x/y)_B \qquad (1)$$

where the last term on the RHS is the 158 KeV radiation resulting from the 2n, γ reaction on the gold contamination in the Pt standard.

If $x'_A$ is the corrected value of the 158 KeV peak area in the sample, then

$$x'_A = x_A - y_A(x/y)_B \qquad (2)$$

where the last term in the RHS is the 158 KeV radiation from the 2n, γ reaction in the sample gold.

If $Pt_A$ and $Pt_C$ are the platinum concentration of sample and standards respectively, then

$$x'_A/x'_C = Pt_A/Pt_C \qquad (3)$$

The 320 KeV photopeak of Ir was used for measurement of this element. However, the 320 KeV photopeak of some oxide and composite grain samples was overlapped by the 322 KeV photopeaks of $^{51}Cr$ because of high Cr contamination in some samples. In this case the 470 KeV photopeak of $^{192}Ir$ was used for measurement. This eliminates the Cr interference but gives poorer counting statistics. To test whether the 322 KeV photopeak of $^{51}Cr$ contributed to the 320 photopeak of $^{192}Ir$ or not, the ratio of the 320 KeV to the 470 KeV photopeaks of $^{192}$ Ir samples was always compared with the ratio for the standards.

The activity of $^{109}$Pd was determined by graphical analysis of a decay curve. Pd samples were usually counted for 3 weeks after the end of the irradiation in order to subtract activities due to long-lived contaminants. The long-lived activities were extrapolated back graphically to $t_o$ (reference time for the calculation of the Pd content) and subtracted from the total sample activity at $t_o$, resulting in the activity of $^{109}$Pd alone. The activities of long-lived contaminants were usually less than 2% of the total activity at $t_o$.

A possible competing reaction which could cause interference is $^{235}U(n,f)^{112}Pd, ^{109}Pd$. This interference is not significant in chromite (Skippen, 1963), sulphides (Crocket, 1969) and ultrabasic rocks (Skippen, 1963). The error due to self-absorption of the 0.96 MeV $^{109}$Pd beta was not considered in this study, as this error is 1 to 2% if the sample and standard chemical yields are within 20% (Chyi, 1972) and is negligible compared with the error due to sample inhomogeneity.

Concentrations were calculated by comparing the specific activity of the element in the samples with that in the standards. The following equation was used for the calculation:

$$m_x = m_s \frac{I_{x_o} Y_s}{I_{s_o} Y_x}$$

where $m_x$ = weight of the element in the sample (gm)

$m_s$ = weight of the element in the standard (gm)

$I_{x_o}$ = count rate from the sample at $t_o$

$I_{s_o}$ = count rate from the standard at $t_o$

$Y_x$ = radiochemical yield in the sample

$Y_s$ = radiochemical yield in the standard

The sources of error inherent in the nuclear aspects of this analytical method have been discussed by Skippen (1963), Keays (1968) and Chyi (1968).

It is considered that sensitivities for Pt, Pd, Ir and Au for a one week irradiation of a 100 mg. sample at $10^{13}$ n/cm$^2$/sec. are as follows (Crocket, 1971):

| N.A.A. | Pt | Pd | Ir | Au | |
|---|---|---|---|---|---|
| | 90 | 0.3 | 0.11 | 0.05 | ppb. |

Precision error was not thoroughly evaluated in this study for the following reasons. The natural inhomogeneity of noble metals in the Merensky horizon is known to be large. Secondly, sufficient sample for many of the mineral analyses could not be obtained. The

analytical component of the precision error is certainly no larger than that obtained by Crocket et al. (1968) in W-1 using a nearly identical analytical method. These errors, in terms of coefficients of variation, are 2.6%, 7.7% and 3.5% for Pd, Ir and Au respectively. That component of precision error due to sample inhomogeneity is probably greater for Pt and Pd than Ir and Au due to the very large concentration variation of Pt and Pd, particularly in certain parts of the core. Thus, replicate analyses of sample 9 for Pt gave 0.13, 2.1, 97.4, 2.2, 1.7 and 0.44 ppm. These results almost certainly reflect the presence of discrete platinoid minerals in this sample. The average coefficient of variation was established as 12% on the basis of duplicate Ir analyses of ten samples. This result suggests that sample inhomogeneity is a negligible source of precision error for Ir as compared with Pt.

# CHAPTER IV

# EXPERIMENTAL RESULTS

## 4.1. Microscopic Observation of Thin Sections

The results of point counting carried out by J.M. Garth are presented in Table 2 and Fig. 7. Concerning the point-counting analyses, many papers have been published since Chayes' work (1954), e.g. Shaw and Harrison (1955), Bayly (1960), Solomon (1963) and Kalsbeek (1969). According to Shaw & Harrison (1955) the chief sources of error are as follows: (a) variability of hand specimens, (b) variability of thin sections from any hand specimen, and (c) operator and mechanical error in the point-counter method. Solomon (1963) stated that there are three principal sources of error involved in modal analyses by point counting: (a) operator variation, (b) the determination of area by grid counting, (c) the determination of volumes from areal analyses and that operator variation is likely to be negligible but (b) and (c) may combine to give a major error. Kalsbeek (1969) gave a convenient chart for evaluating errors in terms of total number of points in a thin section and estimated modal percents. If Kalsbeek's chart is applicable to the data obtained

Table 2.* Modal Analyses of Total Pyroxenes, Plagioclase and Biotite

| Sample No. | Pyroxenes % | Plagioclase % | Biotite % | Spinels % |
|---|---|---|---|---|
| 1 | 72 | 23 | 0.2 | 5 |
| 2 | 80 | 16 | 1.3 | 2 |
| 3 | 89 | 6 | 1.9 | 2 |
| 4 | 71 | 26 | 0 | 4 |
| 5 | 72 | 25 | 0 | 3.5 |
| 6 | 80 | 18 | 0.3 | 1.5 |
| 7 | 85 | 8 | 1.1 | 4 |
| 8 | 90 | 2 | 2.0 | 2 |
| 9 | 91 | 3 | 2.2 | 2 |
| 10 | 89 | 0.2 | 1.1 | 3 |
| 11 | 76 | 0.7 | 1.1 | 2.5 |
| 12 | 70 | 22 | 0.2 | 3 |
| 13 | 68 | 28 | 0 | 5 |
| 14 | 79 | 19 | 0.1 | 0.75 |
| 15 | 90 | 1.2 | 0.4 | 1 |
| 16 | 80 | 19 | 0 | 1 |
| 17 | 74 | 23 | 0.1 | 1 |
| 18 | 80 | 17 | 0.3 | 0.75 |
| 19 | 86 | 8 | 0.3 | 1 |
| 20 | 88 | 3.8 | 1.1 | 0.5 |
| 21 | 67 | 26 | 6.8 | ~0.1 |
| 22 | 81 | 18 | 0.9 | ~0.1 |
| 23 | 85 | 14 | 1.0 | ~0.1 |
| 24 | 78 | 21 | 0.1 | ~0.25 |
| -- | 86 | 12 | | |

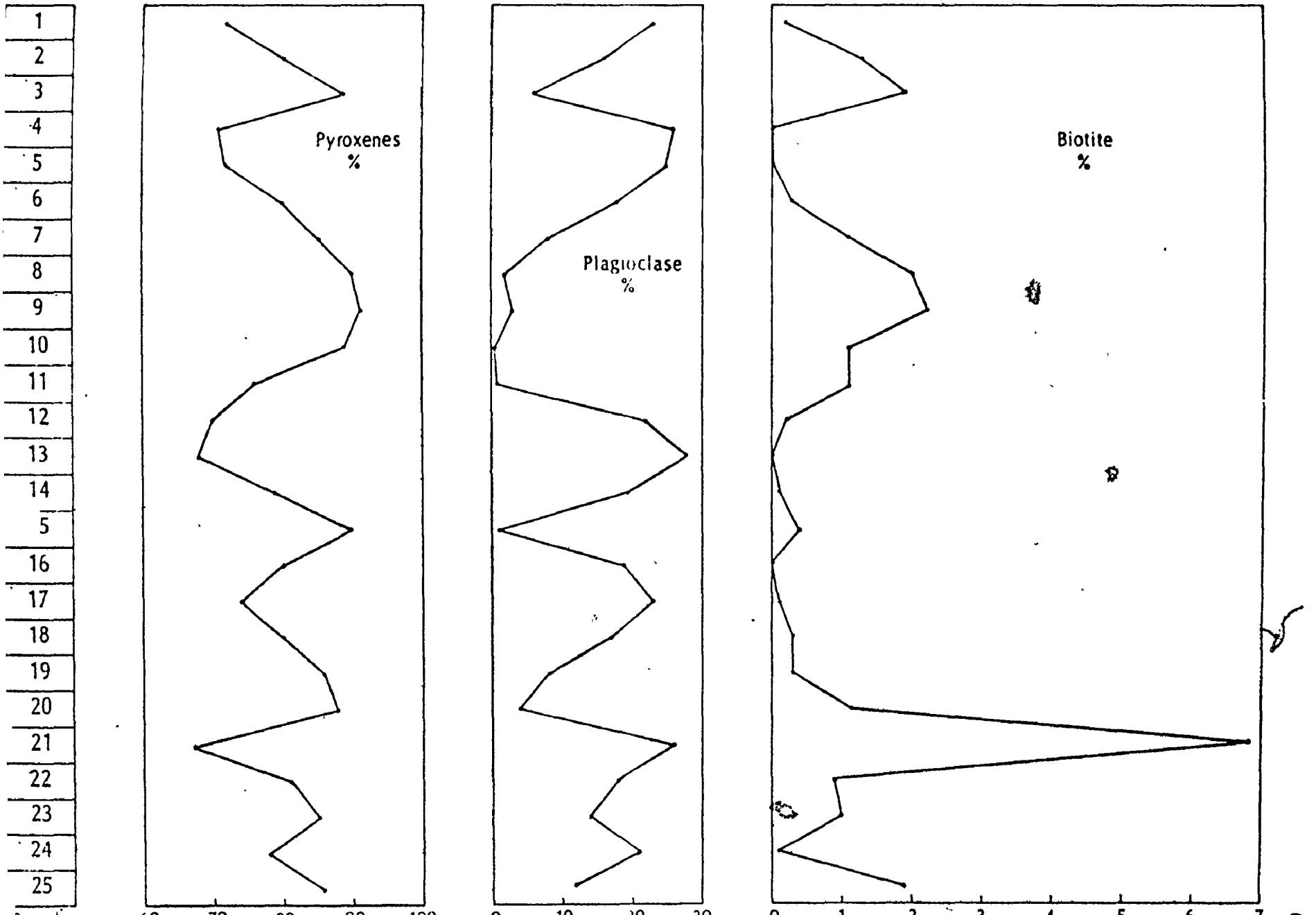


Fig. 7 MODAL ANALYSES OF TOTAL PYROXENES, PLAGIOCLASE AND BIOTITE

by Garth, the average modal percentage of pyroxene is found to be 80±2.8% and plagioclase, 13±2%.

Modal percentages of spinel group minerals, chromite and magnetite, may be associated with large errors due to small grain size and irregular distribution of these minerals.

From observation of 25 thin sections covering the entire core length at approximately 1" intervals the following essential petrographic characteristics were noted.

1) In all sections the essential minerals are pyroxene and plagioclase. The average modal percentages are 80% and 13% respectively (i.e. both comprise about 93% of the rock). These estimates agree closely with the averages of 83 and 14% pyroxene and plagioclase reported by van Zyl (1970) for the same section at Rustenburg. Hence a rock name such as pyroxenite or feldspathic pyroxenite describes the core.

2) The most common accessory silicates are clinopyroxene and biotite. Much of clinopyroxene is characterized by very prominent parting parallel to {100} and may be referred to as diallage, a variety of ferroan diopside (Keer, 1959, p. 308). Biotite is irregularly scattered throughout and its distribution seems to be unrelated to that of the oxides. It forms irregular grains which are always interstitial to pyroxene. Where biotite and orthopyroxene are in contact, orthopyroxene is rounded and locally embayed.

Chromite, magnetite and sulphides are also common accessory constituents. Olivine is not observed in these thin sections, but is occasionally noted in the X-ray powder diffraction of whole rock samples. Small amounts of a fibrous mineral occur as reaction rims around pyroxene grains. The optical properties are compatible with amphibole which is occasionally identified in the X-ray patterns. Amphibole appears to have been formed by magmatic reaction of the pyroxene with residual magma or deuteric fluids. Sulphides are described under the microscopic observation of polished sections. Trace amounts of quartz-like mineral are often observed and this seems to be cordierite as noted in the X-ray data, although its identification by optical methods is very difficult for Bushveld rocks as reported by Willemse (1970).

3) The main petrographic variant observed is the local presence of significant quantities of secondary silicate minerals as alteration of pyroxene. Samples 10 and 11 contain 10 to 20% secondary minerals and sample 15 about 8%. Some of the alteration is talc (optical and X-ray diffraction identification) but much of it occurs as fibrous aggregates of acicular individuals following pyroxene cleavage. It is invariably accompanied by sulphide occurring both as an envelope around the silicate and as blades or lamellar aggregates intimately mixed with silicate and following primary pyroxene cleavages. On

a basis of whole rock X-ray diffraction analyses, this mineral is thought to be pyrophyllite.

4) Orthopyroxene is a cumulus phase. Following the terminology of Wager and Brown (1967, p. 61) the rock is described as dominantly an orthopyroxene orthocumulate (i.e. there is little evidence of adcumulus growth of orthopyroxene and this is the only definite cumulus phase). Commonly the orthopyroxene has exsolved fine lamella of augite parallel to (100) and small blebs of exsolved augite.

All plagioclase is either interstitial to the pyroxene or encloses it poikilitically. It has crystallized from the intercumulus liquid and whether the textural effect is interstitial or poikilitic depends on the pyroxene to plagioclase ratio with the latter texture developing mainly in rocks with 20% plagioclase or more. Clinopyroxene occurs rarely as mega-poikilitic plates enclosing orthopyroxene, as small grains with the intercumulus plagioclase or as patches on the margins of orthopyroxene. It has crystallized almost exclusively from the intercumulus liquid. Biotite is also intercumulus and looks mainly primary.

Magnetite grains, black with a metallic luster in reflected light, exhibited triangular, square, or rhombic sections of octahedra.

They are interstitial to and enclosed by other minerals, such as pyroxene and plagioclase.

Almost all scattered crystals of chromite are at or close to the peripheries of the orthopyroxene grains. Other chromite also occurs both within orthopyroxene as small euhedral grains sometimes surrounded by a thin rim of plagioclase and as euhedral grains in the intercumulus plagioclase. Some chromite may be cumulus phase but this is controversial (see van Zyl, 1970, Wager and Brown, 1967, p. 397).

4.2. Microscopic Observation of Polished Sections

As to the previous textural studies of sulphide minerals in the Merensky Reef, Schneiderhöhn and L. Liebenberg's publications must be reviewed before representing the results of this work. According to Schneiderhöhn (1929, pp. 208-214) sulphides in the Merensky Reef Suite occur as follows: irregular patches and grains occupying the intersticies between silicates, smaller grains along the margins of individual silicate grains, intimate intergrowths with hornblende and biotite, inclusions in several primary silicates, and finally, with serpentine formed by hydrothermal alteration of olivine and bronzite.

He concluded that nickeliferous pyrite is the earliest of the sulphide minerals, being corroded and replaced by all the other sulphides. The nickeliferous pyrite is commonly found enclosed in

pentlandite and forms ring-shaped bodies encasing smaller rounded grains of pyrrhotite. Pyrrhotite occurs in big granular masses and is free of inclusions of other sulphides apart from secondary pentlandite. Pentlandite occurs in two forms; as a discrete primary mineral younger than nickeliferous pyrite and pyrrhotite, but older than chalcopyrite; and as younger, secondary, oriented lamellae in pyrrhotite. Chalcopyrite is usually found rimming the other sulphides and often seen to penetrate into the cleavages of the biotite, pyroxene and hornblende. This mineral is the youngest of the primary sulphides. Included in it are oriented lamellae of cubanite.

L. Liebenberg (1970) also indicates that all the sulphides are interstitial to the silicates and that contacts are noticeably irregular. In general, pyrrhotite is the principal sulphide in the disseminated ore of the Merensky Reef Suite of rocks. The textures and paragenesis of the sulphide minerals reported by Liebenberg are similar to those of Schneiderhöhn's. A semi-eutectic intergrowth of chalcopyrite and pyrite is also reported in ore from the Merensky Reef. Cubanite is rare and generally subordinate to chalcopyrite.

Microscopic observation of the Lonrho polished sections was carried out to identify sulphide mineral phases, examine textures and select grains for chemical analysis. A diamond indentation hardness tester (Leitz Wetzlar) was used to aid in mineral identification.

Sulphide grains were so irregular and variable in grain size that point-counting could not be used to estimate modal mineral proportions. Thus, a photograph of each sulphide grain was taken with a Vickers Projection Microscope and the areal proportion of pyrrhotite, pentlandite and chalcopyrite, etc. was measured on the photograph using the Coradi Compensation Planimeter. This instrument is guaranteed in accuracy to within a maximum deviation of 0.2%. The operational error may be added to this value. To estimate the operational error twenty measurements of an area, 4 x 4 cm (16.00 $cm^2$) on a standard section (grid) paper (JIS A4 180 x 250 mm) were performed. The mean value, standard deviation, and coefficient of variation were found to be 15.95 $cm^2$, $6.07 \times 10^{-4}$ $cm^2$, and 0.38%, respectively.

Twenty nine sulphide grains were chosen from core samples 7, 11, 12, 15-16, 17, 18-19, 20 and 21 for determination of the areal proportions of different sulphide mineral in single grains. The size of each grain was also measured with the micrometer attached to the Leitz Wetzlar microhardness tester. The average size and proportion of each mineral is shown in Table 11.

The main sulphide minerals present were pyrrhotite, pentlandite, chalcopyrite and pyrite. The particle size of sulphides was extremely variable (0.3--5 mm), even in the same section.

Sections with a high sulphide content had the greatest range of particle sizes. The textural relations between sulphides and silicates were variable. Three different textural relationships between sulphides and silicates were observed:

1) Type I: Roundish or oval sulphide blebs with both irregular and smooth edges entirely enclosed in large optically continuous silicate grains, mainly plagioclase (Separate Grain No. 11-1, 11-2, 12-1, 21-1 and 21-3). A typical example is shown in Plates 1 and 2.

2) Type II: The most common texture observed was patches of sulphide interstitial to early pyroxene, the shape of the sulphide grain being controlled entirely by surrounding silicates (Separate Grain No. 7-1, 7-2, 11-3, 15-1, 15-16-1, 17-1, 18-19-1, 20-1, 20-2, 20-3, 21-2, 21-4 and 21-5). Plates 3 and 4 show this texture.

3) Type III: Localization of sulphides along cleavages, particularly in pyroxene and where alteration to pyrophyllite or talc has been extensively developed. Examples are shown in Plates 5 and 6. Such sulphide is often of acicular or bladed habit. The outlines of original sulphide grain have been almost completely destroyed (Separate Grain No. 7-1, 7-2, 11-3, 15-1, 17-2, 18-19-1, 20-1, 21-2, 21-4 and 21-5).


Plate 1. Sulphide Type I: Separate Grain No. 11-1

A: Plagioclase; B: Pyroxene; C: Chromite


Plate 2. Sulphide Type I: Separate Grain No. 11-2

A: Plagioclase; B:Pyroxene; C: Chromite

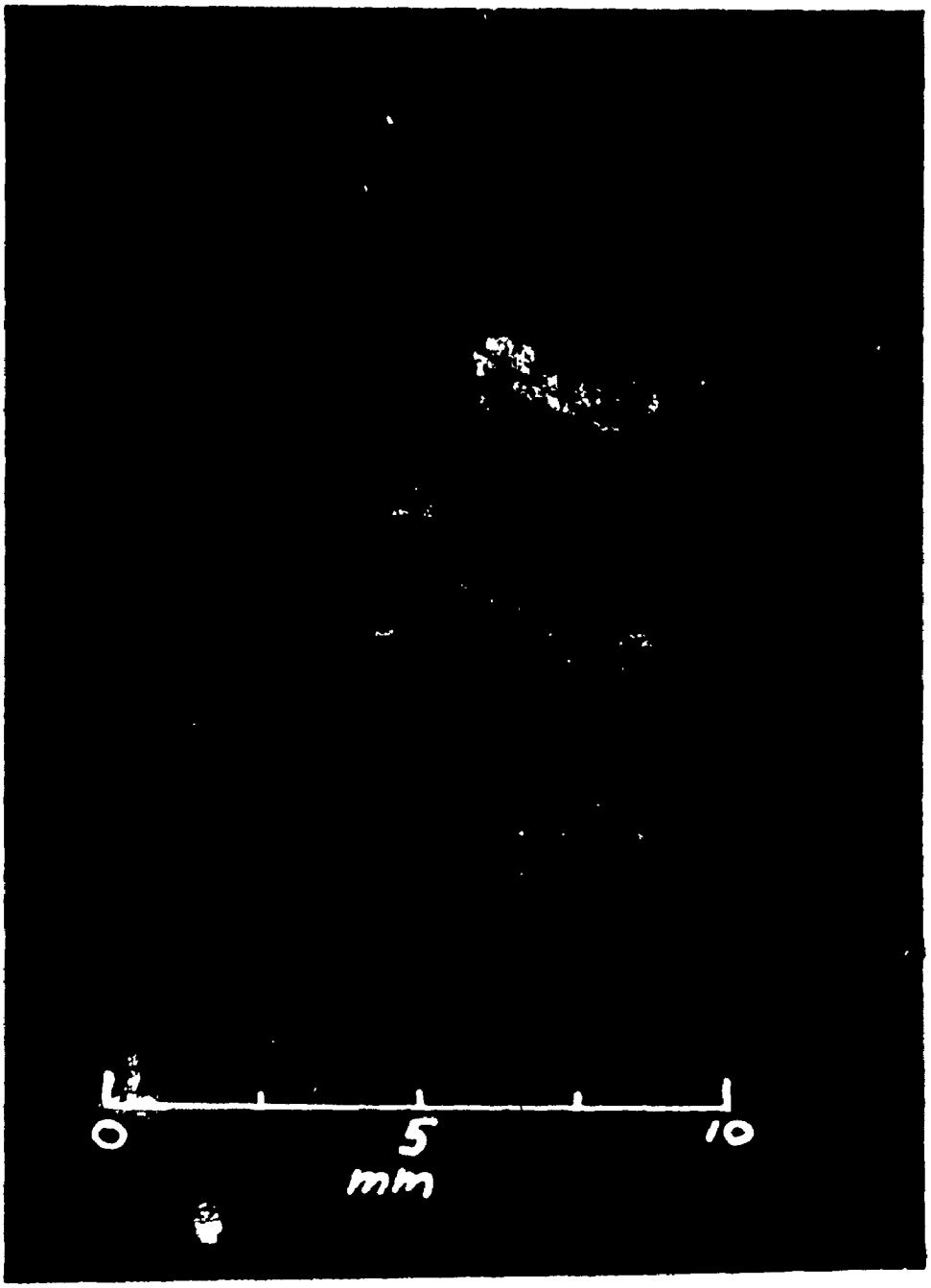


Plate 3. Sulphide Type II: Separate Grain No. 15-16-1

A: Plagioclase; B: Pyroxene

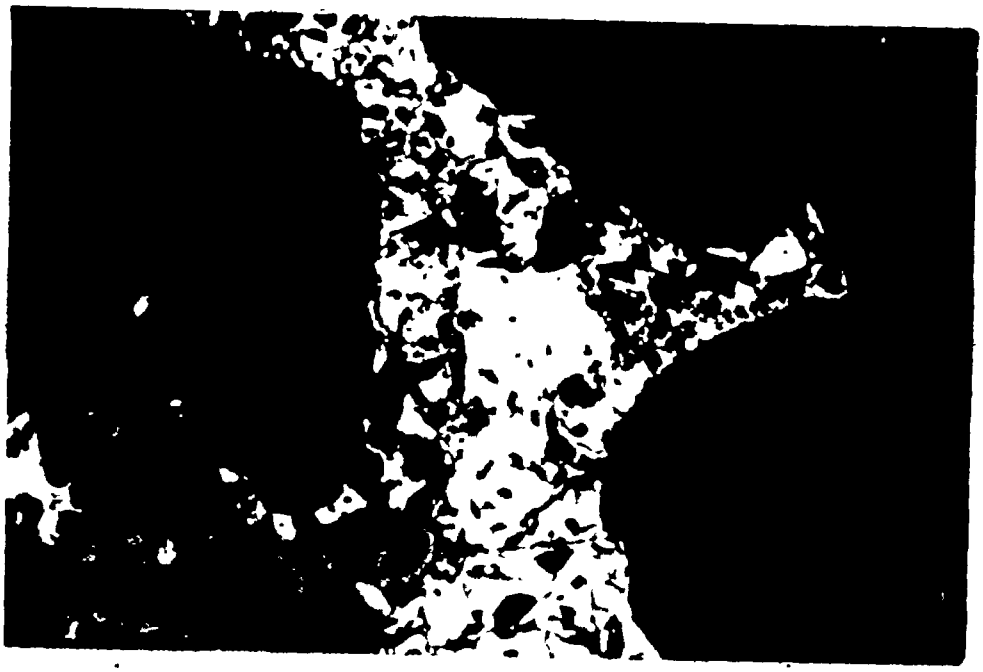

Plate 4. Sulphide Type II: X 53

Sulphide Interstitial to Silicates

Plate 5. Sulphide Type III: X 53

Sulphide with Secondary Silicates

Plate 6. Sulphide Type III: X 53

Sulphide affected by hydrous alteration

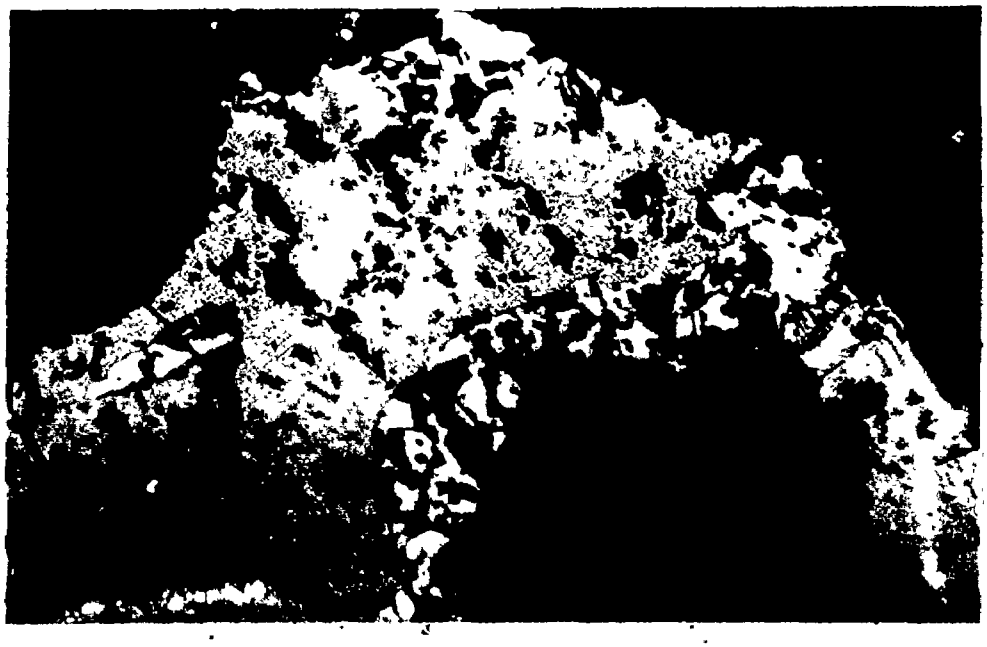

Plate 7. Sulphide Type I: X 106

Exsolution of pentlandite (light yellow) with pyrrhotite (cream-coloured) and chalcopyrite (bright yellow)

The sulphide blebs of Type I appear to have precipitated contemporaneously with the surrounding silicate grain and to be in chemical equilibrium with it, as indicated by the absence of secondary alteration along the boundaries between silicate and sulphide. Pyrrhotite makes up the bulk of these sulphide blebs with pentlandite and chalcopyrite developed as rims around the pyrrhotite core, forming a zonal arrangement. The silicate mineral surrounding these sulphides is dominantly plagioclase. The cumulus mineral is orthopyroxene with the plagioclase bearing an interprecipitate relationship to it. Thus, this, and all other sulphides, appear to have crystallized from the interprecipitate liquid. No silicate veinlets inside sulphides were observed.

In general, pyrrhotite was the principal sulphide. It was seldom found alone but always in association with pentlandite, chalcopyrite and pyrite. In this type of sulphide, pyrrhotite was coarse, anhedral and never contained silicate gangue.

Pentlandite occurred as blocky rims surrounding pyrrhotite or as flames within pyrrhotite. The coarse pentlandite was mostly restricted to the rims of the sulphide blebs occurring with or without chalcopyrite at the outermost rim. It sometimes contained small islands of silicate gangue (No. 11-2). Coarse pentlandite showed a characteristic octahedral parting. They were occasionally enclosed by pyrrhotite (No.

11-1 and 21-3), where coarse pentlandite formed veins of blocky crystals cutting across the basal cleavage of pyrrhotite. These veins followed former cracks in pyrrhotite or its grain boundaries. Fine-grained pentlandite was generally found as feathery or brush-like lamellae parallel to or subparallel to (0001) of pyrrhotite (No. 11-1, 11-2 and 12-1). These occurred as single minute flames or aggregates of flames. This pentlandite usually flared out from boundaries of pyrrhotite crystals (No. 11-2 and Plate 7) from the contact of pyrrhotite with chalcopyrite (No. 11-1), or from cracks (No. 21-3). In the Type I sulphides the amount of exsolved pentlandites was less than in other sulphide types.

The relative percent of chalcopyrite present in sulphide grains was highest in Type I sulfide as compared with the other types of sulphide occurrences. It was restricted to the rim of a sulphide bleb and penetrated into the cleavages of surrounding silicate (Separate Grain No. 11-1, 11-2, 12-1, 21-1 and 21-3). In almost all the samples very fine chalcopyrite grains were observed in surrounding silicate close to sulphide blebs. The grain boundaries between chalcopyrite and pentlandite were relatively smooth.

Pyrite was only found in Type I sulphide blebs where it occurred as round grains or as cubic and octahedral crystals, less than 0.01 mm in diameter. It was present usually in contact with pyrrhotite and pentlandite where rounded or corroded grains with embayments of pyrrhotite were common (No. 11-1, 11-2 and Plate 8). This mineral appeared to be metastable and to be corroded by pyrrhotite.

In the Type II sulphides, which were interstitial to pyroxene and plagioclase, the shape of the sulphide grains was controlled by the surrounding silicate minerals. Abundant veinlets of silicates cut across the sulphides. A gradual transition from Type II to Type III involved an increasing degree of embayment by secondary silicate minerals, i.e. the only textural distinction between types II and III was the nature of boundaries between sulphides and embaying silicates.

The formation of sulphides of the second type appears to be later than that of all primary silicates. The sulphides in type III were affected by late hydrous alteration. The textural relationships between chalcopyrite, pentlandite and pyrrhotite in sulphide grains of Type II were very similar to those of Type III. The following descriptions are equally valid for both types.

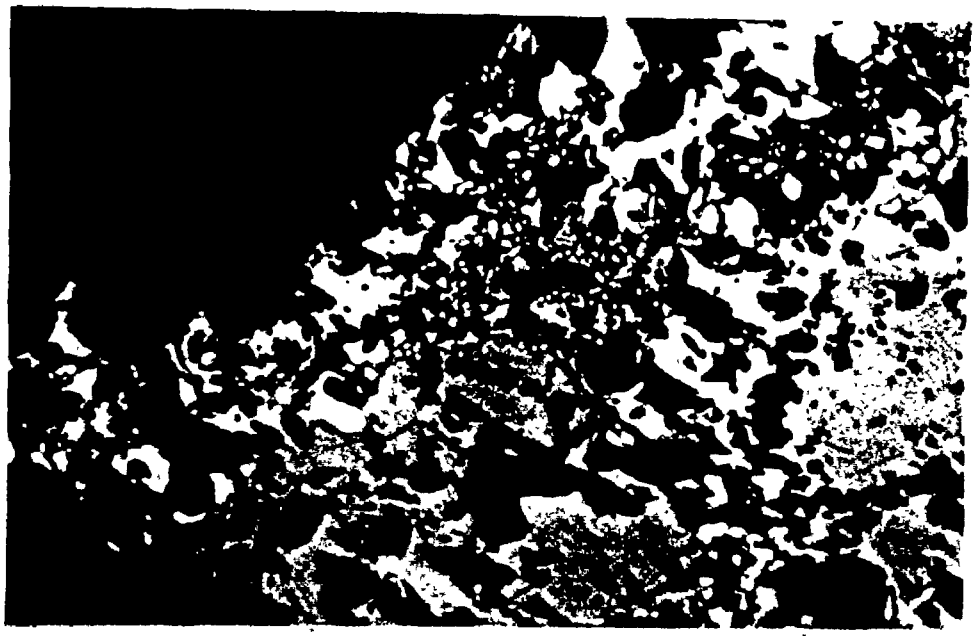

Plate 8. Corroded grain of pyrite (light yellowish white) in pyrrhotite (cream-coloured) and pentlandite (light yellow) X 132

Most of the pyrrhotite in these two types did not form the core of sulphide grains as in Type I but rather, occurred as massive aggregates adjacent to bodies of pentlandite of about the same volume. Near the grain boundaries between pyrrhotite and chalcopyrite (No. 18-19-1) and to a much lesser degree between pyrrhotite and pentlandite, round or angular inclusions of pyrrhotite were found, which had the same optic orientation as the surrounding pyrrhotite. This points to some replacement of pyrrhotite by the minerals mentioned.

Fine grained pentlandite within pyrrhotite appeared to be a product of exsolution. However, the exsolved grains in pentlandites of these types (II and III) were more globular and irregular than those of Type I. These globular bodies graded into bigger, irregular grains which were localized in the central parts of pyrrhotite crystals (No. 15-16-1, 21-1, 21-2 and 21-4). They sometimes formed an intergrowth with pyrrhotite (No. 17-2 and 20-1) and extend along the cracks in pyrrhotite (Separate Grain No. 11-3, 17-1, 18-19-1 and 21-5). Feathery or brush-like lamellae of pentlandite were not common in the present types.

Tiny grains of chalcopyrite were found in pyrrhotite and pentlandite. The amount of exsolved chalcopyrite in pyrrhotite was less than one percent. It is difficult to determine whether grains of

chalcopyrite in pentlandite were due to exsolution or replacement. Chalcopyrites observed in pentlandites usually occurred along cracks as fine veins or lamellae, less than 0.05 mm thick (No. 18-19-1 and 20-3). Grains of chalcopyrite were always associated with inclusions or veinlets of silicate gangue in sulphides (No. 18-19-1, 20-3 and 21-4) or tended to segregate as mono-sulphide patches interstitial to the silicates. Relatively large grains of chalcopyrite, 0.5 mm in diameter, were cut by silicate veinlets.

Although cubanite is reported to be present in minor amounts, it was not observed in the present work. No minerals of the PGM were observed in the present samples.

4.3. X-Ray Powder Diffraction of Whole Rock Samples

A summary of the interpretation of X-ray powder diffraction patterns of each core sample is given in Table 3. The presence of major silicate minerals, hypersthene*, and plagioclase, agrees with the thin section observations. The other silicate minerals, such as diopside, high cordierite, biotite, pyrophyllite and talc, were present in almost all samples as minor components. Of these, diopside, biotite, pyrophyllite and talc were observed in thin section. Olivine was detected

* Orthopyroxene in the Merensky horizon is referred to as bronzite by Wager and Brown (1967). The ASTM X-ray data indicate orthopyroxene whose composition is hypersthene, as defined in Deer et al. (1966). The mineral is hereafter referred to as hypersthene.

Table 3. Minerals Identified in Whole Rock Samples by X-ray Powder Diffraction

| le | Hypers. | Diop. | Plag. | Oliv. | Amph. | H-Cord. | Biot. | Pyroph. | Talc | Pyrrh. | Pentl. | Pyrite | Chromite | Mag. | Graphite |
|---|---|---|---|---|---|---|---|---|---|---|---|---|---|---|---|
| | ++ | + | ++ | | | + | + | + | + | + | | | + | + | |
| | ++ | + | ++ | + | + | + | ++ | + | + | | + | | | + | |
| | ++ | + | ++ | | + | + | ++ | + | + | + | | | + | + | |
| | ++ | + | ++ | | + | + | + | + | + | | + | | + | + | |
| | ++ | + | ++ | | | + | + | + | + | + | + | | + | + | |
| | ++ | + | ++ | | + | + | +- | + | + | | + | | | + | |
| | ++ | + | + | | + | + | + | + | + | | | | + | + | |
| | ++ | + | + | | + | + | ++ | + | + | + | | | + | + | |
| | ++ | + | + | | + | + | ++ | + | + | | | | + | + | |
| | ++ | + | + | | + | ++ | ++ | ++ | + | | | | + | + | |
| | ++ | + | + | + | + | + | + | + | + | + | | + | + | + | + |
| | ++ | + | ++ | | | | | | + | + | | | + | + | |
| | ++ | + | ++ | | | | | | + | + | | | + | + | |
| | ++ | + | ++ | + | | + | | + | + | + | + | | + | + | |
| | ++ | + | ++ | + | | + | + | ++ | + | + | + | | + | + | |
| | ++ | + | + | | | | + | + | + | + | | | + | + | |
| | ++ | + | + | | | + | + | + | + | + | | | + | + | |
| | ++ | + | + | + | | + | + | + | + | + | + | | + | + | |
| | ++ | + | + | | | ++ | + | + | + | + | + | | + | + | |
| | ++ | + | + | | | + | + | + | + | + | | | + | + | |
| | ++ | + | + | | | + | ++ | + | + | | + | | + | + | |
| | ++ | + | + | + | | + | + | + | + | | + | | + | + | + |
| | ++ | + | + | | | + | + | | + | + | | | + | + | |
| | ++ | + | + | | | | | | + | + | | | + | + | |
| | ++ | + | + | + | | | | + | + | + | + | | + | + | |

ers.: Hypersthene; Diop.: Diopside; Plag.: Plagioclase, (Labradorite, Bytownite); Oliv.: Olivine;

mph.: Amphibole (Hornblende, Grunerite); H-Cord:: High Cordierite; Biot.: Biotite; Pyroph.: Pyrophyllite;

rh.: Pyrrhotite; Pentl.: Pentlandite; Mag.: Magnetite

Abundant; + - Minor; Blank - not detected.

only in seven samples (Sample No. 2, 11, 14, 15, 18, 22 and 25) and amphibole was observed exclusively in the samples covering mostly the core above the lowest chromitite seam (Sample No. 2, 3, 4, 6, 7, 8, 9, 10 and 11).

The presence of cordierite is only reported in the Critical Zone from Maandagshock in the Lydenburg district and at the contacts of sedimentary rocks and ultramafic rocks in the Eastern Transvaal (Willemse, 1964 and 1970). In the present study, however, the d-spacings, 8.49 and 4.07 Å, fit best with high cordierite and these peaks tentatively are assigned to cordierite. According to Deer et al. (1966, p. 88) cordierite is found in some norites which are commonly considered to be derived from gabbroic magma contaminated by argillaceous material. In many such norites cordierite is not xenocrystal in origin but crystallizes directly from the contaminated magma.

Vallance (1967) studied mafic rock alteration and isochemical development of some cordierite-anthophyllite rocks and noted that cordierite appears in the rocks which are marked by poverty in Ca and alkalis (especially K) and relative richness in Al and the mafic components. Based on a detailed study of orthopyroxene mineralogy, Hess (1960) defined the Bushveld type as orthopyroxene with a low Ca content (ca. 3%). Atkins (1969) also stated that a Ca-poor pyroxene

persists as a cumulus phase throughout most of the Layered Sequence and gave the same Ca content in Ca-poor pyroxene at the Merensky Reef. In fact, Oen et al. (1973) reported that an unusual paragenesis of chromite, nickeline, cordierite and red-brown mica occurs in veins, pods and schlieren in serpentinized ultramafic rocks at La Gallega and Los Jarales, Spain, and concluded that the chromite-nickeline-cordierite-mica paragenesis is derived from a magma of peculiar, highly differentiated composition, with relatively high concentrations of water and such elements as Cr, Ni, Co, Zn, As and V.

The intercumulus minerals, such as cordierite, are to be expected as products of relatively late stage fractionation. According to Duchesne (1972) if, after the orthomagmatic stage an interstitial fluid rich in volatiles such as $H_2O$ and $H_2$ remains trapped in the interstices between the minerals, equilibrium between oxides and the fluid may be maintained during slow cooling. He called this deuteric readjustment. The presence of cordierite in the present core samples may be caused by the process mentioned above.

Concerning the sulphide minerals, all those observed in polished section except chalcopyrite were detected in the X-ray diffraction patterns. The presence of pyrite was observed only in sample No. 11, which agrees with the microscopic observation of polished samples, No. 11-1 and 11-2.

Chromite and magnetite were ubiquitous as minor components. Graphite was noticed only in two samples, i.e. No. 11 and 22.

Regarding runs on separated grains of oxides, the samples (Separate Grain No.: 1-1, 1-2, 1-3, 4-1a,b, 4-2a,b,c, 4-3, 13-2, and 13-3a,b in Table 12) which contained more than 80% spinel group grains, showed peaks of magnetite and chromite only. The one sample, No. 13-1, indicated the presence of magnetite only. The samples of composite grains (Separate Grain No.: 1-4, 4-4, 7-1, 7-2a,b, 10-1, 10-2 and 13-4) contained hypersthene, pyrophyllite, talc and cordierite besides magnetite and chromite.

## 4.4. Contents of Total S, Cr, Ni and Cu in Whole Rock Samples

The results of chemical analyses of total S, Cr, Ni and Cu are shown in Table 4 and Fig. 8. The general trend of total S in whole rock samples agrees approximately with the results of microscopic observations. Contents of Ni and Cu varied closely with changes in the amounts of S in the samples. Contents of Cr, however, did not follow the trend of S contents. The amounts of Cr present were found to roughly correlate with modal spinel from thin section counts.

Table 4. Contents of Total S, Cr, Ni and Cu in Whole Rock Samples

| Sample No. | Total S % | Cr ppm | Literature value | Ni ppm | Literature value | Cu ppm | Literature value |
|---|---|---|---|---|---|---|---|
| 1 | 0.03 | 12,931 | | 796 | | 48 | |
| 2 | 0.01 | 4,403 | | 596 | | 92 | |
| 3 | 0.002 | 3,834 | | 674 | | 163 | |
| 4 | 0.05 | 17,683 | | 799 | | 73 | |
| 5 | 0.02 | 7,567 | | 627 | | 186 | |
| 6 | 0.03 | 5,281 | | 691 | | 173 | |
| 7 | 0.17 | 10,452 | | 1,213 | | 353 | |
| 8 | 0.43 | 6,843 | | 1,349 | | 1,711 | |
| 9 | 0.32 | 5,288 | | 1,154 | | 1,682 | |
| 10 | 0.65 | 6,788 | | 1,381 | | 3,406 | |
| 11 | 1.40 | 5,115 | | 4,796 | | 1,918 | |
| 12 | 0.67 | 10,241 | | 2,729 | | 942 | |
| 13 | 0.39 | 9,311 | | 2,218 | | 682 | |
| 14 | 0.21 | 4,593 | | 1,491 | | 794 | |
| 15 | 1.04 | 3,930 | | 4,638 | | 1,025 | |
| 16 | 0.10 | 4,596 | | 914 | | 568 | |
| 17 | 0.25 | 5,273 | | 1,366 | | 647 | |
| 18 | 0.15 | 5,228 | | 1,085 | | 444 | |
| 19 | 0.86 | 5,024 | | 3,381 | | 1,456 | |
| 20 | 0.77 | 3,611 | | 2,739 | | 1,046 | |
| 21 | 0.62 | 2,382 | | 2,455 | | 1,069 | |
| 22 | 0.14 | 2,355 | | 911 | | 267 | |
| 23 | 0.06 | 2,724 | | 641 | | 114 | |
| 24 | 0.03 | 2,748 | | 940 | | 217 | |
| 25 | 0.06 | 2,431 | | 1,021 | | 729 | |
| W-1 | | 147) | 114 | 73) | 70 | 122) | 110 |
| W-1 | | 115) | 120 | 92) | 78 | 115) | 112 |
| | | | | | 90 | | 121.5 |
| DTS-1 | | | | 2,235) | 2,250 | 12) | 7.0 |
| DTS-1 | | 3,624) | 4,000 | 2,309) | 2,330 | 7.1) | 7.9 |
| | | | | | 2,500 | | 8.5 |
| | | | | | | | 15.0 |

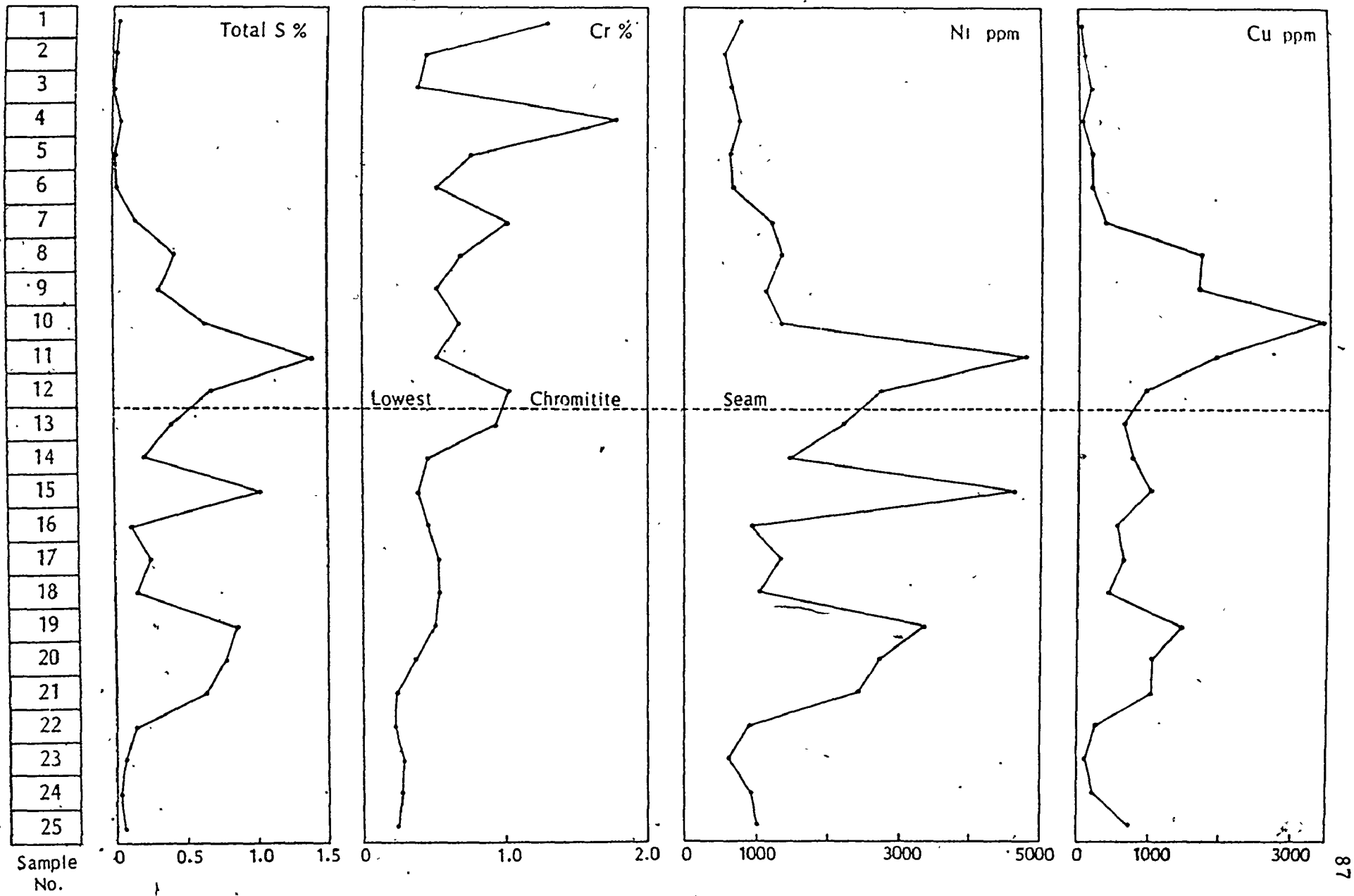


Fig. 8 CONTENTS OF S, Cr, Ni AND Cu IN WHOLE ROCK

The proportion of the sulphides, pyrrhotite, pentlandite and chalcopyrite, was calculated for whole rock samples from the chemical analyses on the following assumtions:

1) The content of Ni in silicates, such as olivine and orthopyroxene, is 400 ppm, which seems to be reasonable for the orthopyroxene in the Merensky horizon (440 ppm for unmineralized Merensky Reef according to L. Liebenberg, 1970).

2) Ni in excess of 400 ppm is contributed by pentlandite.

3) Cu is contributed entirely by chalcopyrite, neglecting small amounts of cubanite.

4) The ideal formula of pentlandite is $(Fe,Ni)_9S_8$ with moles Fe = moles Ni; chalcopyrite, $CuFeS_2$; and pyrrhotite, $Fe_{0.8}S$.

5) Total S is contributed by sulphides only.

The calculation of mineral weight percent was carried out as follows. Firstly, the weight percent of pentlandite for each sample was calculated from the value of (Total Ni content - 400 ppm). Secondly, the weight percent of chalcopyrite was calculated from the total Cu content. Then the amount of S left, i.e. total S minus S contributed by pentlandite and chalcopyrite, was used to calculate weight % of pyrrhotite. These calculations and results are presented in Tables 5-8.

Table 5. Calculation of Weight Percent of Pentlandite $(Fe,Ni)_9S_8$, in Whole Rock Samples from the Atomic Absorption Analyses F. Wt. = 771.955

(4.5Ni/F. Wt.) = 0.34224

| Sample No. | Weight of Sample gm | Content of Ni in Sample, ppm | $A_p$ ppm | $B_p$ microgm | $C_p$ micro-mole | $D_p$ micro-mole | $E_p$ microgm | $F_p$ ppm | Weight % of Pentlandite % |
|---|---|---|---|---|---|---|---|---|---|
| 7 | 1.13374 | 1,213 | 813 | 921.73 | 15.686 | 27.886 | 2,693.2 | 2,375.5 | 0.24 |
| 8 | 1.03751 | 1,349 | 949 | 984.60 | 16.756 | 29.788 | 2,876.9 | 2,772.9 | 0.28 |
| 9 | 1.04007 | 1,154 | 754 | 784.21 | 13.346 | 23.726 | 2,291.4 | 2,203.1 | 0.22 |
| 10 | 1.04961 | 1,381 | 981 | 1,029.7 | 17.524 | 31.154 | 3,008.7 | 2,866.5 | 0.29 |
| 11 | 1.01655 | 4,796 | 4,396 | 4,468.7 | 76.050 | 135.20 | 13,057. | 12,845. | 1.28 |
| 12 | 1.03507 | 2,729 | 2,329 | 2,410.7 | 41.026 | 72.935 | 7,043.9 | 6,805.0 | 0.68 |
| 13 | 1.02568 | 2,218 | 1,818 | 1,864.7 | 31.734 | 56.416 | 5,448.5 | 5,312.0 | 0.53 |
| 14 | 1.03954 | 1,491 | 1,091 | 1,134.1 | 19.300 | 34.311 | 3,313.8 | 3,188.0 | 0.32 |
| 15 | 1.02418 | 4,638 | 4,238 | 4,340.5 | 73.868 | 131.32 | 12,683. | 12,383. | 1.24 |
| 16 | 1.01183 | 914 | 514 | 520.08 | 8.8509 | 15.735 | 1,519.6 | 1,501.9 | 0.15 |
| 17 | 1.04296 | 1,366 | 966 | 1,007.5 | 17.146 | 30.482 | 2,943.8 | 2,822.6 | 0.28 |
| 18 | 1.01380 | 1,085 | 685 | 694.45 | 11.818 | 21.010 | 2,029.1 | 2,001.5 | 0.20 |
| 19 | 1.06485 | 3,381 | 2,981 | 3,174.3 | 54.021 | 96.038 | 9,275.1 | 8,710.2 | 0.87 |
| 20 | 1.00390 | 2,739 | 2,339 | 2,348.1 | 39.961 | 71.042 | 6,861.0 | 6,834.3 | 0.68 |
| 21 | 1.02866 | 2,455 | 2,055 | 2,113.9 | 35.975 | 63.956 | 6,176.7 | 6,004.6 | 0.60 |
| 22 | 1.12517 | 911 | 511 | 574.96 | 9.7849 | 17.395 | 1,680.0 | 1,493.1 | 0.15 |

$A_p$ = Content of Ni - 400 (ppm); 400 ppm is estimated Ni contribution from silicates.
$B^p$ = Content of Ni in Sample, (gm)
$C^p$ = Ni in Samples (moles), $(B_p/58.76)$
$D^p$ = S in Pentlandite (moles), $^p(16/9)C_p$
$E^p$ = Microgram Pentlandite, $B_p/0.34224$
$F^p_p$ = $E_p$/Wt. of Sample, (ppm)

Table 6. Calculation of Weight Percent of Chalcopyrite, $CuFeS_2$, in Whole Rock Samples

from the Atomic Absorption Analyses F. Wt. = 183.515 Cu/F. Wt. = 0.34624

| Sample No. | Weight of Sample gm | Content of Cu in Sample ppm | $B_c$ microgm | $C_c$ micro-mole | $D_c$ micro-mole | $E_c$ microgm | $F_c$ ppm | Weight % of Chalco-pyrite % |
|---|---|---|---|---|---|---|---|---|
| 7 | 1.13374 | 353 | 400.21 | 6.30 | 12.60 | 1,155.9 | 1,019 | 0.10 |
| 8 | 1.03751 | 1,711 | 1,775.2 | 27.94 | 55.88 | 5,127.0 | 4,942 | 0.49 |
| 9 | 1.04007 | 1,682 | 1,749.4 | 27.53 | 55.06 | 5,052.6 | 4,858 | 0.49 |
| 10 | 1.04961 | 3,406 | 3,575.0 | 56.26 | 112.52 | 10,325. | 9,837 | 0.98 |
| 11 | 1.01655 | 1,918 | 1,949.7 | 30.69 | 61.38 | 5,631.2 | 5,540 | 0.55 |
| 12 | 1.03507 | 942 | 975.04 | 15.35 | 30.70 | 2,816.1 | 2,721 | 0.27 |
| 13 | 1.02568 | 682 | 699.51 | 11.01 | 22.02 | 2,020.3 | 1,970 | 0.20 |
| 14 | 1.03954 | 794 | 825.39 | 12.99 | 25.98 | 2,383.9 | 2,293 | 0.23 |
| 15 | 1.02418 | 1,025 | 1,049.8 | 16.52 | 33.04 | 3,031.9 | 2,960 | 0.30 |
| 16 | 1.01183 | 568 | 574.61 | 9.04 | 18.08 | 1,659.6 | 1,640 | 0.16 |
| 17 | 1.04296 | 647 | 674.80 | 10.62 | 21.24 | 1,948.9 | 1,869 | 0.19 |
| 18 | 1.01380 | 444 | 450.13 | 7.08 | 14.16 | 1,300.1 | 1,282 | 0.13 |
| 19 | 1.06485 | 1,456 | 1,550.4 | 24.40 | 48.80 | 4,477.9 | 4,205 | 0.42 |
| 20 | 1.00390 | 1,046 | 1,050.1 | 16.53 | 33.06 | 3,032.8 | 3,021 | 0.30 |
| 21 | 1.02866 | 1,069 | 1,099.6 | 17.31 | 34.62 | 3,175.9 | 3,087 | 0.31 |
| 22 | 1.12517 | 267 | 300.42 | 4.73 | 9.46 | 867.66 | 771 | 0.08 |

$B_c$ = Content of Cu in Sample (gm)

$C_c$ = Cu in Sample (moles), ($B_c$/63.54)

$D_c$ = S in Chalcopyrite (moles), $2C_c$

$E_c$ = Microgram Chalcopyrite, $B_c$/0.34624

$F_c$ = $E_c$/Wt. of Sample, (ppm)

Table 7. Calculation of Weight Percent of Pyrrhotite, $Fe_{0.8}S$, in Whole Rock Samples from the Atomic Absorption Analyses

F. Wt. = 76.7416 S/F. Wt. = 0.41782

| Sample No. | Total S in Sample | Weight of Sample | $B_s$ | $C_s$ | $D_c$ | $D_p$ | $D_s$ | Sulphur in Pyrrhotite $32.06D_s$ | $E_s$ | $F_s$ | Weight % of Pyrrhotite |
|---|---|---|---|---|---|---|---|---|---|---|---|
| | % | gm | microgm | micromole | micromole | micromole | micromole | microgm | microgm | ppm | % |
| 7 | 0.167 | 1.13374 | 1893.4 | 59.05 | 12.60 | 27.89 | 18.57 | 595.35 | 1424.9 | 1257 | 0.13 |
| 8 | 0.426 | 1.03751 | 4419.8 | 137.86 | 55.88 | 29.79 | 52.19 | 1673.2 | 4004.6 | 3860 | 0.39 |
| 9 | 0.325 | 1.04007 | 3380.2 | 105.43 | 55.06 | 23.73 | 26.64 | 854.1 | 2044.1 | 1965 | 0.20 |
| 10 | 0.651 | 1.04961 | 6833.0 | 213.13 | 112.52 | 31.15 | 69.46 | 2226.9 | 5329.8 | 5078 | 0.51 |
| 11 | 1.402 | 1.01655 | 14252. | 444.54 | 61.38 | 135.20 | 247.96 | 7949.6 | 19026. | 18720 | 1.87 |
| 12 | 0.669 | 1.03507 | 6924.0 | 215.99 | 30.70 | 72.94 | 112.35 | 3601.9 | 8620.8 | 8329 | 0.83 |
| 13 | 0.389 | 1.02568 | 3989.0 | 124.45 | 22.02 | 56.42 | 46.01 | 1475.1 | 3530.4 | 3442 | 0.34 |
| 14 | 0.211 | 1.03954 | 2193.4 | 68.42 | 25.98 | 34.31 | 8.13 | 260.65 | 623.83 | 600 | 0.06 |
| 15 | 1.039 | 1.02418 | 10641 | 331.92 | 33.04 | 131.32 | 167.56 | 5372.0 | 12857. | 12554 | 1.26 |
| 16 | 0.100 | 1.01183 | 1011.8 | 31.56 | 18.08 | 15.74 | | | | | |
| 17 | 0.253 | 1.04296 | 2638.7 | 82.30 | 21.24 | 30.48 | 30.58 | 980.4 | 2346.4 | 2249.8 | 0.22 |
| 18 | 0.149 | 1.01380 | 1510.6 | 47.12 | 14.16 | 21.01 | 11.95 | 383.1 | 916.95 | 904.5 | 0.09 |
| 19 | 0.861 | 1.06485 | 9168.4 | 285.98 | 48.80 | 96.04 | 141.14 | 4525.0 | 10830. | 10170. | 1.02 |
| 20 | 0.774 | 1.00390 | 7770.2 | 242.36 | 33.05 | 71.04 | 138.26 | 4432.6 | 10609. | 10568. | 1.06 |
| 21 | 0.616 | 1.02866 | 6336.6 | 197.65 | 34.62 | 63.96 | 99.07 | 3176.2 | 7601.8 | 7390. | 0.74 |
| 22 | 0.137 | 1.12517 | 1541.5 | 48.08 | 9.46 | 17.40 | 21.22 | 680.3 | 1628.2 | 1447. | 0.14 |

$B_s$ = Total S in Sample (gm)

$C_s$ = S in Sample (moles), $B_s/32.06$

$D_c$ = S in Chalcopyrite (moles), ($D_c$ in Table 6)

$D_p$ = S in Pentlandite (moles), ($D_p$ in Table 5)

$D_s$ = S in Pyrrhotite (moles), $C_s - (D_c + D_p)$

$E_s$ = Microgram Pyrrhotite, S in Pyrrhotite (gm)/0.41782

$F_s$ = $E_s$/Wt. of Sample (ppm)

Table 8. Proportion of Sulphide Minerals in Whole Rock Samples

| Sample No. | Pentlandite Wt.% Table 5 | Chalcopyrite Wt.% Table 6 | Pyrrhotite Wt.% Table 7 | Pentlandite % | Chalcopyrite % | Pyrrhotite % |
|---|---|---|---|---|---|---|
| 7 | 0.238 | 0.102 | 0.126 | 51 | 22 | 27 |
| 8 | 0.277 | 0.494 | 0.386 | 24 | 43 | 33 |
| 9 | 0.220 | 0.486 | 0.197 | 24 | 54 | 22 |
| 10 | 0.287 | 0.984 | 0.508 | 16 | 55 | 29 |
| 11 | 1.28 | 0.554 | 1.87 | 35 | 15 | 50 |
| 12 | 0.680 | 0.272 | 0.833 | 38 | 15 | 47 |
| 13 | 0.531 | 0.197 | 0.344 | 50 | 18 | 32 |
| 14 | 0.319 | 0.229 | 0.060 | 52 | 38 | 10 |
| 15 | 1.24 | 0.296 | 1.26 | 44 | 11 | 45 |
| 16 | 0.150 | 0.164 | - | - | - | - |
| 17 | 0.282 | 0.187 | 0.225 | 41 | 27 | 32 |
| 18 | 0.200 | 0.128 | 0.09 | 48 | 31 | 21 |
| 19 | 0.871 | 0.421 | 1.02 | 38 | 18 | 44 |
| 20 | 0.683 | 0.302 | 1.06 | 33 | 15 | 52 |
| 21 | 0.600 | 0.309 | 0.739 | 36 | 19 | 45 |
| 22 | 0.149 | 0.077 | 0.145 | 40 | 21 | 39 |
| | | | Average | 38 | 27 | 35 |

Table 9. Determination of Chromite Content of Whole Rock Samples calculated from the Atomic Absorption Analyses

($Cr/Cr_2O_4$=0.309515) Average $Cr_2O_4$ Wt.% in Chromite=38.85

| Sample No. | Weight of Sample gm | Content of Cr in sample gm | $A_{Cr}$ ppm | $B_{Cr}$ microgm | $E_{Cr}$ microgm | $E'_{Cr}$ microgm | $F_{Cr}$ ppm | Weight % of Chromite % | Spinel Vol.* % |
|---|---|---|---|---|---|---|---|---|---|
| 1 | 1.03627 | 12,931 | 11,931 | 12,364 | 39,946 | 102,820 | 99,221 | 9.9 | 5.0 |
| 2 | 1.09019 | 4,403 | 3,403 | 3,710 | 11,986 | 30,853 | 28,300 | 2.8 | 2.0 |
| 3 | 1.07594 | 3,834 | 2,834 | 3,049 | 9,852 | 25,358 | 23,568 | 2.4 | 2.0 |
| 4 | 1.03204 | 17,683 | 16,683 | 17,218 | 55,627 | 143,185 | 138,740 | 14. | 4.0 |
| 5 | 1.07704 | 7,567 | 6,567 | 7,073 | 22,852 | 58,820 | 54,613 | 5.5 | 3.5 |
| 6 | 1.01310 | 5,281 | 4,281 | 4,337 | 14,012 | 36,068 | 35,601 | 3.5 | 1.5 |
| 7 | 1.13374 | 10,452 | 9,452 | 10,716 | 34,622 | 89,118 | 78,605 | 7.9 | 4.0 |
| 8 | 1.03751 | 6,813 | 5,843 | 6,062 | 19,586 | 50,414 | 48,592 | 4.9 | 2.0 |
| 9 | 1.04007 | 5,288 | 4,288 | 4,460 | 14,409 | 37,089 | 35,660 | 3.5 | 2.0 |
| 10 | 1.04961 | 6,788 | 5,788 | 6,075 | 19,628 | 50,522 | 48,134 | 4.8 | 3.0 |
| 11 | 1.01655 | 5,115 | 4,115 | 4,183 | 13,515 | 34,788 | 34,221 | 3.4 | 2.5 |
| 12 | 1.03507 | 10,241 | 9,241 | 9,565 | 30,903 | 79,546 | 76,850 | 7.7 | 3.0 |
| 13 | 1.02568 | 9,311 | 8,311 | 8,524 | 27,541 | 70,891 | 69,116 | 6.9 | 5.0 |
| 14 | 1.03954 | 4,593 | 3,593 | 3,735 | 12,067 | 31,062 | 29,880 | 3 0 | 0.75 |
| 15 | 1.02418 | 3,930 | 2,930 | 3,001 | 9,695 | 24,956 | 24,367 | 2.4 | 1.0 |
| 16 | 1.01183 | 4,596 | 3,596 | 3,639 | 11,756 | 30,259 | 29,905 | 3.0 | 1.0 |
| 17 | 1.04296 | 5,273 | 4,273 | 4,457 | 14,399 | 37,062 | 35,535 | 3.6 | 1.0 |
| 18 | 1.01384 | 5,228 | 4,228 | 4,287 | 13,849 | 35,648 | 35,161 | 3.5 | 0.75 |
| 19 | 1.06485 | 5,024 | 4,024 | 4,285 | 13,844 | 35,635 | 33,465 | 3.3 | 1.0 |
| 20 | 1.00390 | 3,611 | 2,611 | 2,621 | 8,469 | 21,798 | 21,714 | 2.2 | 0.5 |
| 21 | 1.02866 | 2,382 | 1,382 | 1,422 | 4,593 | 11,822 | 11,493 | 1.1 | 0.1 |
| 22 | 1.12517 | 2,355 | 1,355 | 1,525 | 4,926 | 12,679 | 11,269 | 1.1 | 0.1 |
| 23 | 1.09220 | 2,724 | 1,724 | 1,883 | 6,084 | 15,659 | 14,338 | 1.4 | 0.1 |
| 24 | 1.03697 | 2,748 | 1,748 | 1,813 | 5,855 | 15,074 | 14,537 | 1.5 | 0.25 |
| 25 | 1.02850 | 2,431 | 1,431 | 1,472 | 4,755 | 12,240 | 11,901 | 1.2 | 0.5 |

$A_{Cr}$=Content of Cr - 1000 (ppm); 1000 ppm is estimated Cr contribution from pyroxene. $B_{Cr}$=Content of Cr in Sample (gm)
$E_{Cr}$=$Cr_2O_4$ (microgm), $B_{Cr}/0.309515$ $E'_{Cr}$=$FeCr_2O_4$ (microgram), $E_{Cr}/0.3885$ $F_{Cr}$=$FeCr_2O_4$ (ppm), $E'_{Cr}$/Wt. of Sample

* Estimated to the nearest 0.25% by point-counting of the thin sections by J.M. Garth

The weight percent of chromite was estimated in a similar way, assuming the weight percent $Cr_2O_4$ is 38.85% as indicated by a complete chromite analysis given by Cousins (1969). The result of the calculation is shown in Table 9. The chemical estimate of chromite and the microscopic estimate of spinel volume do not agree well in absolute value (although the trend in relative values is similar). The reason is largely that chromium content in pyroxene is assumed to be 1,000 ppm for the whole rock samples and the microscopic values may be of low accuracy because of irregular distribution and small grain size of spinels. The chemical values are used to estimate the contribution of chromite to whole rock PGMs and therefore give a maximum value for this component.

## 4.5. Contents of Pt, Pd, Ir and Au by Neutron Activation Analysis

### 4.5.1. Whole Rock Analyses

The PGM values obtained from neutron activation analyses of whole rock samples are given in Table 10 and Fig. 9, which also show the results of S and modal spinels. The sample number 1 through 25 refer to the 25 slices cut perpendicular to the core axis, each sample representing about 1.08 inches. Core footages giving distances of sample

Table 10. Neutron Activation PGM Values for Whole Rock Samples

| Sample No. | Pt ppm | Pd ppm | Ir ppm | Au ppm |
|---|---|---|---|---|
| 1 | 2.75 | 0.511 | 0.0884(2) | 0.0315 |
| 2 | 1.20 | 0.217 | 0.033 | 0.0097 |
| 3 | 1.34(2) | 0.177(2) | 0.0378(3) | 0.0798(2) |
| 4 | 4.2 | 0.722 | 0.100 | 0.033 |
| 5 | 3.9 | 2.2 | 0.0579(2) | 0.0343 |
| 6 | 2.1 | 0.683 | 0.0236 | 0.087 |
| 7 | 4.5 | 1.6 | 0.0853(2) | 0.109 |
| 8 | 7.8 | 1.7 | 0.0306 | 0.366 |
| 9 | 14.8(6) | 1.31(4) | 0.0193(5) | 0.963(5) |
| 10 | 8.1 | 13.8 | 0.0735(2) | 3.4 |
| 11 | 15.0 | 7.7 | 0.0793(2) | 0.286 |
| 12 | 4.3 | 1.8 | 0.0501(2) | 0.395 |
| 13 | 1.2 | 1.1 | 0.0255(2) | 0.549 |
| 14 | 1.6 | 0.541 | 0.0116 | 0.333 |
| 15 | 3.1 | 2.1 | 0.0435(2) | 0.680 |
| 16 | 0.375 | 0.157 | 0.0071 | 0.0849 |
| 17 | 3.8 | 0.444 | 0.0133(2) | 0.918 |
| 18 | 0.721 | 0.148 | 0.0071 | 0.134 |
| 19 | 0.926 | 1.1 | 0.0294(2) | 0.332 |
| 20 | 4.5 | 1.4 | 0.0216 | 1.5 |
| 21 | 1.56(2) | 1.08(2) | 0.083(2) | 0.362(2) |
| 22 | not det. | 0.217 | 0.0678 | 0.344 |
| 23 | 0.38(2) | 0.114(2) | 0.0134(2) | 0.0409(2) |
| 24 | 0.56(2) | 0.055(2) | 0.0183(2) | 0.0661(2) |
| 25 | 0.79(2) | 0.096(2) | 0.0144(2) | 0.237(2) |
| Average | (3.73) | (1.64) | (0.0414) | (0.455) |
| | 3.7 | 1.6 | 0.04 | 0.46 |

The determinations of Pt, Pd, Ir and Au without duplicate (or replicate) number were carried out by J.M. Garth.

( ) = number of determinations

not det. = not detected.

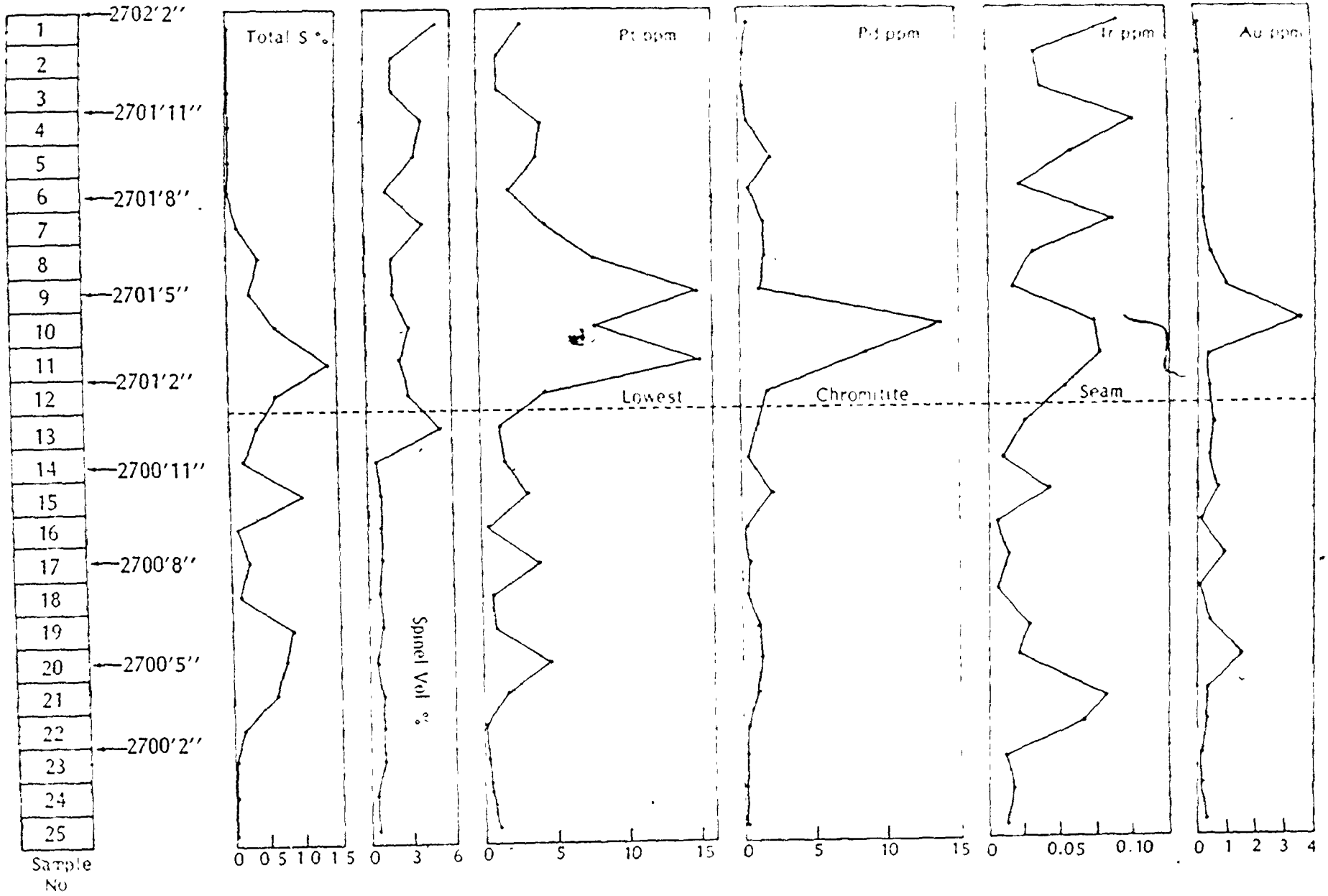


Fig. 9 PROFILES FOR Pt, Pd, Ir, AND Au ACROSS THE CHROMITITE SEAM

above and below the chromitite seam are also shown. The core top is about 2 feet below the hanging wall of the Merensky feldspathic pyroxenite unit.

4.5.2. Separated Mineral Samples

The contents of Pt, Pd, Ir and Au in sulphide grains drilled from polished sections are shown in Table 11 and Figs. 10, 11 and 12. The contents of the four PGMs in oxides and composite grain samples are given in Table 12 and Figs. 10, 11 and 12, which also show whole rock PGM values for comparison.

Percents of total whole rock metals contributed by sulphides and oxides (T in Table 13) were calculated from the following equation:

$$T = \frac{(SxSsi) + (CxOsi)}{Ri} \times 100\%$$

where S=weight fraction of sulphides in the whole rock (Table 8)

C=weight fraction of chromite in the whole rock (Table 9)

Ri=metal concentration in the whole rock in ppm (Table 10)

Ssi=average metal concentration in separated sulphide grains in ppm (Table 11)

Osi=average metal concentration in separated oxides in ppm (Table 12)

i = Pt, Pd, Ir and Au

and the results of the calculation are shown in Tables 13 and 13a.

Table 11. Neutron Activation PGM Values for Sulphide Grains

| Sample No. | Separate Grain No. | Number of Sulphide Grains | Weight of Sample mg | Metal Contents of Sulphides ppm | | | | Model Percent | | | Average Grain Size, mm | Type of Sulphide Grains II, III |
|---|---|---|---|---|---|---|---|---|---|---|---|---|
| | | | | Pt | Pd | Ir | Au | $CuFeS_2$ | $(Fe,Ni)_9S_8$ | $Fe_{0.8}S$ | | |
| 7 | 7-1 | 1 | 6.429 | 0.41 | 28.5 | 1.21 | 0.44 | *trace | trace | 99 | 2.6 | II, III |
| | 7-2 | 3 | 4.155 | 0.96 | 32.0 | 1.41 | 0 23 | 0.63 | 2.9 | 96.4 | 1.9 | II, III |
| 11 | 11-1 | 1 | 8.474 | 0.30 | 36.8 | 1.41 | 0.02 | 0.91 | 38.1 | 60.9 | 3.0 | I |
| | 11-2 | 1 | 7.309 | 1.33 | 20.6 | 0.81 | 0.08 | 4.0 | 16.8 | 79.2 | 1.8 | I |
| | 11-3 | 1 | 7.687 | 0.82 | 0.8 | 1.31 | 0.50 | 0.1 | 0.6 | 99.3 | 3.0 | II, III |
| 12 | 12-1 | 1 | 3.385 | 5.44 | 22.0 | 3.91 | 0.77 | 4.6 | 25 7 | 69.7 | 1.6 | I |
| 15 | 15-1 | 2 | 0.832 | 4.44 | 18.8 | 0.51 | 0.61 | 0.6 | 0.6 | 98.8 | 1.4 | II, III |
| 15-16 | 15-16-1 | 1 | 8.869 | 24.6 | 19.4 | 0.85 | 6.11 | 1.4 | 22.6 | 76 0 | 2.1 | II |
| 17 | 17-1 | 1 | 3.356 | 0.60 | 5.1 | 0.68 | 0.22 | 0 | 8.5 | 91.5 | 1.8 | II |
| | 17-2 | 3 | 3.000 | 1 44 | 22.5 | 0 58 | 0.07 | 0.3 | 17.0 | 82.7 | 1.6 | III |
| 18-19 | 18-19-1 | 1 | 10 436 | 0.75 | 3.12 | 0.98 | 0 62 | 0.5 | 17.6 | 81.9 | 2.7 | II, III |
| 20 | 20-1 | 2 | 19.715 | 2.22 | 38.4 | 1.15 | 0 79 | 0 | 28.9 | 71.1 | 2.8 | II, III |
| | 20-2 | 2 | 6.416 | not det. | 24.7 | 0.97 | 9.32 | 0.2 | 0 3 | 99.5 | 2.9 | II |
| | 20-3 | 4 | 6.820 | 2.70 | 27.6 | 0.64 | 11.94 | 1.5 | 42.8 | 55.7 | 1.4 | II |
| 21 | 21-1 | 1 | 5.710 | 9.51 | 43.5 | 3.38 | 1.20 | 0.6 | 34.8 | 64 6 | 2.2 | I |
| | 21-2 | 1 | 20.080 | 3 96 | 42.3 | 1.52 | 0.89 | 0 | 39.5 | 60.5 | 3 8 | II, III |
| | 21-3 | 1 | 21.810 | 12.84 | 38.9 | 1.74 | 1.35 | 6.10 | 25.3 | 68.6 | 3.5 | I |
| | 21-4 | 1 | 9.428 | 2.31 | 47.0 | 1.62 | 0 35 | 0 | 46 5 | 53 5 | 3 7 | II, III |
| | 21-5 | 1 | 15.244 | 5.01 | 85.0 | 1.33 | 0.16 | 0.1 | 42 6 | 57.3 | 4.1 | II, III |

not det. = not detected  Types of Sulphide Grains I--III (see text)

* = poor section, sample taken from edge

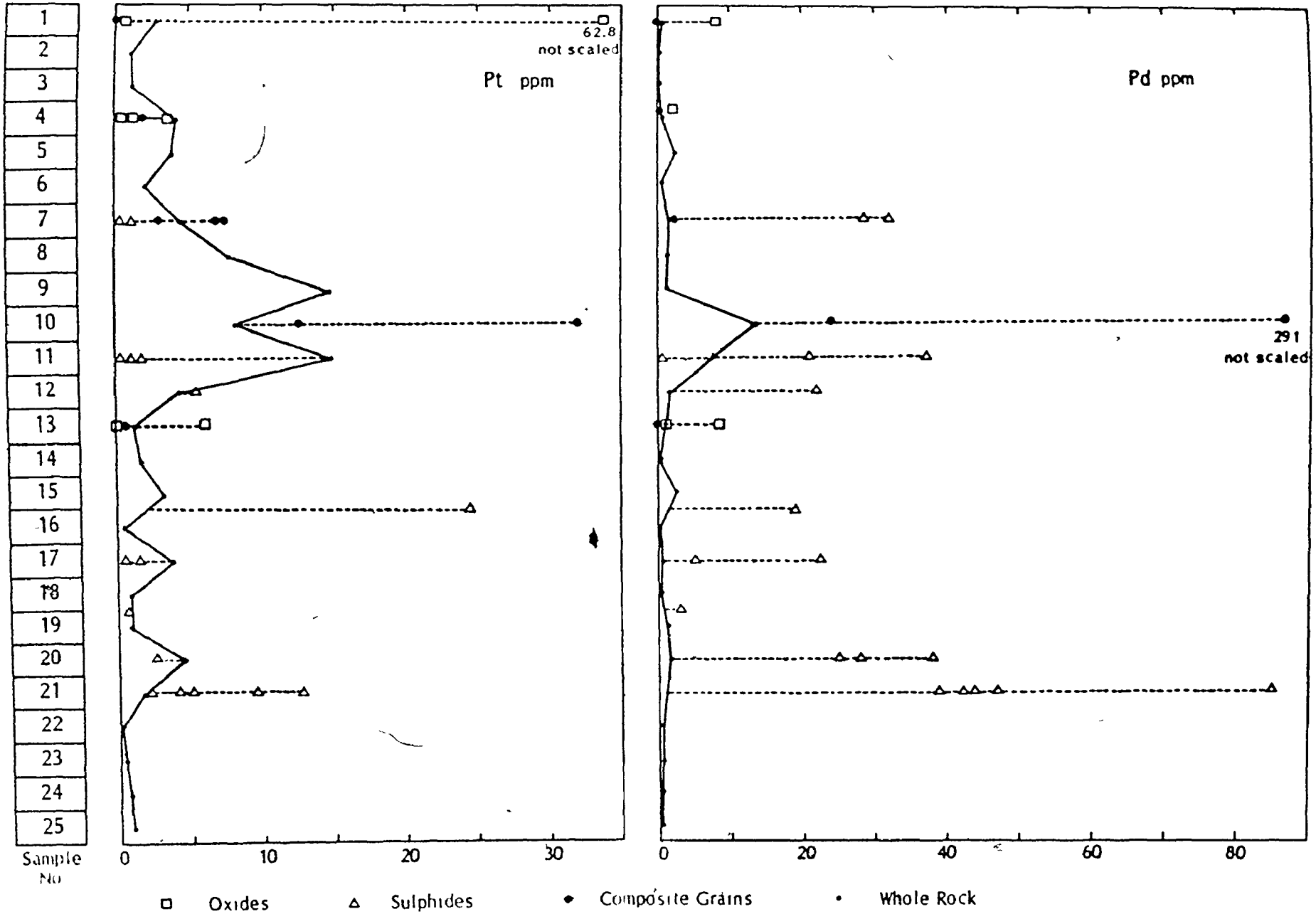


Fig.10 CONTENTS OF Pt AND Pd IN OXIDES, SULPHIDES, COMPOSITE GRAINS AND WHOLE ROCK

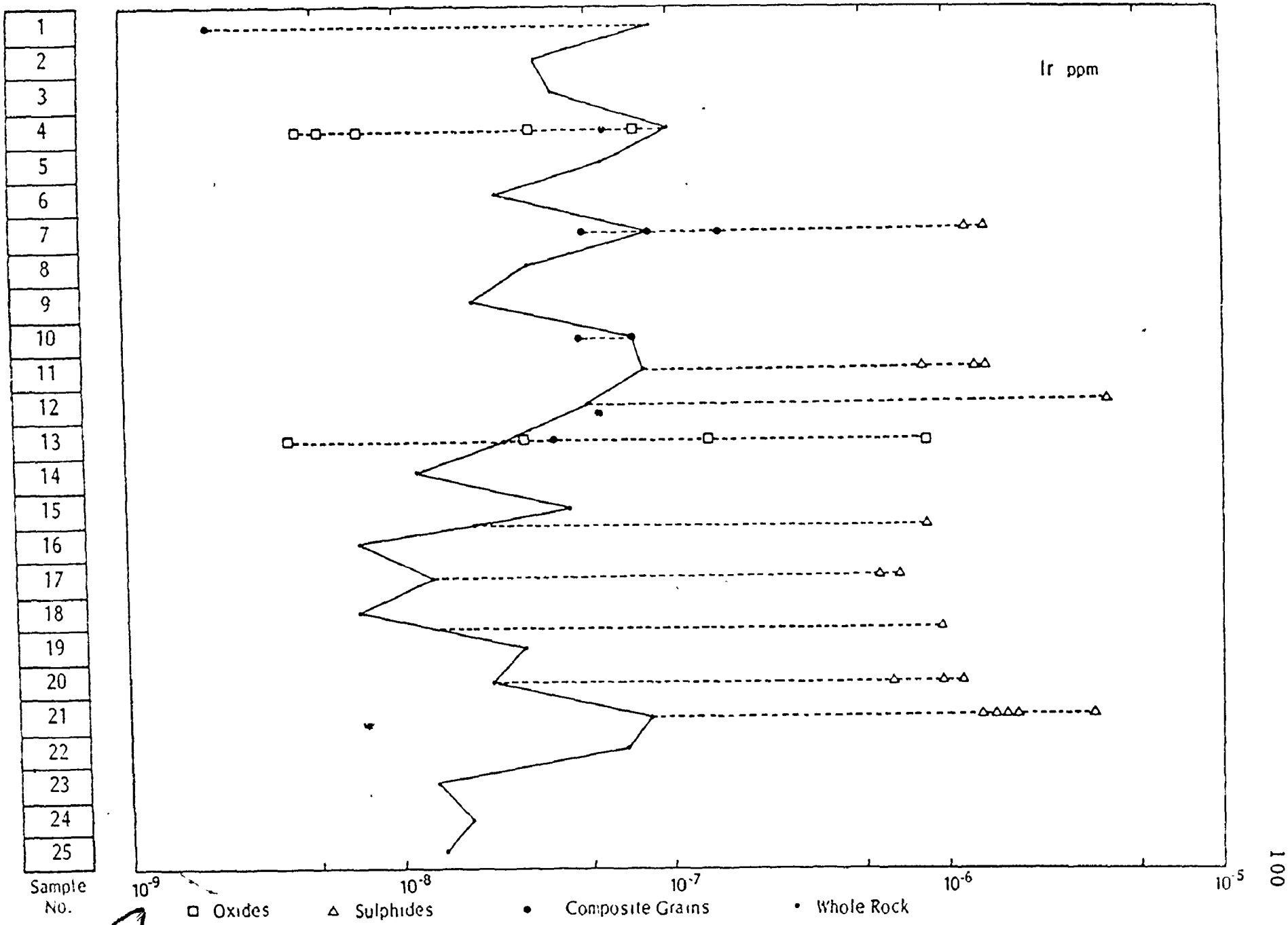


Fig. 11 CONTENTS OF Ir IN OXIDES, SULPHIDES, COMPOSITE GRAINS AND WHOLE ROCK

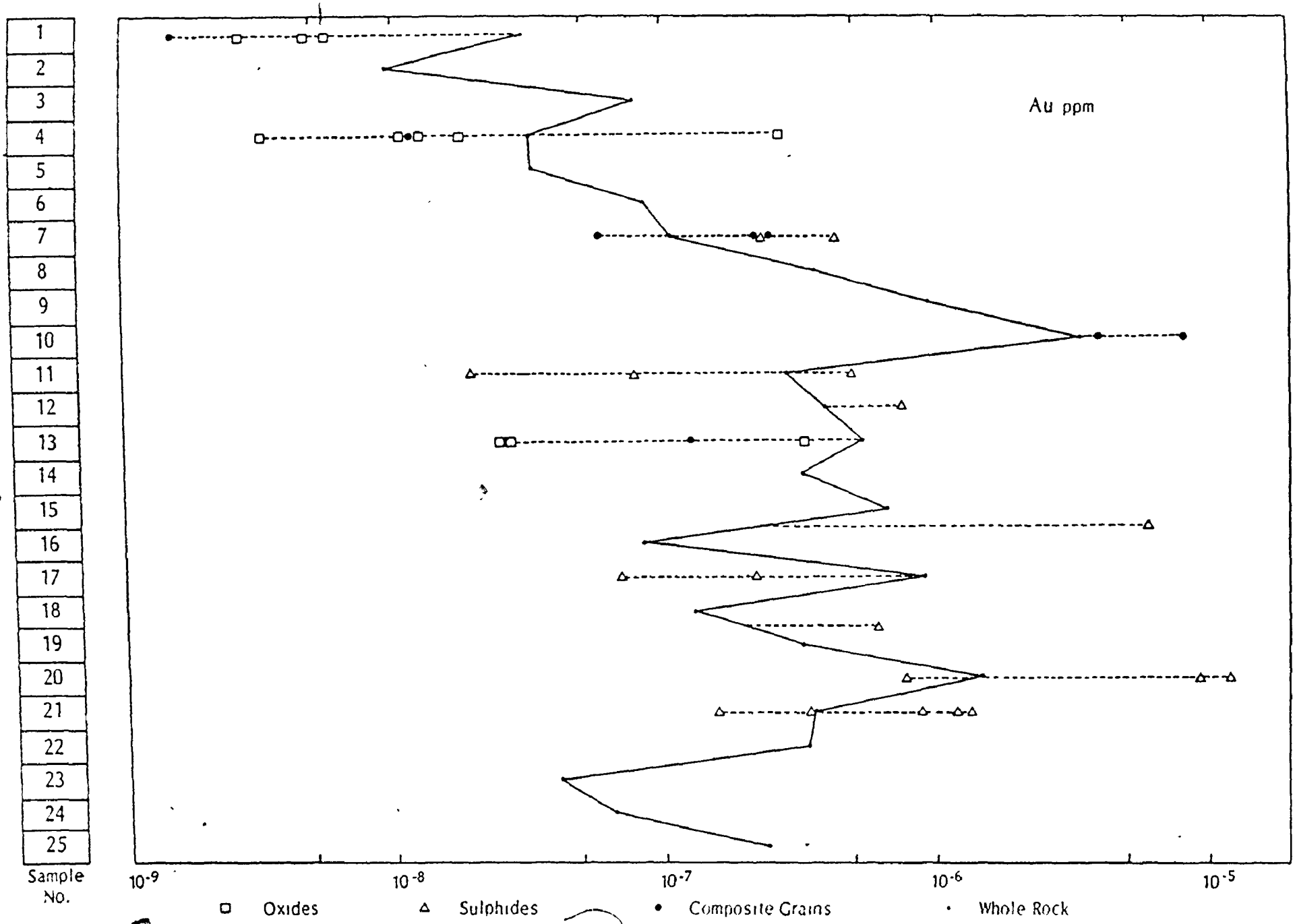


Fig. 12 CONTENTS OF Au IN OXIDES, SULPHIDES, COMPOSITE GRAINS AND WHOLE ROCK

Table 12. Neutron Activation PGM Values for Oxides and Composite Grain Samples

| Sample No. | Separate No. | Weight of Sample mg | Magnetic Susceptibility[1] | Purity % of Oxides | Metal Contents of Oxides Pt ppm | Pd ppm | Ir ppb | Au ppb | Main Minerals after X-ray Powder Diffraction |
|---|---|---|---|---|---|---|---|---|---|
| 1 | 1-1 | 27 00 | I | 94 | 0.45 | 0 13 | )not | 2.8 | Magnetite, Chromite |
| | 1-2 | 41.00 | II | 94 | 0.14 | 0 15 | )deter- | 4.8 | Magnetite, Chromite |
| | 1-3 | 18.49 | III | 94 | 63. | 8.2 | )mined | 5.7 | Magnetite, Chromite |
| | 1-4 | 45.19 | IV | ~50 | 0 06 | 0.07 | 2.1 | 1.6 | Hypersthene, Pyrophyllite, Magnetite, Chromite |
| 4 | 4-1a | 26.56 | I | 95 | 3.7 | 0.67 | 75 | 268 | Magnetite, Chromite |
| | 4-1b | 38.09 | I | 95 | 1 1 | 2.1 | 31 | 13. | " " |
| | 4-2a | 40.56 | II | 95 | 0.47 | 0.13 | 4 4 | 11. | " " |
| | 4-2b | 29.60 | II | 95 | 0 78 | 0.10 | 7 3 | 3 4 | " " |
| | 4-2c | 42.22 | II | 95 | 0 40 | 1 0 | 5.3 | 18 | " " |
| | 4-3 | 26 87 | III | 95 | 0 95 | 0 79 | 75 | 3.4 | |
| | 4-4 | 56 00 | IV | ~50 | 1 8 | 0 52 | 59 | 12 | Hypersthene, Pyrophyllite, Magnetite, Chromite |
| 7 | 7-1 | 53 85 | I | ~50 | 3.1 | 2.3 | 50 | 59. | Magnetite, Chromite, Pyrophyllite |
| | 7-2a | 54 31 | II | ~30 | 7.3 | 2 8 | 151. | 249 | Hypersthene, Pyrophyllite, Cordierite |
| | 7-2b | 80.99 | II | ~50 | 7.0 | 2 3 | 84. | 23. | Talc, Hypersthene, Chromite, Cordierite |
| 10 | 10-1 | 57 45 | I | ~50 | 32. | 24 | 47. | 8220. | Hypersthene, Pyrophyllite, Magnetite |
| | 10-2 | 80 85 | II | ~50 | 13. | 291. | 74 | 3930 | Hypersthene, Cordierite, Talc |
| 13 | 13-1 | 15 88 | I | 83 | 6 0 | 8 6 | 850. | 327. | Magnetite |
| | 13-2 | 47.85 | II | 93 | 0 14 | 0.05 | 4 0 | 26. | Magnetite, Chromite |
| | 13-3a | 40 18 | III | 90 | 0.79 | 1.8 | 137. | 28. | Magnetite, Chromite |
| | 13-3b | 26 81 | III | 90 | 0.14 | 0.41 | 29 | 27. | Magnetite, Chromite |
| | 13-4 | 33 75 | IV | ~50 | 0 69 | 0.52 | 38 | 129 | Hypersthene, Pyrophyllite, Magnetite, Chromite |

' Composite grains

[1] Oxides have wide range of magnetic susceptibility, generally two to four fractions of progressively lower magnetic susceptibilities separated on a Franz magnetic separator. Each separate was assigned sequential No. I through IV Letters a, b, and c are used to indicate the same sample, i.e. same magnetic susceptibility.



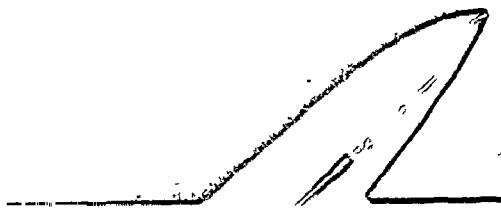

Table 13. Calculation of Percent of Total PGM+ Contributed by Sulphides and Oxides

| Sample No. | Ri Metal Concentrations in Whole Rock Samples, ppm | | | | (SxSsi) + (CxOsi) Sum of Metals in Sulphides and Oxides ppm | | | | T Percent of Total Whole Rock Metal Contributed by Sulphides and Oxides, % | | | |
|---|---|---|---|---|---|---|---|---|---|---|---|---|
| | Pt | Pd | Ir | Au | Pt | Pd | Ir | Au | Pt | Pd | Ir | Au |
| 1 | 2.75 | 0.51 | 0.0884 | 0.0315 | 0.03 | 0.014 | (0.0002) | 0.0004 | 1.1 | 2 7 | (0.23) | 1.3 |
| 4 | 4.2 | 0.72 | 0.100 | 0.033 | 0.17 | 0.11 | 0 0046 | 0.0014 | 4 0 | 15. | 4.6 | 4.2 |
| 7 | 4.5 | 1.6 | 0.0853 | 0.109 | 0.245 | 0 32 | 0.010 | 0.0053 | **5.5 | 20. | 12. | 5.8 |
| 10 | 8.1 | 13.8 | 0.0735 | 3.4 | 1.07 | 1.15 | 0.0029 | 0.29 | (13. | 8.3 | 3.9 | 8 5) |
| 11 | 15.0 | 7.7 | 0.0793 | 0.286 | 0.030 | 0.72 | 0.044 | 0.007 | *0 2 | -9.3 | 55. | 2.6 |
| 12 | 4.3 | 1.8 | 0.0501 | 0.395 | 0.097 | 0.39 | 0.070 | 0.014 | *2 3 | 22. | ~100 | 3 5 |
| 13 | 1.2 | 1.1 | 0.0255 | 0.549 | 0.025 | 0.052 | 0.0012 | 0.0019 | 2.1 | 4.7 | 4.7 | 0 3 |
| 15-16 | 1.74 | 1.13 | 0 0253 | 0.382 | 0.35 | 0.28 | 0.012 | 0.087 | *20. | 24. | 48. | 23 |
| 17 | 3.8 | 0.44 | 0.0133 | 0.918 | 0.007 | 0.095 | 0.0043 | 0 0010 | *0.18 | 22 | 32. | 0.11 |
| 18-19 | 0.825 | 0.625 | 0.0183 | 0.233 | 0.010 | 0 042 | 0 013 | 0.0084 | *1.2 | 6.8 | 73. | 3.6 |
| 20 | 4.5 | 1.4 | 0.0216 | 1.5 | 0.050 | 0.62 | 0.019 | 0.15 | *1 1 | 44. | 88. | 10 |
| 21 | 1.56 | 1.09 | 0.083 | 0.362 | 0.11 | 0.85 | 0 032 | 0.013 | *7.1 | 78. | 38. | 3.6 |
| | | | | | | | | Average | 5. | 21. | 38 | 5.5 |

** = Sulphide and Oxide  * = Sulphide only  No symbol = Oxide only
( ) = Composite grains only

Table 13a. Calculation of Percent of Total PGM+ Contributed by Sulphides and Oxides for Sample No. 7

| | Pt | Pd | Ir | Au |
|---|---|---|---|---|
| Sulphide Contribution, % | 0.07 | 8.9 | 7.3 | 1.5 |
| Composite Grain Contribution, % | 5.4 | 11.0 | 4.6 | 4.3 |

# CHAPTER V

# DISCUSSION

Interpretation of the results obtained in this work and comments on previous studies will be given under the following sub-headings: petrology of the core, mode of occurrence of PGMs and interpretation of the Lonrho Data.

## 5.1. Petrology of the Core

The rock is a feldspathic pyroxenite in which orthopyroxene is the main cumulus phase. The next most abundant minerals, plagioclase and clinopyroxene, are mainly intercumulus phases. Modal analyses of total pyroxenes and plagioclase (Fig. 7) shows that the variation in pyroxenes is nearly the inverse of that of plagioclase. This results from the fact that these minerals make up about 93% of the rock. Biotite is the most persistent accessory silicate averaging 1%, although occasionally as high as 6.8% (No. 21). The ortho- and clinopyroxenes are hypersthene and diopside respectively, and the plagioclase is bytownite and/or labradorite on the basis of X-ray diffraction analyses of whole rock samples. The occurrences of minor

amounts of chromite, magnetite and talc are noted in almost all samples. However, localized concentration of chromite (and magnetite) was noted at four points in the core, sample No. 1, 4, 7 and 13 (Fig. 9). Further, oxides are essentially confined to the top half of the core.

Extensive hydrous alteration was observed in a localized area 0.5 to 1 inch wide in the middle of the core (Sample No. 10 and 11) and occasionally elsewhere (Sample No.: 15, 16, 20 and 21). The X-ray powder diffraction patterns indicate strong reflections for pyrophyllite and biotite in these samples. Olivine was not identified in the thin sections, but was detected in the X-ray diffraction in the samples approximately below the lowest chromitite seam. Its sporadic presence is reported in the Merensky Reef in the Western Transvaal. The presence of high cordierite and pyrophyllite, not reported previously from the Western Merensky Reef, is indicated by the X-ray data (see p. 83 for discussion).

The occurrence of hydrous minerals, such as amphibole, biotite, pyrophyllite and talc, implies localized hydrothermal or deuteric effects. Magmatic blebs of sulphide grains are still preserved in samples No. 11-1, 11-2, 12-1, 21-1 and 21-3 (Plates 1 and 2). This indicates that the hydrothermal effects was not pervasive but highly localized.

The textural relationship between silicates and sulphides indicates that part of the sulphide represents a nickeliferous immiscible sulphide liquid trapped in the intercumulus pores between the silicate crystals. This sulphide crystallized contemporaneously with plagioclase postdating the crystallization of cumulus orthopyroxene. It appears to be at equilibrium with silicates and occasionally is characterized by pentlandite-chalcopyrite rims of exsolution origin. Other sulphides showing close spatial relationship with hydrous silicates including talc, pyrophyllite, biotite and amphibole are particularly prominent in the middle of the core where the highest PGM values occur. This sulphide, although texturally distinct from that noted above, probably resulted from reaction of primary sulphides with hydrous solutions responsible for the alteration of primary silicates. The origin of the hydrous fluids is probably deuteric.

## 5.2. Mode of Occurrence of PGMs (Platinum Group Metals)

The question of whether the platinum group metals occur mainly in solid solution in sulphides and oxides or as discrete minerals is of considerable practical and academic interest. A brief survey of important arguments on this issue is presented below.

According to Wagner (1929, p. 18), part of the platinum present in the sulphidic ores of the Merensky horizon is in the form of cooperite and sperrylite. The remainder, and the bulk of the palladium, is in solid solution in earlier magmatic sulphides. Adam states that (in Wagner, 1929, p. 21) about one half of the platinum and one-tenth of the palladium in these mixed ores are "free". Schneiderhöhn (ibid, p. 242) stated that the platinum metals are present in the sulphides in solid solution and not in mechanical admixture, and emphasized the possibility of solid solution of sperrylite and pyrite on a basis of crystal structure and ionic radii (p. 243). Apparently he arrived at this conclusion because he did not find platinum minerals in sulphide concentrates (ibid, p. 230). Wagner's footnote, however, indicates that Schneiderhöhn's conclusions refer only to the primary ores of the Potgietersrus district which he examined. In the Rustenburg district cooperite has definitely been identified in the sulphide ore.

The results of an analysis of Cu-Fe sulphides and Schneiderhöhn's semiquantitative analyses of the sulphides led Liebenberg (1970) to conclude that the PGMs had a three-fold mode of occurrence in the Merensky Reef:

1. as S, Sb and As minerals, e.g. sperrylite, cooperite, stibiopalladinite and braggite,

2. as alloys of the PGM or in combination with Fe and other metals, e.g. Au, Ni, Cu and Co, and

3. as a solid solution of the PGM in the sulphides.

Based on microscopic observations, L. Liebenberg drew the following generalizations on the mode of occurrence of PGM minerals 1) they are mostly present along sulphides - silicates boundaries, 2) sperrylite is the most abundant platinoid in the Merensky Reef, and is either interstitial to the silicates or cross-cuts sulphides and silicates, and 3) braggite, the main platinum bearer in the Rustenburg Platinum Mine, is usually situated along sulphide-silicate contacts. His mineral A, $BiPd_3$?, is also interstitial to the silicate.

Cousins (1969) thinks that the sulphide correlation with platinoids is not due to chemical association, or solid solution, as suggested by Wagner, but rather, results from gravity concentration. However, he modified this opinion later (1973), stating that the platinoids occur both as individual platinoid minerals and, in base-metal sulphides, the latter representing the main proportion. Those in sulphides are either in solid solution or, to use Cousins' words, as "colloid solid solution".

Cabri (1974), while not referring specifically to the Merensky ores, points out that recent discoveries of numerous new PGM minerals go against the presence of significant PGM in solid solution in sulphides. Rather, their occurrence in sulphides as minute included minerals as well as molecular replacements must be considered.

Stumpfl (1962) noted that the bulk of the Pt-metals in the Novisk deposits, U.S.S.R., is fixed in independent Pt-minerals, but that the possibility that traces of Pt-metals enter the lattice of sulphides and, perhaps, even silicate should not be disregarded.

Wagner (1929, p. 68) and L. Liebenberg (1970) studied the relationship between chromitite and Pt values in the Merensky Suite and concluded that chromitite could have acted as a sponge (Wagner's phrase) as far as the Pt is concerned. The results of spectrographic analyses by Schneiderhöhn (ibid, p. 235) indicate that Merensky chromite does not contain significant PGM concentrations. According to van Zyl (1970) no platinum minerals occur in chromite in the Rustenburg district.

According to Gijbels et al. (1974) high temperature cumulus chromite from the Eastern Bushveld strongly concentrates Ir which is in part subsequently exsolved at lower temperatures. Although van Zyl regards the chromite from the Merensky Reef at Rustenburg as of late magmatic (low temperature) origin, the process suggested by Gijbels

et al. (1974) could potentially result in formation of irregularly distributed platinoid minerals along chromite grain boundaries.

The best indication of PGM in chromite is in the experiments of Grimaldi and Schnepfe (1969) on Stillwater chromite, which very strongly infer a chemical association of Pt and Rh, but not Pd, with chromite. Their experiments do not indicate whether Pt occurs as inclusions within the chromite lattice or in true solid solution. Palladium, however, apparently is neither in solid solution nor as inclusions in chromite. According to Page et al. (1972) major Pt and Pd values occur in the various chromitite seams which are much higher in PGMs than any other rock type in the Stillwater Complex.

## 5.3. Interpretation of the Lonrho Data

### 5.3.1. Whole Rock Data

The general pattern of metal distribution across the core as reflected in whole rock analyses (see Fig. 9) shows sympathetic overall variation of three metals, Pt, Pd, and Au. For these metals maxima occur at approximately the same position in the core, immediately above the chromitite marker horizon. The variation in Ir content is irregular and different from that of the other metals. Although there is a peak above the chromitite marker comparable to

Pt, Pd and Au, there are five additional peaks on the Ir profile, four of which represent Ir contents as high as that at the chromitite marker.

To aid in evaluation of the noble metal trends the contents of S, Cr, Ni and Cu were determined on the same samples (Fig. 8). The Ni and Cu values vary sympathetically with S as might be expected from the presence of Ni and Cu sulphides in the samples. Some regions of the noble metal profiles also correlate positively with the S profile. The maxima in the middle of the core (Sample No. 10 and 11) is matched by a maximum in sulphur content (Sample No. 11). Two lesser highs on the S profile in the region of samples 15 and 20 correspond to above-background values in the same sample regions for all four noble metals, although the effect is not very pronounced for Au. All the sulphur highs are corroborated by observed sulphide in corresponding polished sections. It is, therefore, concluded that in general, the presence of sulphide is correlated with increased noble metal content.

The correlation of noble metal content with Cr differs in several aspects from the noble metal-sulphur relationships. The main variation in Cr content generally correlated with observable chromite occurs above the chromitite marker horizon with highs recorded in

samples 1, 4, 7, 12 and 13, the latter two representing the marker horizon itself. Firstly, it is to be noted that the Cr content in the vicinity of the chromitite marker horizon, where the noble metal maxima occur, is exceeded by samples above it. Thus, although there is a Cr high coincident with the highest noble metal contents, it does not represent the highest Cr content of the core. This contrasts with S where highest noble metal values are coincident with highest S value in the core. Secondly, there are no obvious correlations of Pt, Pd or Au with Cr above the marker chromitite. In contrast, Ir exhibits maxima in samples 1, 4 and 7, precisely the same samples characterized by Cr (and chromite) maxima. Indeed, the highest Cr and Ir values in the entire core are found in the same sample, No. 4. It is suggested then that the Ir profile reflects local chromite accumulation above the marker band whereas most of the profile variance below the marker (where chromite is low and relatively constant) reflects sulphide variation. To explore these generalizations further, oxides and sulphides were separated and analysed. As noted below (oxides and composite grain samples) this interpretation presents some problems when the Ir content of separated oxides and composite grains is considered.

5.3.2. Mineral Data: Sulphides

Pd and Ir are consistently enriched in sulphides. Except for one sample out of nineteen, and in this case for Pd only, these two metals were always significantly enriched in sulphides relative to the whole rock. Enrichments of Pd and Ir in sulphides are 18 and 34 times that of the whole rock values respectively, based on the average concentration of each element. High concentrations of Pd in sulphide grains (Separated Grain No. 11-1, 20-1, 21-1, 21-2, 21-3, 21-4 and 21-5) are observed in the samples with relatively high modal percentages of pentlandite (38, 29, 35, 40, 25, 47, and 43% respectively). The influence of sulphide mineralogical composition can be seen in Fig. 13 in which samples are plotted on a three component compositional diagram using mineral composition in percent as determined with the planimeter from enlargements of polished section mineral photographs. Metal concentrations of each grain are indicated. The concentration contours show a significant displacement of high Pd samples toward the pentlandite apex. A similar plot for Ir showed little evidence of a significant correlation of Ir with pentlandite. Yushko-Zakharova et al. (1970) reported 1 ± 0.08 ppm Pd and 0.02 ± 0.01 ppm Pt for pentlandite specimens from Cu-Ni ores (8 analyses) which were free from microscopically detectable platinum metals. Chyi (1972) also found that in pyrrhotite-pentlandite-chalcopyrite-magnetite assemblages from Strathcona Mine, Sudbury, Pd was consistently

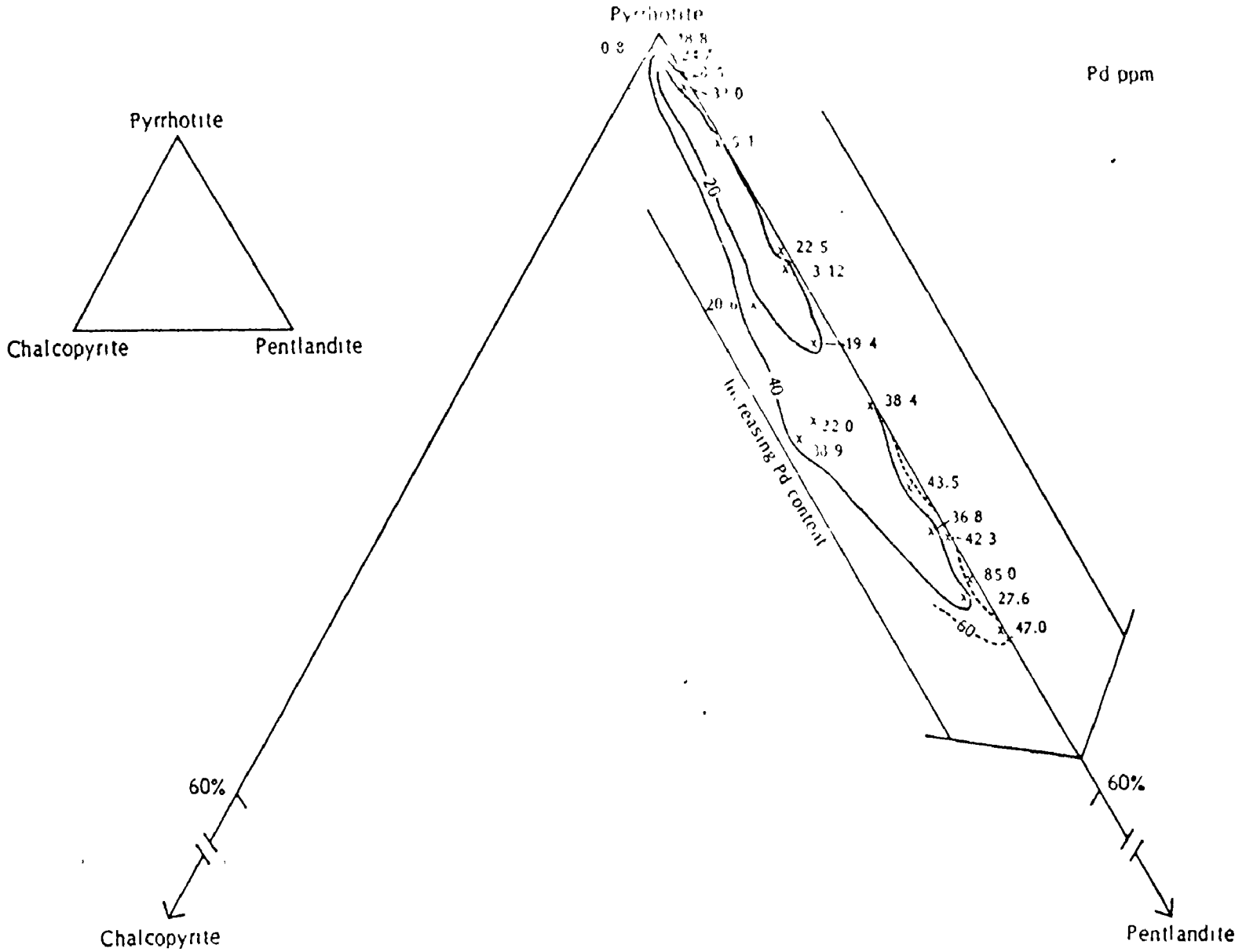


Figures give Pd content of individual samples. Pd contents contoured at 20 ppm interval.
60 ppm contour (dashed line) only suggested due to insufficient data

Fig. 13 MODAL COMPOSITION OF SULPHIDES IN PERCENT PYRRHOTITE, PENTLANDITE AND CHALCOPYRITE

enriched in pentlandite relative to the other three phases. Thus, Pd appears to be closely related to Ni and/or to pentlandite-rich sulphide samples.

Strong enrichment of Pt in sulphides is shown by two core samples, No. 15-16 and 21 only. It is depleted in core samples Nos. 7, 11, 17 and 20 relative to the whole rock values. It appears that sulphides are not as consistently enriched in platinum as either Pd or Ir although the Pt enrichments in the vicinity of samples 15 and 21 do correspond to instances where Pt in sulphides is significantly higher than in the whole rock.

In the case of gold (Fig. 12), enrichment in sulphide is not consistent. Core samples Nos. 15-16 and 20 do show marked (X 10) enrichment of Au in sulphides, possibly accounting for the whole rock trends. However, nearly half the individual sulphide grains analysed were lower in gold than their corresponding whole rock values.

The dispersion of noble metal sulphide values is also worthy of comment. Table 14 presents some simple statistics on the sulphide data which bear on the degree of dispersion of the noble metal values. From Table 14 the average coefficient of variation calculated for individual core sections with replicate analyses indicates the variability of noble metals in sulphides increases in the order $Ir < Pd \leq Pt < Au$.

Thus, Pd variability in individual sulphide grains separated from the same ~1" core section is considerably greater than that of Ir (compare visually Figs. 10 and 11). Both these considerations strongly suggest that the distribution of Pd in sulphides is far more heterogeneous than that of Ir. It is suggested that the cause of this heterogeneity is the presence of much Pd in discrete platinoid minerals within sulphides. In contrast, the uniformity of Ir content, both with respect to the dispersion about the average value for the entire suite of sulphides and the dispersion within a single ca. 1" core sample, is best explained by a highly homogeneous Ir distribution such as would result from solid solution.

5.3.3. Mineral Data: Oxides and Composite Grain Samples

The nature of the genetic relationships, if any, between chromite (and magnetite) and the noble metals are not immediately obvious in the case of the Lonrho samples. Oxide and composite grain samples are generally lower in noble metals than their host whole rock samples. The percentages of oxide analyses giving lower values than the corresponding whole rock values are 70%, 50%, 67% and 70% for Pt, Pd, Ir and Au respectively. Nearly all the oxide and composite grain samples contain both magnetite and chromite according to the X-ray diffraction data although chromite predominates. Important exceptions

Table 14. Mean and Coefficient of Variation for Replicate Sulphide Analyses

| Metal | Sample No. with Replicate Sulphide Analyses | | Mean with Standard Deviation of a Single Measurement, ppm | Coefficient of Variation $(\sigma/\bar{x})X100$ % |
|---|---|---|---|---|
| Pt | 7 | (2) | 0.69±0.39 | 57 |
| | 11 | (3) | 0.82±0.52 | 63 |
| | 17 | (2) | 1.02±0.59 | 58 |
| | 20 | (2) | 2.46±0.34 | 14 |
| | 21 | (5) | 6.73±4.34 | 64 |
| | | | Average | 51 |
| Pd | 7 | (2) | 30.25± 2.47 | 8 |
| | 11 | (3) | 19.40±18.03 | 93 |
| | 17 | (2) | 13.80±12.30 | 89 |
| | 20 | (3) | 30.23± 7.22 | 24 |
| | 21 | (5) | 51.34±19.04 | 37 |
| | | | Average | 50 |
| Ir | 7 | (2) | 1.31±0.14 | 11 |
| | 11 | (3) | 1.18±0.32 | 27 |
| | 17 | (2) | 0.63±0.07 | 11 |
| | 20 | (3) | 0.92±0.26 | 28 |
| | 21 | (5) | 1.92±0.83 | 43 |
| | | | Average | 24 |
| Au | 7 | (2) | 0.34±0.15 | 44 |
| | 11 | (3) | 0.20±0.26 | 130 |
| | 17 | (2) | 0.15±0.11 | 73 |
| | 20 | (3) | 7.35±5.83 | 79 |
| | 21 | (5) | 0.79±0.52 | 66 |
| | | | Average | 78 |

( ) gives number of individual analyses

are samples 10-1 and 10-2, separates from whole rock core sections having the highest noble contents. In these samples the oxide phase is magnetite alone and the composite grain samples have very high Pt and Pd values relative to the whole rock. Thus, the high noble metal values do not appear to be associated with chromite in these samples. Further, it is noted that the oxide separate with the highest noble metal values, sample 13-1, is also magnetite with no chromite detectable by X-ray diffraction.

The Ir data present a special problem because the whole rock Ir values show good correlation with chromite (Sample Nos.: 1, 4 and 7) whereas the oxide mineral separates from the same whole rock samples are generally lower than the whole rock values. A tentative explanation is that the distribution of Ir in these oxides is sufficiently irregular that the sample weights of mineral separates taken were too small to generally include discrete Ir-containing minerals. The widely divergent Pt values on oxide separates in sample No. 1 is certainly suggestive of very heterogeneous metal distribution in chromite. Thus, it does not appear from the present data that concentration of noble metals in oxides is a major factor responsible for high PGM values in this part of the Merensky Reef.

It must be realized that the extension of this conclusion to other PGM deposits or even to other parts of the Merensky Reef is likely not justified. For example, the thicker and more prominent chromite band at the base of the Merensky pyroxenite in the Lonrho area is known to carry platinum values locally (H.H. Bird, written communication).

### 5.3.4. Relative Contribution of Sulphides and Oxides to Total Whole Rock PGMs

The percent of total whole rock noble metals contributed by sulphides and oxides (Table 13 and 13a) appears to be rather variable. For both Pt and Au only 5% of their total whole rock PGM content can, on the average, be accounted for by that attributable to sulphides and oxides. A more important contribution from sulphides and oxides is found for Pd and Ir where averages of 21 and 38% are calculated.

Although the main generalizations noted above are considered realistic, the calculation is subject to a number of uncertainties and is regarded as an estimate. The main sources of error include the following:

1. Both Cr and Ni are partly present in pyroxene as well as chromite and pentlandite. Chemical estimates of mineral proportions require a correction for Ni and Cr in pyroxene (Häkli, 1963). Point

counting estimates are also subject to uncertainty (see p. 61). Although mineral estimates are difficult, the chromite-related PGM contribution to the whole rock total is small, and so a fairly large error in the estimated mineral proportion of chromite would not significantly affect this conclusion.

2. Mineral volume estimates are further complicated by the variable composition of chromite and pentlandite with respect to Cr and Ni. However, literature estimates of $Cr_2O_3$ in Merensky chromites are fairly consistent (Cousins, 1969; van Zyl, 1970).

3. Finally, sulphides which could be sampled are mainly textural Types I and II. Type III sulphides, fine grained replacements along silicate cleavages and disseminations throughout silicates, could not be sampled individually. Type III is an important component of total sulphide in sample Nos. 10 and 11 where high noble metal values occur. Thus, the influence of sulphides could be underestimated, particularly in No. 10.

Neither Pt nor Au appear to be accounted for by the contents found in sulphides and oxides. In the case of Pt rather high solubility in silicates would be required if they (orthopyroxene and plagioclase) are to be significant carriers of Pt. The extremely heterogeneous Pt distribution found in the high Pt region of the core argues strongly for the presence of discrete platinoid minerals, at least in the area. The

general observation that Pt correlates somewhat with sulphur suggests that although sulphides were better hosts for Pt than silicates, the Pt content of the Merensky magma exceeded that which could be accommodated by sulphides alone and the remainder crystallized as discrete platinoid minerals. According to Cousins (1969) the sulphide braggite, (Pt, Pd, Ni)S, occurs in Merensky Reef ores and would be a potential mineralogical constituent of the high sulphur region of the core (Nos. 10, 11 and 12) where very high Pt values are found.

Like Pt, only a small fraction of the gold is accounted for by sulphides and oxides. The average gold content of the core is 455 ppb (332 ppb excluding No. 10) which is approximately 100 times the 1 to 5 ppb commonly found in basic igneous rocks (Crocket, 1971). There is little geochemical evidence that silicate structures accept gold in the hundreds of ppb range. It is suggested that metallic gold is a significant contributor to total whole rock gold.

Both Pd and Ir, on the other hand, appear to be much more strongly associated with sulphides (much less with oxides). In the case of Pd the association appears to be specific to pentlandite. Even so only about one-quarter, of the Pd can be accounted for by sulphides (and oxides). Much the same arguments can be made for the presence of much of the Pd as discrete minerals as were noted for Pt. Although

extreme Pd heterogeneity in peak value region was not tested, very high dispersion of Pd in different samples from the same one inch core specimen was noted (p. 117). It is inferred from this observation that even in the case of obvious association of Pd with sulphides, the Pd is probably not in lattice type solid solution. Rather, it is likely that the Pd was incorporated into the sulphide at a very high temperature magmatic stage when the sulphide was an immiscible liquid. On cooling with subsolidus exsolution of pentlandite from a pyrrhotite host, Pd is expelled from the pyrrhotite host along with Ni resulting in the Pd pentlandite association. This may well increase the Pd concentration (by redistributing it in a smaller volume) and leading to its crystallization as discrete minerals. At any rate the sulphide (pentlandite) - Pd association should not be taken as definite evidence that the Pd is in lattice solid solution in sulphide.

Finally, Ir exhibits the strongest sulphide-oxide association in the sense that nearly 40% of the metal is accounted for by these accessory constituents. In the half of the core below the chromitite seam the sulphide-related Ir accounts for 46% of total Ir. Furthermore, the dispersion of Ir (see Table 14) in these sulphides is considerably less than for the other PGMs. Also the absolute Ir concentration is the lowest of the four metals involved. These factors suggest that

much of the Ir may be present in true lattice solid solution or perhaps as an extremely uniform dispersion of very fine particles in a sulphide host.

## 5.4. Conclusions

To summarize, the following conclusions have been drawn from this study:

1. Pt, Pd and Au are all highly enriched above background in the central portion of the core in association with strong development of hydrous secondary silicate and secondary sulphide. From this association it is inferred that hydrous solutions, probably of deuteric magmatic origin, have played an important role in producing the highest concentrations of PGMs observed.

2. Pd and Ir are enriched in sulphides throughout the core and closely related to pentlandite, although more than 75% of the Pd and 50% of the Ir are not accounted for by a sulphide (and oxide) association. In the case of Pd there are good arguments for the occurrence of much Pd in platinoid minerals.

3. In general, Pt and Au do not show clear enrichment in separated sulphides and oxides. The heterogeneous distribution of Pt in the high concentration area strongly suggests the presence of discrete Pt minerals as a source of much of this metal. Metallic gold is probably a significant contributor to total whole rock gold.

# REFERENCES

American Society for Testing and Materials (1967) (Inorganic). Index to the Powder File, X-ray Powder Data File.

Atkins, F.B. (1969) Pyroxenes of the Bushveld Intrusions, South Africa. J. Petrology, 2, 10:222-49.

Bayley, M.B. (1960) Modal Analysis by Point-counter the Choice of Sample Area. J. Geol. Soc. Australia, 2, 6:119-129.

Berry, L.G. and Thompson, R.M. (1962) X-ray Powder Data for Ore Minerals: the Peacock Atlas. Geol. Soc. Amer. Memoir 85, 281 p.

Borg, I.Y. and Smith, D.K. (1969) Calculated X-ray Powder Patterns for Silicate Minerals. Geol. Soc. Amer. Memoir 122, 896 p.

Brown, G. (1961) The X-ray Identification and Crystal Structures of Clay Minerals. Mineralog. Soc., London, 544 p.

Cabri, L.J. (1974) Some Observations on the Geochemistry of the Platinum-group Elements. Trans. Geol. Soc. S. Afr. 77:65-67.

Chayes, F. (1954) Petrographic Modal Analysis, John Wiley, 113 p.

Chilton, D.A. (1971) Platinum-markets and Mines. Mining Mag, 2, 125:109-115.

Chyi, L.L. (1968) The Geochemistry of Pd, Os, Ir and Au in the Mount Albert Pluton. M.Sc. Thesis, McMaster University.

_____ (1972) Distribution of Some Noble Metals in Sulphide and Oxide Minerals in Strathcona Mine, Sudbury. Ph.D. Thesis, McMaster University.

Coertz, F.J. (1958) Intrusive Relationships and Ore Deposits in the Western Part of the Bushveld Igneous Complex. Trans. Geol. Soc. Sth. Afr., 61:387-392.

Cousins, C.A. (1956) The Value Distribution of Economic Minerals with Special Reference to the Witwatersrand Gold Reefs. Trans. Geol. Soc. Sth. Afr., 59:95-113.

_____ (1962) The Stratigraphy, Structure and Igneous Rocks of the Transvaal System at the Western Areas Gold Mine. Trans. Geol. Soc. Sth. Afr., 65:13-40.

_____ (1969) The Merensky Reef of the Bushveld Igneous Complex, Magmatic Ore Deposits, Monograph No. 4, ed. by Wilson, H.D.B. Econ. Geol., 239-251.

_____ (1973) Notes on the Geochemistry of the Platinum Group Elements. Trans. Geol. Soc. Sth. Afr., 76:77-81.

Crocket, J.H. (1969) Platinum Metals, Handbook of Geochemistry, ed. by Wedepohl, K. Springer-Verlag, Berlin, pp. 78-D-1 - 78-O-2.

_____ (1971) Neutron Activation Analysis for Noble Metals in Geochemistry, in Activation Analysis in Geochemistry and Cosmochemistry, ed. by Brunfelt, A.O. and Steinnes, E. Universitetsforlaget, pp. 339-351.

_____ and Skippen, G. (1966) Radioactivation Determination of Palladium in Basaltic and Ultrabasic Rocks. Geochim. Cosmochim. Acta 30:129-141.

_____, Keays, R.R. and Hsieh, S.S. (1968) Determination of Some Precious Metals by Neutron Activation Analysis. J. Radioanal. Chem. I, 487-507.

Davies, R.D., Allsopp, H.L., Erlandk, A.J. and Manton, W.I. (1970) Sr-isotopic Studies on Various Layered Mafic Intrusions in Southern Africa, Symposium on the Bushveld Igneous Complex and other Layered Intrusions, ed. by Visser, D.J.L. and von Gruenewaldt, G.V. Spec. Publ. No. 1, Geol. Soc. Sth. Afr. pp. 576-593.

Deer, W.A., Howie, R.A. and Zussman, J. (1966) An Introduction to the Rock-forming Minerals. Longmans, 528 p.

Duchesne, J.C. (1972) Iron-titanium Oxide Minerals in the Bjerkrem-Sogndal Massif, South-western Norway. J. Petrol., 13:57-81.

Ferguson, J. and Botha, E. (1964) Some Aspects of Igneous Layering in the Basic Zones of the Busvheld Complex. Trans. Geol. Soc. Sth. Afr., 67:259-278.

_____ and Wright, I.H. (1970) Compositional Variation of Plagioclases in the Critical Series, Bushveld Igneous Complex and Other Layered Intrusions, ed. by Visser, D.J.L. and von Gruenewaldt, G. Spec. Publ. No. 1, Geol. Soc. Sth. Afr., pp. 59-66.

Flanagan, F.J. (1969) U.S. Geological Survey Standards-II. First Compilation of Data for the New U.S.G.S. Rocks. Geochim. Cosmochim. Acta, 33:81-120.

Fleischer, M. (1969) U.S. Geological Survey Standards-I. Additional Data on Rocks G-1 and W-1, 1965-1967. Geochim. Cosmochim. Acta, 33:65-79.

Gijbels, R.H., Millard, H.T. Jr., Desborough, G.A. and Bartel, A.J. (1974) Osmium, Ruthenium, Iridium and Uranium in Silicates and Chromite from the Eastern Bushveld Complex, South Africa. Geochim. Cosmochim. Acta, 38:319-337.

Griffith, W.P. (1967) Iridium in the Chemistry of the Rarer Platinum Metals. Interscience, 227-312.

Grimaldi, F.S. and Schnepfe, M.M. (1969) Mode of Occurrence of Platinum, Palladium and Rhodium in Chromite. U.S. Geol. Survey, Prof. Paper 650-C, pp. C149-C151.

Häkli, A. (1963) Distribution of Nickel between the Silicate and Sulphide Phases in Some Basic Intrusions in Finland. Geologiska Kommission Finland Bulletin No. 209, pp. 37-54.

Hall, A.L. (1932) The Bushveld Igneous Complex of the Central Transvaal. Mem. Geol. Surv. Sth. Afr. 28.

Hartford, W.H. (1963) Chromium in Treatise on Analytical Chemistry ed. by Kolthoff, I.M., Elving, P.J. and Sandell, E.B. Part II, 8:273-377, Wiley.

Heinrich, B.J., Grimes, M.D. and Puckett, J.E. (1961) Sulphur in Treatise on Analytical Chemistry ed. by Kolthoff, I.M., Elving, P.J., and Sandell, E.B. Part II, 7:1-135, Wiley.

Hess, H.H. (1960) Complementary Evidence from the Bushveld Complex, Great Dyke, and Skaergaard Intrusion in Stillwater Igneous Complex, Montana. Geol. Soc. Amer. Mem. 80, pp. 151-167.

_____ and Poldervaart, A. (1968) Basalts. Vols. 1 and 2. Interscience, 862 p.

Jackson, E. D. (1967) Ultramafic Cumulates in the Stillwater, Great Dyke, and Bushveld Intrusions in Ultramafic and Related Rocks, ed. by Wyllie, P.J. Wiley, pp. 20-38.

Jeffery, P.G. (1974) Chemical Methods of Rock Analysis, Pergamon Press, 509 p.

Joint Committee on Powder Diffraction Standards (1974). Powder Diffraction File, Search Manual, Minerals. 1st Edition, U.S.A. 119 p.

_____ (1974) Selected Powder Diffraction Data for Minerals. Publication DBM-1-23, 262 p.

Kalsbeek, F. (1969) Note on the Reliability of Point Counter Analyses. N. Jahrbuch f. Mineralogie, Monatshefte, pp. 1-6.

Keays, R.R. (1968) A Neutron Activation Analysis Technique for Determination of the Precious Metals and its Application to a Study of their Geochemistry. Ph.D. Thesis, McMaster University.

Keer, P.F. (1959) Optical Mineralogy, 3rd edition. McGraw-Hill, 442 p.

Liebenberg, C.J. (1960 and 1961) The Trace Elements of the Bushveld Igneous Complex, Univ. Pretoria, Publ. 12 and 13.

Liebenberg, L. (1970) The sulphides in the Layered Sequence of the Bushveld Igneous Complex, Symposium on the Bushveld Igneous Complex and Other Layered Intrusions, ed. by Visser, D.J.L. and von Gruenewaldt, G. Sp. Publ. No. 1, Geol. Soc. Sth. Afr., pp. 108-207.

Lombaad, B.V. (1934) On the Differentiation and Relationships of the Rocks of the Bushveld Complex. Trans. Geol. Soc. Sth. Afr., 37:5-52.

Newman, S.C. (1973) Platinum Institution of Mining and Metallurgy, Transactions/Section C, Vol. 82, Bull. No. 797, pp. A52-68.

Nicolaysen, L.O., de Villiers, J.W.L., Burger, A.J. and Strelow, F.W.E. (1958) Trans. Geol. Soc. Sth. Afr., 61:137-163.

Oen, I.S., Kieft, C. and Westerhof, A.B. (1973) Composition of Chromites in Cordierite- and Mica-bearing Cr-Ni Ores from Mélaga Province, Spain. Mineral. Mag. 39:193-203.

Page, N.J., Riley, L.B. and Haffty, J. (1972) Vertical and Lateral Variation of Platinum, Palladium and Rhodium in the Stillwater Complex, Montana. Econ. Geol. 67:915-923.

Ramdohr, P. (1969) The Ore Minerals and their Intergrowth. Pergamon Press, 1174 p.

Razin, L.V., Khvostov, V.P. and Novikov, V.A. (1965) Platinum metals in the Essential and Accessory Minerals of Ultramafic Rocks. Trans. from Geokhimiya, No. 2, pp. 159-174.

Schmidt, E.R. (1952) The Structure and Composition of the Merensky Reef and Associated Rocks of the Rustenburg Platinum Mine. Trans. Geol. Soc. Sth. Afr., 55:233-279.

Schneiderhöhn, H. (1929) The mineragraphy, spectrography and genesis of the platinum-bearing nickel-pyrrhotite ores of the Bushveld Igneous Complex in the Platinum Deposits and Mines of South Africa, ed. by Wagner, P.A. and C. Struik, Cape Town, 1973, pp. 206-246.

_____ and Moritz, H. (1931) Spektrographische Untersuchungen über die Verteilung der Platinmetalle in der Mineralien der Südafrikanischen platinlagerstätten. Festschrift, z.50, jährr. Bestehen der Platinschmelze G. Siebert GmbH. Hanau, S. 257.

Shaw, D.M. and Harrison, W.D. (1955) Determination of the Mode of a Metamorphic Rock. Amer. Min. 40:614-623.

Skippen, G.B. (1963) A Study of the Distribution of Palladium in Igneous Rocks. M.Sc. Thesis, McMaster University.

Skoog, D.A. and West, D.M. (1966) Sulphur in Fundamentals of Analytical Chemistry. Holt, Rinehart and Winston, pp. 203-205.

Solomon, M. (1963) Counting and Sampling Errors in Modal Analysis by Point Counter. J. Petrology, 3, 4:367-82.

Stumpfl, E.F. (1962) Some Aspects of the Genesis of Platinum Deposits. Econ. Geol., 57:619-623.

Truter, F.C. (1955) Modern Concepts of the Bushveld Igneous Complex. C.C.T.A. South Reg. Com. Geol. 1, pp. 77-92.

Turekian, K.K. and Wedepohl, K.H. (1961) Distribution of the Elements in Some Major Units of the Earth's Crust. Bull. Geol. Soc. Amer. 72:175-192.

Vallance, T.G. (1967) Mafic Rock Alteration and Isochemical Development of Some Cordierite-Anthophyllite Rocks. J. Petrology, 1, 8:84-96.

van Zyl, J.P. (1970) The Petrology of the Merensky Reef and Associated Rocks on Swartklip 988, Rustenburg, Symposium on the Bushveld Igneous Complex and other Layered Intrusions, ed. by Visser, D.J.L. and von Gruenewaldt, G. Geol. Soc. Sth. Afr. Sp. Publ. No. 1, pp. 80-107.

Vinogradov, A. P. (1962) Average Contents of Chemical Elements in the Principal Types of Igneous Rocks of the Earth's Crust. Geochem., 7:641-664.

Vogel, A. I. (1961) Palladium in Quantitative Inorganic Analysis. 3rd edition, Longmans, pp. 511-513.

Yushko-Zakharova, O. Ye., Bykov, V. P., Kulagov, E. A., Avdonin, A. S., Chernyayev, L. A. and Yurkina, K. V. (1970). Isomorphism in the Platinum Metals. Geochem. Int., 7:788-796.

Wager, L. R. (1968) Rhythmic and Cryptic Layering in Mafic and Ultramafic Plutons in Basalt, ed. by Hess, H. H. and Poldervaart, A. Interscience, 2:573-622.

_____ and Brown, G. M. (1967) Layered Igneous Rocks. Freeman, San Francisco, 588 p.

Wagner, P. A. (1929) The Platinum Deposits and Mines of South Africa, 2nd impression, C. Struik, Cape Town 1973, 338 p.

Walsh, T. J. and Hausman, E. A. (1963) Iridium in Treatise on Analytical Chemistry, ed. by Kolthoff, I. M., Elving, P. J. and Samdell, E. B., Part II, 8:379-522.

Willard, H. H., Furman, N. H. and Bricker, C. E. (1956) Sulphur in Elements of Quantitative Analysis, 4th edition, van Nostrand, pp. 358-360 and 328-332.

Willemse, J. (1964) A brief Outline of the Geology of the Bushveld Igneous Complex in the Geology of Some Ore Deposits of South Africa II. Geol. Soc. Sth. Afr., pp. 91-128.

_____ (1969) The Geology of the Bushveld Igneous Complex, the Largest Repository of Magmatic Ore Deposits in the World, Magmatic Ore Deposits, Monograph No. 4, by Wilson, H.D.B. Econ. Geol., pp. 1-22.

_____ and Viljoen, E.A. (1970) The Fate of Argillaceous Material in the Gabbroic Magma of the Bushveld Complex, Symposium on the Bushveld Igneous Complex and Other Layered Intrusions, ed. by Visser, D.J.L. and von Gruenewaldst, G. Sp. Publ.1,Geol. Soc. Sth. Afri. pp. 336-366.

Wyllie, P.J. (1967) Ultramafic and Related Rocks. Wiley, 464 p.

# APPENDIX I

## Analytical Procedures for the Determination of S, Cr, Ni and Cu Contents in Whole Rock Samples

Mixture of 1 gm of sample and 4 gm of $Na_2CO_3$ in Pt crucible — Roasting at 500°C for 1 hr.

↓

Sprinkle 0.1 gm $Na_2O_2$ and 1 gm $Na_2CO_3$ over the above mixture — Fusion at 950°C for 0.5-1 hr.

↓

Cool to R. T. Transfer quantitatively to a 250 ml beaker

↓

Add approx. 50 ml $H_2O$-5 ml ethyl alcohol and stirring bar to the melt — Stir overnight; Digest at a temp. hot to hands, without boiling

↓

Filter through Whatman No. 40 paper into a 400 ml beaker. Wash with hot 1% $Na_2CO_3$

↓

**Residue**

↓

Wash with hot 20% v/v HCl

↓

Filtrate

250 ml

↓

Determination of Cr, Ni and Cu by Atomic Absorption

**Filtrate, 250 ml solution**

↓

100 ml

↓

Determination of Cr by Atomic Absorption

100 ml

↓

Determination of S (gravimetric)

## Determination of S

100 ml solution

Dilute to 150 ml with $H_2O$

Add a few drops of methyl orange
Stir and acidify with HCl
Add 1 ml in excess

Boil a few minutes to expel $CO_2$

At a boiling temp. precipitate S with 20 ml 5% w/v $BaCl_2$ stirring vigorously

Precipitates in the supernatant liquid

Leave on steam bath overnight

Add ashless analytical grade filter paper pulp

Filter through Whatman No. 42 paper

Precipitates

Wash with hot $H_2O$ until no chlorine is indicated by the addition of $AgNO_3$

Precipitates in silica crucible

Char and ignite at 900°C for 15 mins.

Weigh